RARE EARTH ELEMENTS IN THE SUDBURY NICKEL IRRUPTIVE

By

Hsiao-Yu Kuo, B.Sc., M.Sc.

A Thesis

Submitted to the School of Graduate Studies

in Partial Fulfilment of the Requirements

for the Degree

Doctor of Philosophy

McMaster University

September 1975

RARE EARTH ELEMENTS IN THE SUDBURY NICKEL IRRUPTIVE

Abstract is on page XV

DOCTOR OF PHILOSOPHY (1975)   McMASTER UNIVERSITY
(Geology)   Hamilton, Ontario.

TITLE: RARE EARTH ELEMENTS IN THE SUDBURY NICKEL IRRUPTIVE

AUTHOR: Hsiao-Yu Kuo, B.Sc. (National Taiwan University)
                       M.Sc. (McMaster University)

SUPERVISOR: Dr. James H. Crocket

NUMBER OF PAGES: xvii, 242.

SCOPE AND CONTENTS:

Rare earth elements have been determined by group

separation, radiochemical neutron activation analysis in rocks from

the main Irruptive, the sub-layer and sub-layer inclusions from the

Sudbury Nickel Irruptive, Ontario, Canada.

Rare earth behaviour in layered intrusions is discussed and

applied to the Sudbury Nickel Irruptive. The petrogenesis and mutual

relationships of the Sudbury rocks are discussed in the light of their rare

earth properties.

ACKNOWLEDGEMENTS

TABLE OF CONTENTS.

iv

v

LIST OF TABLES

ABSTRACT

Radiochemical neutron activation analysis procedures for rare earth elements (REE) are described and applied to the determination of REE in samples of main Irruptive, sub-layer, sub-layer inclusions, Onaping Formation, and basement rock from the Sudbury Nickel Irruptive, Ontario, Canada.

Rare earth (RE) distribution in several layered basic intrusions are reviewed. Features of RE behaviour in layered intrusions are, in general, in accordance with Rayleigh fractionation considerations. The magnitude of negative europium anomaly in final granophyres and europium compensation effects observed in layered intrusions may have their petrogenetic significance. These findings are then compared with the observed RE patterns in Sudbury rocks.

Compared to other layered basic intrusions, the Sudbury main Irruptive rocks are characterized by enrichment in total RE abundances and chondrite normalized RE patterns showing strong enrichment of light REE over heavy REE. Corresponding rock units from the north and south ranges of the main Nickel Irruptive have very similar RE fractionation patterns. The micropegmatite and norite are characterized by negative and positive Eu anomalies respectively, whereas the border

norite shows no significant Eu anomaly. The main Irruptive border

norites are considered to have been solidified as a relatively closed

system with respect to REE and should preserve the RE fractionation

patterns of the undifferentiated main Irruptive magma. The mirror-

image RE fractionation patterns of the micropegmatite and norite are

considered to result from gravitational fractional crystallization of

the main Irruptive magma with norite representing cumulates and micro-

pegmatite forming from residual liquid. RE mass balance considerations

favour a funnel-shaped model for the main Irruptive.

The RE fractionation patterns of the sub-layer rocks are

generally similar to those of the main Irruptive border norites pointing

to possible genetic links. However, the wider range of variation in sub-

layer RE patterns suggests that several batches of magma were involved

and that their history is probably complicated.

The sub-layer ultramafic and mafic inclusions have RE

fractionation patterns generally similar to those of the main Irruptive

border norites and sub-layer rocks, although they are somewhat less

fractionated. After comparing with RE patterns of different types of

ultramafic rocks, the sub-layer inclusions are considered to represent

fragments from pre-existing mafic-ultramafic cumulates, which were

probably in equilibrium with a liquid that had a RE fractionation pattern

similar to the main Irruptive magma. Varying amounts of inter-
cumulus material appear to be the factor governing the RE fractiona-
tion patterns in these inclusions.

The Onaping Formation rocks have total RE contents
lower than the main Irruptive rocks. When compared with RE frac-
tionation patterns in rocks from known ash-flows and meteorite impact
sites, the Onaping Formation rocks favour a meteorite impact fall-
back breccia origin in the sense that the RE patterns of the lower
Onaping Formation rocks can be represented by mechanical mixtures of
country rocks.

CHAPTER ONE

INTRODUCTION

The Sudbury district is distinctive both economically and geologically. Economically, the area hosts the world's greatest producer of nickel sulfide ore. Geologically, the occurrence of the Sudbury basin at the junction of three major tectono-structural provinces has provided the focus for genetic interpretation by some authors. Others have maintained that the shock metamorphic features and abundance and variety of breccias in the area point to a large scale impact of an extraterrestrial body which was the key event in producing the Sudbury structure.

Nickel-copper ores were discovered at Sudbury in 1883. A close association of these ores with the Sudbury Nickel Irruptive is generally accepted. However, during the nearly 100 years since discovery, controversies over the origin of the ores and Nickel Irruptive itself have never subsided. Whether the main Irruptive is a folded sill, a ring-dike complex, or a funnel-shaped intrusion and whether the norite and the micropegmatite were emplaced as a single magma or as separate intrusions, have never been fully resolved.

1

Numerous models have been proposed to account for the unusual features observed at Sudbury. Early interpretations considered the Onaping Formation and Nickel Irruptive to be extrusive and intrusive respectively (Collins, 1934; Thomson, 1956; Williams, 1956; Speers, 1957; etc.). Dietz's (1964) suggestion that the Sudbury structure is an astrobleme and the subsequent discoveries of shock metamorphic features in the country rocks (Dietz and Butler, 1964; Bray et al., 1966; French, 1967, 1970) have raised renewed interest in the genesis of the Irruptive. Increasing numbers of geologists now maintain that a meteorite impact model can most satisfactorily explain the shock metamorphic features and abundant breccias at Sudbury. The formation of the Nickel Irruptive magma and its ores was probably triggered at depth by the impact. Some suggest that the Nickel Irruptive is formed directly from the impact melt (Dence, 1972). One authority (Dietz, 1972) argues that the ores are cosmogenic in origin; that is, that the copper, nickel and noble metals are original constituents of the impacted bolide. Others who disagree with the impact theory point out that the uniqueness of the regional tectonic setting may be responsible for the Sudbury structure (Card and Hutchinson, 1972). They consider that a meteorite impact at the site of the Sudbury basin, which is near the junction of the Superior, Southern and Grenville structural provinces of the Canadian Shield and at the intersection of the regional Onaping-Timiskaming and Murray fault

systems, requires a high degree of coincidence. They consider that the Sudbury structure is just one component of a prolonged series of geological events in which tectonics, stratigraphy, petrogenesis and mineralization are all interrelated.

The main points of current debate on Sudbury geology emphasize several questions critical to the interpretation of the geological history of the Irruptive. Some of the more important include the following: is the Onaping Formation a volcanic ash-flow deposit or was it produced by country rock fall-back after the meteorite impact? What are the age relationships of the various rock units of the Irruptive? Did the norite and micropegmatite crystallize from two separate magmas or are they differentiates from a single magma? Are the mafic and ultramafic inclusions of the sub-layer rocks derived directly from the upper mantle or from some pre-existing layered rocks, or could they represent early cumulates from the Irruptive magma? What are the petrogenetic relationships between the main Irruptive, the sub-layer, and the Onaping Formation rocks?

The Sudbury Nickel Irruptive has been carefully mapped and a number of modal and major element analyses of its constituent rocks and minerals have been published (Collins, 1934; Naldrett and Kullerud, 1967; Cowan, 1968; Souch et al., 1969; Naldrett et al., 1970, 1972). However, few trace element studies on the Irruptive Rocks have been

1

reported except for several studies (mainly Rb-Sr) attempting to establish an emplacement age for the Nickel Irruptive (Fairbairn et al., 1960; 1965; 1968; Faure et al., 1964; Souch et al., 1969; Fullagar et al., 1971; Gibbins, 1973; Hurst and Wetherill, 1974; Krogh and Davis, 1974).

The similarity in chemical properties and the extremely coherent behaviour of REE in geological systems have long been recognized (Rankama and Sahama, 1950; Goldschmidt, 1954). However, recent developments in analytical techniques have revealed that relative fractionation among individual elements in the group occurs in various geological processes. With increasing understanding of the relationships between the RE fractionation trends in rocks and the evolutionary history of magmas, REE have become useful tools in petrogenetic studies. Their usefulness is self-evident by the ever increasing number of RE papers reported in the literature during the past few years.

Many recent RE studies are concerned with determination of RE distribution coefficients for rock-forming minerals (see section 5-1) and RE patterns in basalts (Frey et al., 1968; Schilling and Winchester, 1969; Jakes and Gill, 1970; Kay and Gast, 1973; Condie and Barager, 1974; etc.). Since partial crystallization of basalt magma prior to eruption does not drastically change its RE fractionation pattern, REE are useful guides to possible compositions of source rocks and probably mechanisms of partial melting responsible for the generation of basalt magma.

RE studies on plutonic rocks are fewer than those on basalts and are mainly concerned with establishing RE patterns in ultramafic rocks of possible mantle origin (see section 5-7). Determinations of RE abundances in several differentiated intrusions can be found in recent literature (see section 5-2). The only systematic discussion on RE behaviour in a layered intrusion is that of Haskin and Haskin (1968) and Paster et al. (1974) on the Skaergaard intrusion.

The most common techniques used by geochemists for RE determinations are isotope dilution mass spectrometry (IDMS) and neutron activation analysis (NAA). The main advantage of NAA is relative freedom from contamination while IDMS, in general, gives better precision and probably better accuracy. Both methods provide sufficient sensitivity to routinely determine REE in a wide variety of rocks including ultramafics.

In this work, REE in the Sudbury rocks were determined by a wet chemical, group separation, neutron activation technique. The objective was to provide additional constraints on the various petrogenetic models for the Nickel Irruptive and related rocks. The main points considered are: the petrogenetic relationships between the micropegmatite and norite; the petrogenetic relationship of the sub-layer to the main Irruptive; the origin of the sub-layer mafic and ultramafic inclusions

and their relationship to the main Irruptive rocks; and finally, the origin of the Onaping Formation and its relationship to the main Irruptive.
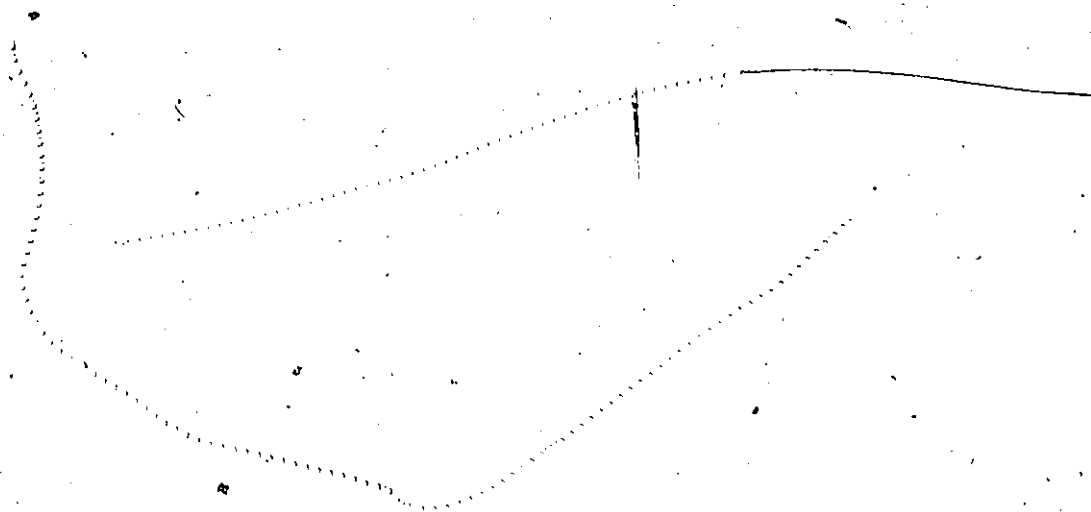
CHAPTER TWO

GEOLOGY

2-1. Regional Geology of the Sudbury Basin

The geological setting and rock units of the Sudbury basin are illustrated in Fig. 2-1. The Sudbury basin is located in a unique position near the junction of the Superior, Southern and Grenville structural provinces of the Canadian Precambrian Shield. The oval-shaped basin outlined by the outcrops of the Sudbury Nickel Irruptive is 60 km long by 27 km across with a long axis oriented east-northeast and lies within the Southern Province 9 to 16 km northwest of the "Grenville Front".

Bounding the basin on its northern and eastern flanks are Archean granites and gneisses of the Superior Province. On the south a series of apparently conformable, steeply dipping, metamorphosed Huronian volcanic and sedimentary rocks of the Southern Province is in contact with the Irruptive. Within the basin is a succession of rocks known as the Whitewater Series whose lowest unit, the Onaping Formation, lies directly on top of the Nickel Irruptive. The Onaping Formation

6

Fig. 2-1. Geological Map of the Sudbury Basin

(modified after Hawley, 1962).

GEOLOGICAL MAP

SUDBURY BASIN

0   2   4   6   8 mi

LEGEND

Nickel Irruptive

Olivine diabase dikes

Micropegmatite

Transition zone

Norite and sub-layer rocks

Chelmsford sandstone

Onwatin slate

Onaping tuff

Granite and gneiss
C - Creighton
M- Murray

Quartzites

Greywacke, acid and basic volcanics

Faults

SUPERIOR - PROVINCE

GRENVILLE PROVINCE

SOUTHERN PROVINCE

Toronto

0   100   200

grades upwards into the Onwatin slate which in turn is overlain by a
massive greywacke known as the Chelmsford sandstone which occupies
the center of the basin. The members of the Whitewater Series together
with the Nickel Irruptive outcrop in concentric rings and dip inward
towards the center of the basin.

Regionally, the basin is divided into the north and the south
ranges by the Cameron Creek and Airport faults,which result in an
apparent uplift of the south range of approximately 5 km relative to the
north range (Souch et al., 1969). Across the north range between
Levack and Maclennan is a series of northerly trending, steeply
dipping faults which have an accumulated vertical displacement of
about 1 km, west side up relative to the east. The Maclennan block
on the east range is thus the highest stratigraphic segment of the
Sudbury basin and the south range is the lowest.

The Sudbury Nickel Irruptive was emplaced 1.7 to 2.0 billion
years ago (Fairbairn et al., 1968; Gibbins, 1973) along the contact be-
tween the Whitewater Series and the underlying basement rocks. The
outcrops of the main Irruptive consist of an inner ring of granophyre
(the micropegmatite) and an outer ring of norite with a transition zone
(the oxide-rich gabbro) between the two. The inner and outer contacts
of the main Irruptive dip, for the most part, toward the center of the basin

at a weighted average angle of 42° on the north range and 65° on the south range and define a bowl-shaped structure.

The majority of the Sudbury nickel-copper sulfide ores, consisting mainly of pyrrhotite, pentlandite and chalcopyrite, are associated with the mafic sub-layer which is a sulfide- and inclusion-rich noritic unit occurring between the main Irruptive and the country rocks (Naldrett and Kullerud, 1967; Cowan, 1968; Souch et al., 1969; Hewins, 1971). The sulfides are believed to have been introduced together with the sub-layer magma. Sulfides and inclusions also occur in offsets, which are dike-like, steeply dipping bodies of quartz diorite that project away from the outer perimeter of the main Irruptive. Offsets run for as much as 13 km into the surrounding country rocks.

The Nickel Irruptive has been variously interpreted as the surface expression of: (1) a folded, differentiated sill (Walker, 1897; Coleman, 1905, 1913; Collins, 1934, 1935, 1936, 1937); (2) a ring-dike complex (Knight, 1917, 1923; Phemister, 1925); (3) a differentiated, funnel-shaped intrusion (Wilson, 1956; Naldrett et al., 1970).

2-2. The Main Irruptive

Detailed petrographic studies on rocks collected at Strathcona mine of the north range and from five traverses across the main Irruptive have been reported by Naldrett and Kullerud (1967),

Cowan (1968) and Naldrett et al. (1970, 1972). Comparison and correlation of partially idealized north and south range sections from Naldrett et al. (1972) are shown in Fig. 2-2.

Although the north and south range rocks have been mapped as a single stratigraphic group, petrographic differences between the north and south range main Irruptive rocks have been noted and are attributed to the uplifting of the south range by faulting, thereby exposing a deeper section of south range rocks (Stevenson and Colgrove, 1968; Naldrett et al., 1970). Naldrett et al. (1970) have demonstrated that while the micropegmatite and transition zone are very similar on the north and south ranges, the bulk of the south range norite does not appear on the north range and the north range felsic norite corresponds only to the extreme upper part of the south range norite (Fig. 2-2).

The presence of cryptic variation in hypersthene, augite, plagioclase and opaque oxides on both ranges (Naldrett et al., 1970; Gasparrini and Naldrett, 1972) strongly suggests that the norites and gabbros of the main Irruptive have been gravitationally differentiated in situ. Based on their work Naldrett et al. (1970) further interpreted the south range quartz-rich norite as a rapidly cooled marginal facies of the norite and therefore suggest that its composition approximates the liquid composition of the original main Irruptive magma. A similar

Fig. 2-2. Comparison and Correlation of North and South Range

Sections of the Sudbury Irruptive (after Naldrett et al.,

1972).

14,000'

No data

12,000'

MICROPEGMATITE

A 0.60

MICROPEGMATITE

6,000'

4,000'

10,000'

UPPER GABBRO

8,000'

A 0.50

A 0.42, P 50

OXIDE-RICH
GABBRO

2,000'

A 0.37, P 53

P 50

H 0.38
A 0.31
P 58

FELSIC NORITE

P 55

H 0.33
A 0.30
P 65

MAFIC NORITE

0'

? — ? — ?

A 0.30

6,000'

H 0.32
A 0.27
P 57

SOUTH RANGE
NORITE

North Range Section
(true thickness)

?

?

EXPLANATION

Quartz + Micrographic Intergrowth

Plagioclase

Hypersthene

Augite

Biotite + Primary Amphibole

Opaque Oxides + Apatite + Sphene

4,000'

?

?

?

?

H 0.31
A 0.27
P 61

2,000'

QUARTZ-RICH
NORITE

?

H 0 31 Fe/(Mg + Fe) atomic ratio in Hypersthene

A 0 27 Fe/(Mg + Fe) atomic ratio in Augite

P 61 mole % Anorthite in Plagioclase

H 0.41
A 0.35
P 60

0'

South Range Section
(horizontal distances)

marginal facies (the mafic norite) at the base of the north range

felsic norite has been revealed by recent underground developments.

Electron-microprobe studies demonstrate that cryptic variation in

minerals continues from felsic norite into mafic norite. This suggests

that the mafic norite may represent the rapidly cooled border group of

the main Irruptive magma on the north range analogous to the quartz-

rich norite on the south range (Hewins, 1971). As illustrated in Fig.

2-2 the transition from mafic norite to felsic norite on the north range

is very abrupt, contrasting with the smooth transition from quartz-rich

norite to south range norite on the south. Hewins (1971) attributed this

sharp transition and the localized development of mafic norite at Strathcona

mine to a surge of a large volume of felsic norite magma over the top of

other units scouring away much of the younger, partially consolidated

material. Remnants of mafic norite were preserved in downward em-

bayments of the lower contact in relatively sharp contact with the over-

lying felsic norite. His model suggests that the poikilitic mafic norite

is considered a border group formed by crystallization in situ

and the hypidiomorphic mafic norite a later gravitational accumulate in a

funnel-shaped chamber. The felsic norite was formed by a rapid cry-

stallization in a sill environment during later resurgence of the magma.

The following is a summary of the petrography of the various rock units of the main Irruptive based mainly on the detailed work of Naldrett and Kullerud (1967) and Naldrett et al. (1970). Their terminology of the rock units will be adopted in this study.

2-2-1. North Range Rocks

The north range geology can best be represented by the rocks in the vicinity of the Strathcona mine where much detailed work has been performed (Naldrett and Kullerud, 1967 and Cowan, 1968 for mineralogy and petrology; Keays and Crocket, 1970 and Chyi, 1972 for noble metal distribution; Greenman, 1970 and Hewins, 1971 for petrogenesis of the sub-layer rocks). Four rock units of the main Irruptive are recognized here including in descending order, the micropegmatite, the oxide-rich gabbro, the felsic norite and the mafic norite. The general relations of the rock units and the localities of the samples used in this study are illustrated in Figs. 2-3 and 2-4. Fig. 2-3 is a vertical section extending south-east from the Strathcona mine across and approximately at right angles to the long axis of the main Irruptive. Fig. 2-4 shows horizontal geological sections across Strathcona mine at different levels. In this study the north range samples were collected from a drill core (M-9) through the Strathcona mine. The modal variation within core M-9

Fig. 2-3. Vertical Cross-Section through the Strathcona

Mine showing Contact Relations between Rock Units

(after Naldrett and Kullerud, 1967).

LEGEND

ORE

DIABASE DIKE

MICROPEGMATITE AND
OXIDE-RICH GABBRO

FELSIC NORITE

MAFIC NORITE

XENOLITHIC NORITE

HANGING-WALL BRECCIA

GRAY BRECCIA

GRANITIC GNEISS COMPLEX

1750 LEVEL

2000 LEVEL

2250 LEVEL

2500 LEVEL

2750 LEVEL

3025 LEVEL

SCALE

0   400   800 ft
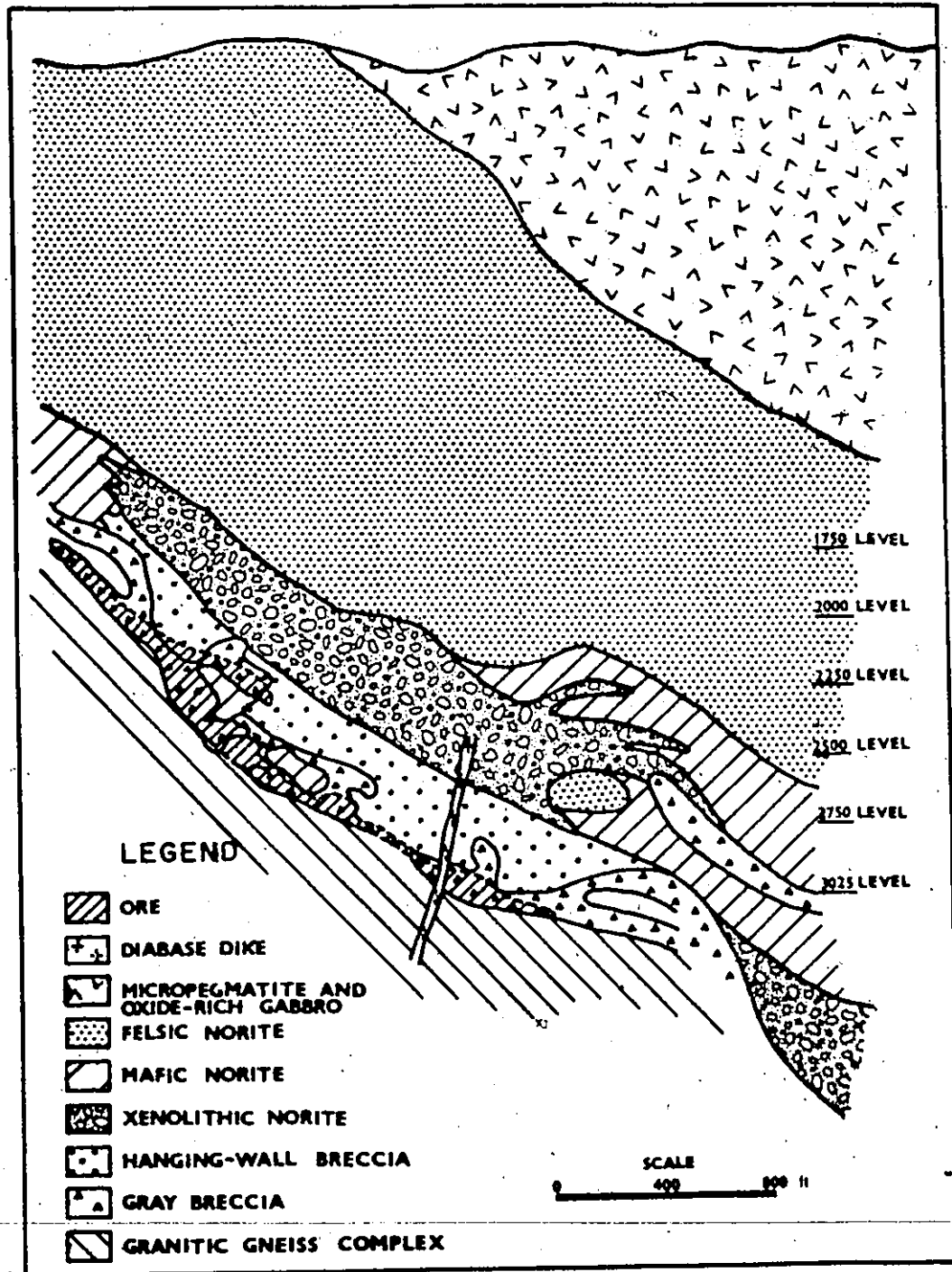
Fig. 2-4. Three Horizontal Levels through the Strathcona Mine
at different Levels showing Contact Relations between
Rock Units and Projected Sub-Layer Inclusion Sample
Locations (geology after Cowan, 1968).

2000 LEVEL

N

10500 N

S-20-40

2250 LEVEL

10500 N

S-23-32

2625 LEVEL

10500 N

S-27-27

20700 E

21500 E

22200 E

LEGEND

ORE

DIABASE DIKES

GRAY BRECCIA

HANGING-WALL BRECCIA
AND XENOLITHIC NORITE

MAFIC NORITE

GRANITIC GNEISS COMPLEX

FAULT

SCALE OF FEET
200   0   200
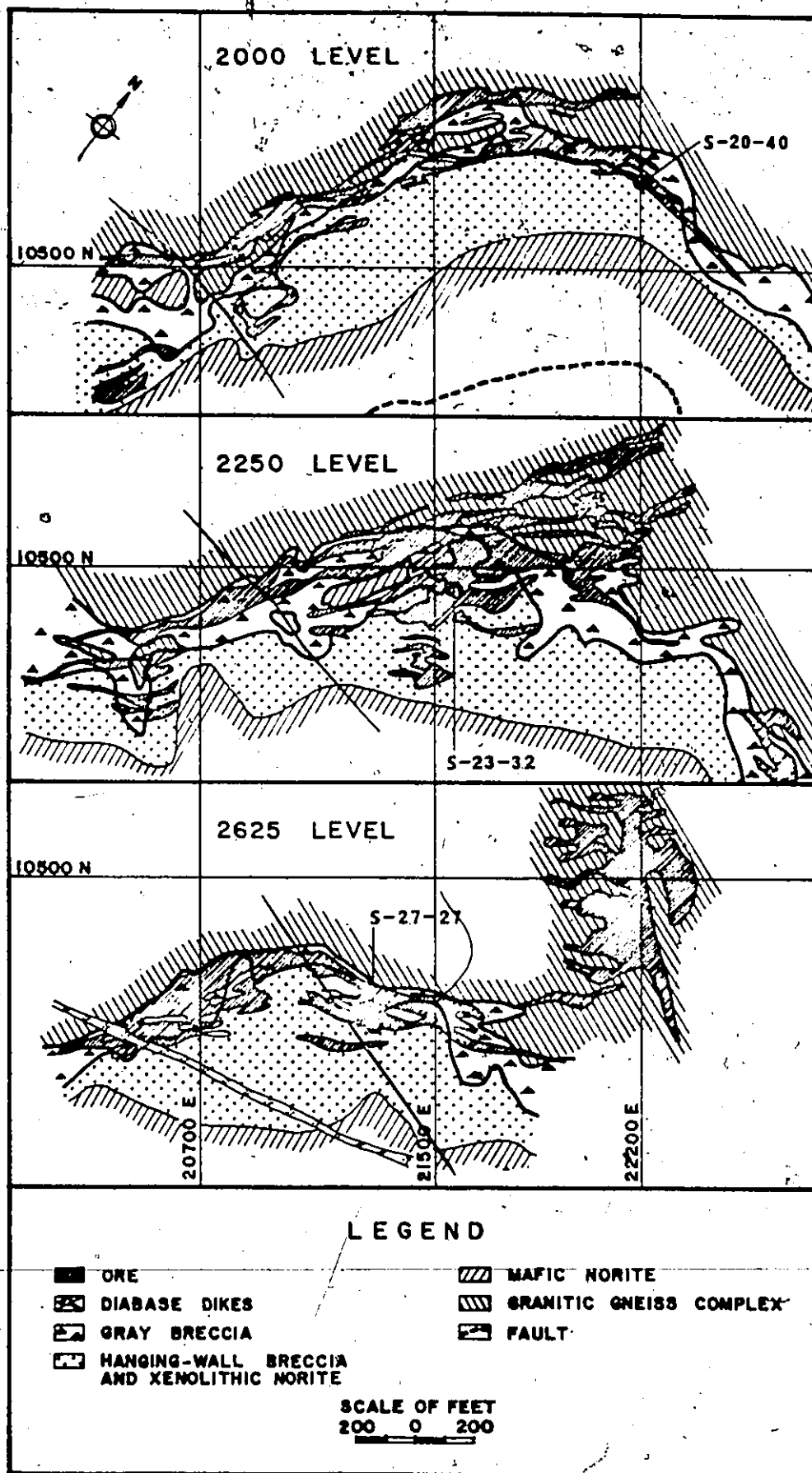
reported by Naldrett et al. (1970) is reproduced in Fig. 2-5. Samples

of core section used in this study are adjacent to the samples of Naldrett

et al. so that their reported modal data are applicable to the samples

of this study.

I) micropegmatite:

The micropegmatite is the uppermost unit of the main Irruptive

and is in direct contact with the overlying Onaping Formation. It is about

1500 meters in thickness and is a coarse-grained granitic rock with sub-

hedral sodic plagioclase in a matrix of more than 60 modal percent micro-

graphic intergrowth of quartz and K-feldspar. The ratio of the plagioclase

to the micrographic intergrowth is about 1 to 3. Mafic minerals (about

15 model percent) include very rare relict augite, green hornblende,

stilpnomelane and chlorite.

II) oxide-rich gabbro:

This "transition zone" rock lies between felsic norite and

micropegmatite. It is a coarse-grained, hypidiomorphic granular rock

consisting of 45 percent plagioclase, 20 percent micrographic intergrowth

and 30 percent mafic minerals. The sharp boundary between the oxide-

rich gabbro and the underlying felsic norite is manifest by an abrupt

increase in the percentage (up to 8 percent) of opaque oxides and by the

disappearance of hypersthene in the oxide-rich gabbro. The content of

Fig. 2-5. Modal Variation along Strathcona Core M-9 (after

Naldrett et al., 1970) showing Sample Locations.
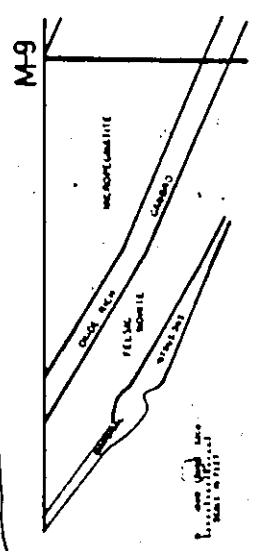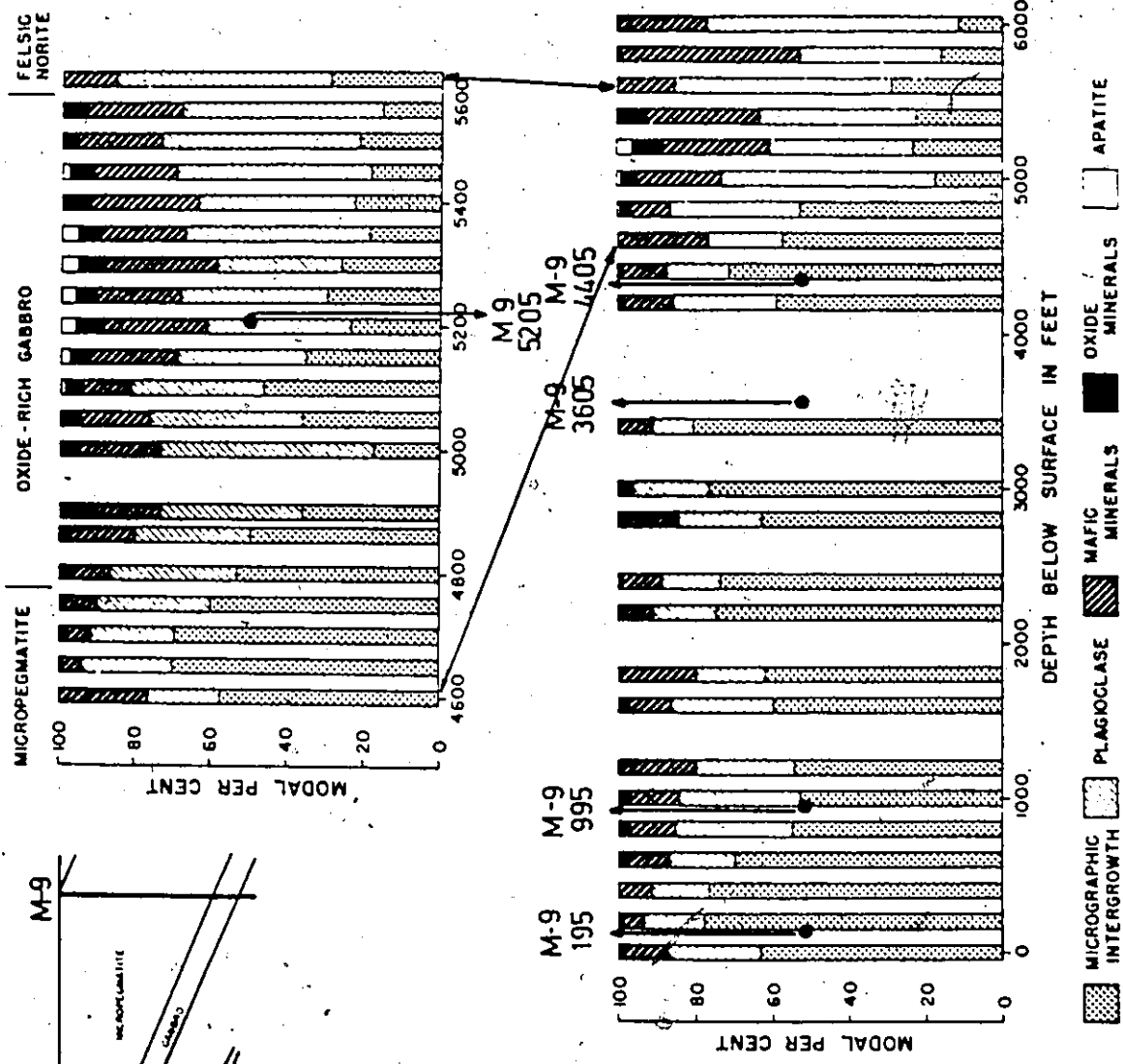
the opaque oxides decreases and the micrographic intergrowth increases in the upper part of the oxide-rich gabbro and the transition into the micropegmatite is gradational.

Much of the plagioclase in the oxide-rich gabbro has a cloudy alteration which gives the plagioclase laths a characteristic white appearance in hand specimen. In the field, this rock often shows a pronounced lamination which is enhanced by the alteration of the plagioclase.

III) felsic norite:

The felsic norite is about 600 meters thick in the vicinity of Strathcona mine. It is a fairly uniform, coarse-grained, hypidio-morphic granular rock composed of 50 percent zoned plagioclase, 25 percent augite and hypersthene in the ratio of about 1 to 2, and 10 percent interstitial micrographic intergrowth with accessory biotite, apatite, and opaque oxides. In the lower two-thirds of this unit hypersthene and plagioclase occur as subhedral tabular cumulus crystals with augite moulded about plagioclase as intercumulus crystals. In the upper third of the unit, hypersthene disappears and augite is more tabular.

IV) mafic norite:

Variable thicknesses of mafic norite (0 to 140 meters) occur at the base of the felsic norite near Strathcona. The mafic norite is

a medium-grained, granular rock. Its texture varies between hypidio-morphic and poikilitic. It is mineralogically similar to the felsic norite except that it is less altered and contains more orthopyroxene. Its contact with the overlying felsic norite varies between transitional to abrupt. The mafic norite was originally thought to be part of the younger mafic sub-layer intrusion (Naldrett and Kullerud, 1967; Cowan, 1968) but a recent study of Hewins (1971) has shown that cryptic layering continued from felsic norite into mafic norite suggesting that the mafic norite is not a separate intrusion but a part of a sequence continuous with the felsic norite. The increase inwards from the contact in the amount of orthopyroxene, in the crystal size and a decrease in the amount of intercumulus material led him to suggest that the mafic norite is the border group of the main Irruptive on the north range.

2-2-2. South Range Rocks

The south range samples were collected along or close to Highway 69 (the Blezard traverse), cutting the south range approximately perpendicular to the strike of the main Irruptive. Sample locations and the modal variation along the Blezard traverse are illustrated in Figs. 2-6 and 2-7.

Four rock units of the south range are recognized. These are the micropegmatite, the upper gabbro, the south range norite, and the quartz-rich norite.

Fig. 2-6. Blezard Traverse Along the South Range of the

Sudbury Irruptive (after Naldrett et al., 1970)

showing Sample Locations.

To Capreol

Whitewater Group

Micropegmatite

W155

Whitson
Lake

Lake

W150

W153

Micropegmatite

Upper Gabbro

W126

Upper Gabbro

South Range Norite

W120

W116

South Range Norite

Quartz-rich Norite

W104

W110

0   1000 2000 3000 4000 5000 FEET

SCALE

Blezard Twp

Outer Perimeter
of Irruptive

-N-

HWY
69

To
Sudbury
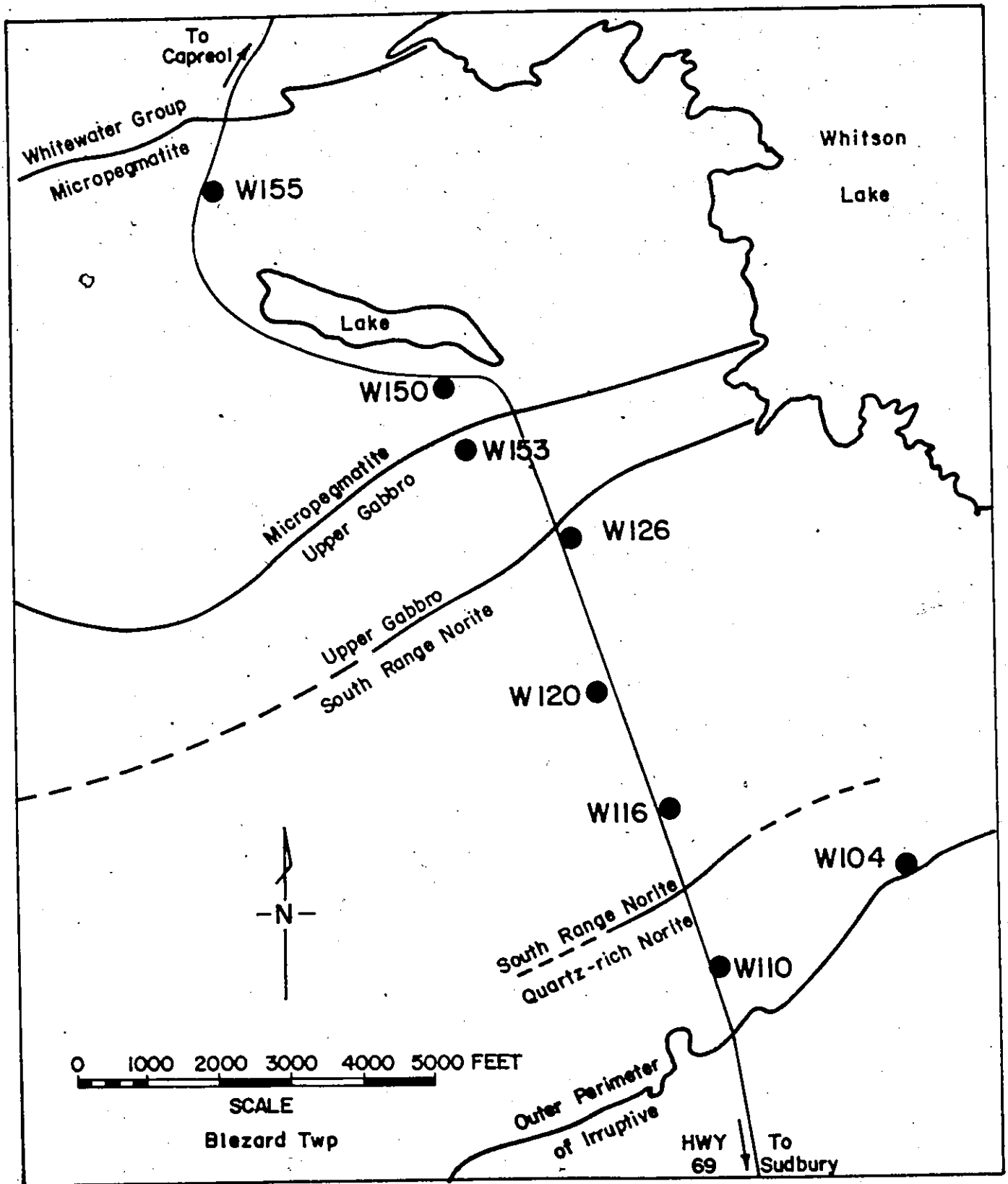
Fig. 2-7. Modal Variation along the South Range Blezard

Traverse (after Naldrett et al., 1970)

LEGEND

- Apatite
- Opaque Oxide
- Sphene
- Biotite + Secondary Amphibole
- Primary Hornblende
- Hypersthene
- Augite
- Plagioclase
- Quartz
- Micrographic Intergrowth
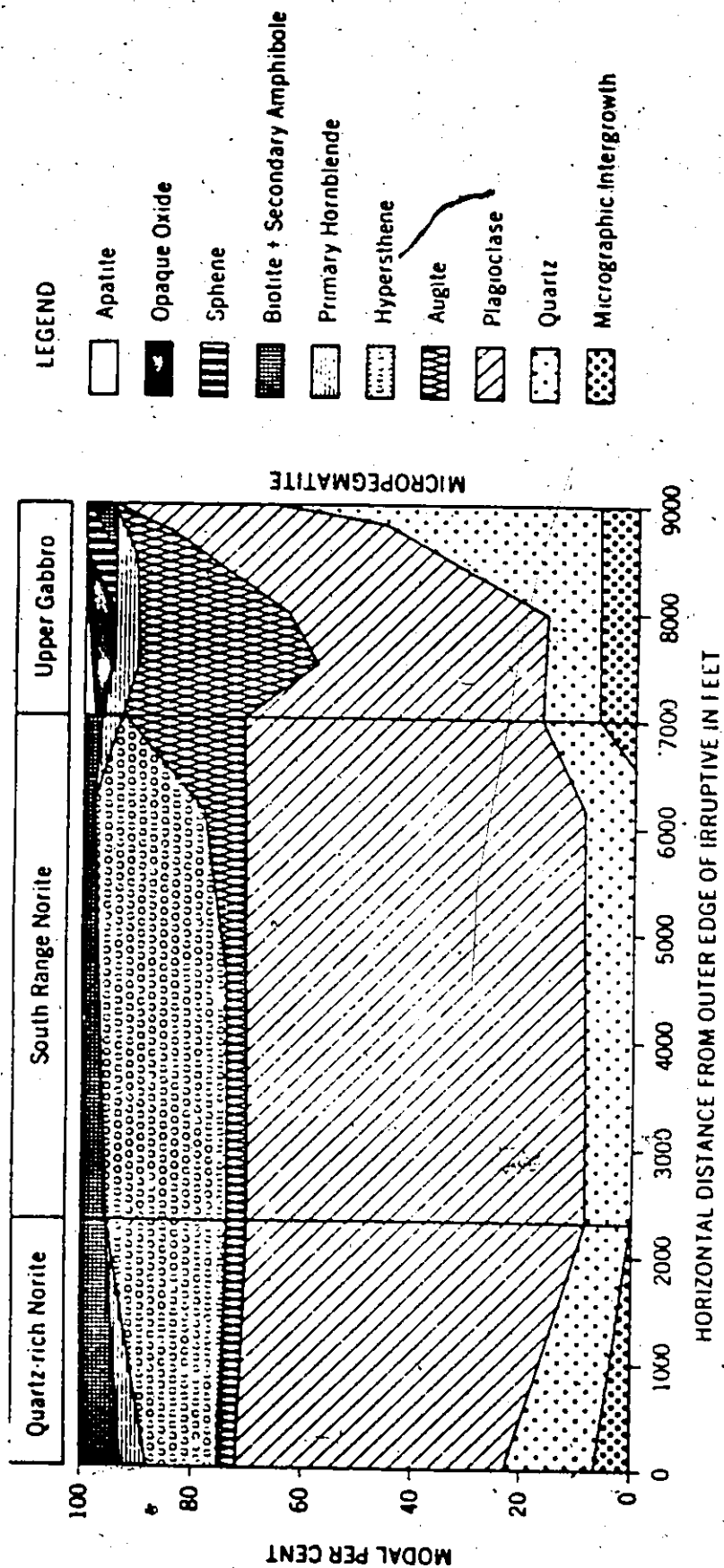
I) micropegmatite:

On the Blezard traverse, the south range micropegmatite is a granulated rock consisting mainly of quartz and plagioclase with rims of antiperthite. Most samples are altered and have a pronounced gneissic foliation, marked by subparallel orientation of biotite, the most common mafic mineral of the rock.

II) upper gabbro:

The south range upper gabbro is stratigraphically equivalent and mineralogically similar to the north range oxide-rich gabbro. Its principal difference with respect to the north range is that the high opaque oxide content of the gabbro is restricted to the lower half of the unit.

As on the north range, the boundary between the upper gabbro and the underlying south range norite is marked by the abrupt increase in opaque oxides (ilmenite and magnetite) and apatite in the gabbro. The contact between the upper gabbro and the overlying micropegmatite is gradational and manifest by a gradual increase in the content of quartz plus micrographic intergrowth from the upper gabbro into the micropegmatite.

III) south range norite:

This is a medium- to coarse-grained rock containing 60 percent plagioclase, 25 percent pyroxenes, 8 percent quartz and minor magnetite and ilmenite as its main primary minerals. Hypersthene and plagioclase occur as subhedral tabular crystals. Augite occurs as anhedral masses, partially molded about plagioclase and hypersthene. Its main differences compared to north range felsic norite are less zoned plagioclase, higher hypersthene to augite ratio (5 to 1 in south range norite and 2 to 1 in north range felsic norite), lower quartz content, and no micrographic intergrowth. Secondary alteration is extensive in the south range norite, and often imparts a greenish color to the more severely altered norite (the so-called "green norite").

IV) quartz-rich norite:

The thickness of this unit is approximately 400 meters and it lies at the base of the main Irruptive on the south range. Mineralogically, it is similar to the south range norite, but has a higher quartz content. The quartz content increases from 8 percent at the contact with the south range norite to over 20 percent at the extreme outer margin of the main Irruptive. Most of the quartz occurs as anhedral interstitial masses or as aggregates of equant grains. Minor amounts of quartz occur in the form of micrographic intergrowth.

At the outer margin, the quartz-rich norite is distinctly finer grained than the south range norite. Naldrett et al. (1970) interpreted this unit as a rapidly cooled border group on the south range and stressed that the extreme outer portion of the quartz-rich norite should closely approximate the composition of the liquid portion of the original main Irruptive magma.

2-3. The Sub-Layer

The sub-layer rocks occur between the main Irruptive and the footwall country rocks. They carry sulfides and inclusions of mafic to ultramafic type unlike any rocks found in the main Irruptive. Frequently they are tectonic breccias consisting of footwall gneiss and overlying norite fragments. They can be divided into three groups: the north and south range mafic sub-layer, the leucocratic sub-layer breccias, and the offset dikes. Recent studies (Cowan, 1968; Souch et al., 1969) show that the majority of the sulfide ore at Sudbury is probably emplaced together with the mafic sub-layer and the offset intrusions.

The distribution of the sub-layer rocks and their close association with the existing mines along the perimeter of the main Irruptive is shown in Fig. 2-8. The contacts between the sub-layer

Fig. 2-8. Distribution of Sub-Layer and Offsets with Occurrences

Sampled in this Study Indicated (modified after Souch

et al., 1969).

Whistle sub-layer

Little Stobie sub-layer
Frood offset
Murray sub-layer

Copper Cliff offset

RANGE

NORTH RANGE

SOUTH RANGE

Foy offset

Strathcona sub-layer

Sultana sub-layer

0   5
MILES
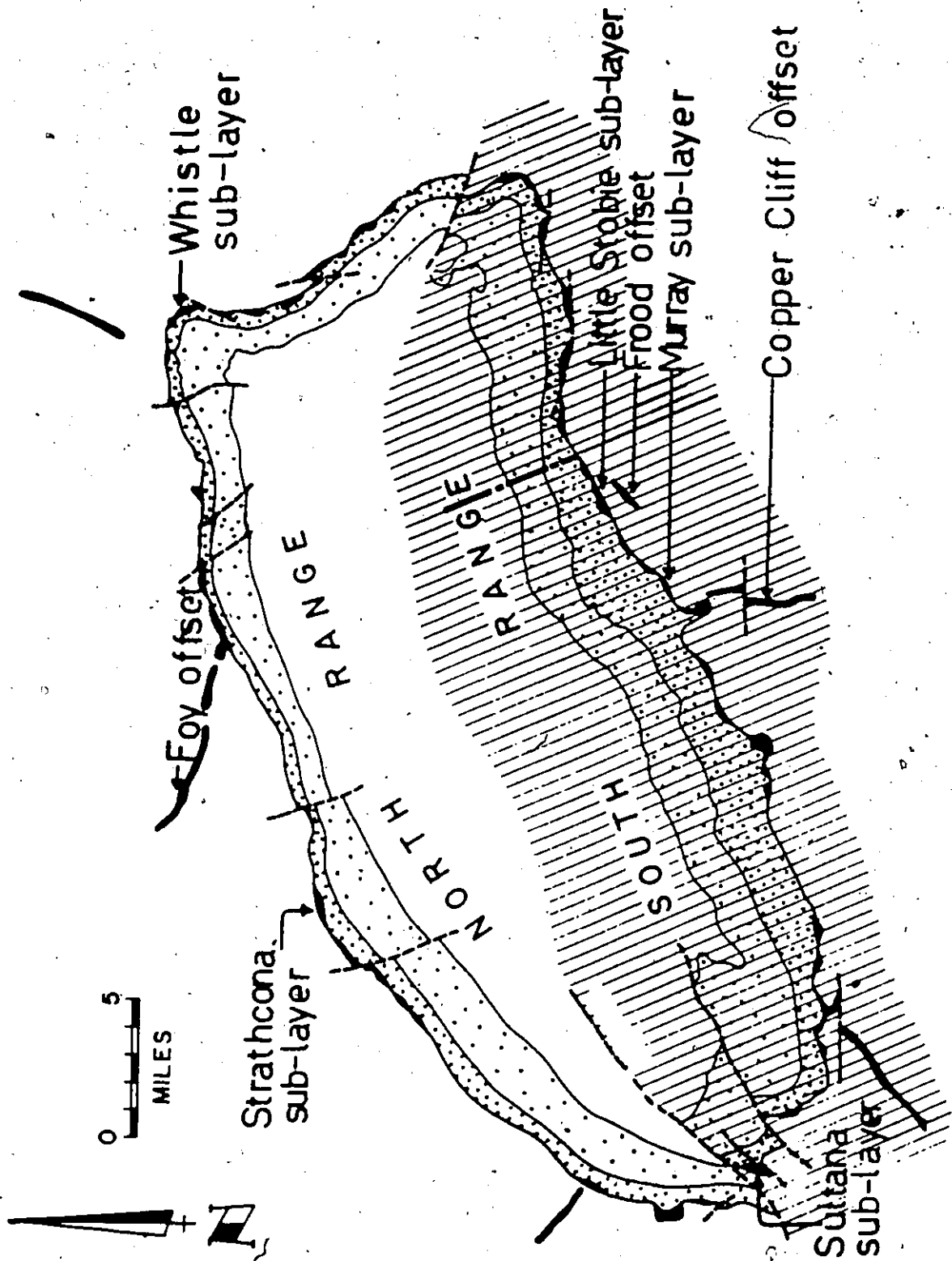
rocks and the overlying main Irruptive are generally abrupt and the sub-layer rocks are considered to be younger than the main Irruptive. (Greenman, 1970; Hewins, 1971). However, the relative ages of individual sub-layer units are not yet clearly established due to their complicated structural relations.

The sulfide content of the sub-layer rocks range from essentially sulfide-free to massive sulfide. When the sulfide content is low it generally occurs as disseminated patches interstitial to the silicate minerals. When the proportion of sulfide increases it forms blebs and eventually the inclusion massive sulfide type ore (terminology from Souch et al., 1969). There is generally an increase in the sulfide content and the inclusion size towards the footwall (Souch et al., 1969). Naldrett and Kullerud (1967) considered the data on the solubility of sulfides in silicate magmas and ruled out the possibility that the bulk of the sulfides were in solution in the noritic magmas during intrusion, and suggested that the sulfides were held in suspension in the sub-layer magma as droplets of immiscible sulfide-oxide liquid. Dietz (1972), in his most recent version of the meteorite impact model, considered that both the sub-layer rocks and the associated ores were formed during the meteorite impact which triggered the intrusion of the main Irruptive.

2-3-1. North and South Range Mafic Sub-Layer Rocks

Mafic sub-layer rocks on the north and south ranges are medium- to fine-grained, inclusion- and sulfide-bearing basic rocks. The inclusions consist of angular footwall fragments and a suite of rounded fragments of ultramafic and mafic rocks including peridotite, pyroxenite, and gabbro. The silicate mineralogy of the matrix is noritic with varying proportions of augite and hypersthene (Souch et al., 1969). Detailed studies are found in Greenman (1970) and Hewins (1971), both in the Strathcona area.

Hewins (1971) reported considerable modal and textural variations within and between mafic sub-layer rocks from mine to mine on the north range. The mafic sub-layer at Strathcona varies in thickness from place to place and is best developed in embayments where the main Irruptive protrudes into the footwall rocks. The contact relations between the sub-layer and the main Irruptive at Strathcona mine are shown in Figs. 2-3 and 2-4.

2-3-2. Leucocratic Sub-Layer Breccias

A group of breccias of complicated origin known as leucocractic sub-layer breccias occur between the main Irruptive and the footwall rocks. Two major types are recognized. They are the Levack breccia and the north range gray breccia.

The Levack breccia is developed extensively around the periphery of the Sudbury basin. It is a tectonic breccia composed of country rock blocks sitting in a fine-grained dark matrix. The bulk of the breccia is barren in sulfide and believed to be pre-Irruptive (Speers, 1957).

The north range gray breccia, locally termed late granite breccia, is well developed at Strathcona mine (see Figs. 2-3 and 2-4), and has been studied in detail by Cowan (1968) and Greenman (1970). This breccia is important economically as it is the most important host for ore in the north range mines. It consists of highly brecciated footwall rock fragments and, in some cases, ultramafic and mafic rocks in a matrix of plagioclase and quartz with gneissic texture. Greenman (1970) concluded that the gray breccia is post-Irruptive and has been intruded in a fluidized state shortly after the injection of the mafic sub-layer rocks.

2-3-3. Offset Rocks

There are five dike-like, steeply dipping, sulfide- and inclusion-bearing offsets that project away from the outer contact of the main Irruptive into the surrounding country rocks. Two occur along the north rim (the Foy offset and the Milnet mine offset) and three along the south rim (the Worthington offset, the Copper Cliff offset, and the Frood-Stobie offset) (see Fig. 2-8). The dominant rock type of the offsets is quartz diorite, a quartz-plagioclase rock with primary hornblende and biotite. They are generally finer-grained than the main Irruptive norite. Their inclusions are fragments of country rocks and mafic to ultramafic xenoliths. As in mafic sub-layer rocks, the sulfide content in the offset matrix may range from a few to one hundred percent. The amount of sulfide in the matrix, however, does not alter the proportions of the silicate minerals (Souch et al., 1969).

In the Frood mine disseminated sulfides occur as blebs in quartz diorite, sparsely distributed in the upper levels and becoming increasingly abundant downward where they gradually grade into inclusion massive sulfide ore, in the same pattern as in the mafic sub-layer ores (Fig. 2-9). The Copper Cliff offset ore bodies consist of a core of inclusion-bearing sulfide fringed by a zone of disseminated

inclusion-bearing quartz diorite: The ore zones grade into barren
or weakly mineralized quartz diorite over distances of several inches
to a few feet.

2-3-4. Sub-Layer Inclusions

A variety of inclusions of exotic rocks, ranging in size
from mineral grains to tens of feet in diameter, invariably occur in
sub-layer rocks. They are either angular pre-Irruptive country rock
fragments or a suite of subrounded mafic to ultramafic rocks differing
from any exposed rocks of the main Irruptive.

The mafic to ultramafic suite includes a wide range of
compositions varying from dunite, pyroxenite, and peridotite to olivine
gabbro and are generally barren in sulfides. They are commonly
olivine-bearing and often show poikilitic texture with large plagioclase
grains enclosing grains of pyroxene and olivine. Naldrett and Kullerud
(1967) have observed that the iron content of mafic minerals from
Strathcona mafic sub-layer inclusions has a positive correlation with the
proportion of felsic minerals in these inclusions. They also observed
that pyroxenes in these inclusions are generally more magnesian than
the pyroxenes of the host rocks and suggested that these inclusions may
have been derived from a cryptically layered, well-fractionated series
of olivine-bearing cumulus rocks.

Possible sources of these mafic and ultramafic inclusions include: (1) the same source as the Irruptive magma (i. e. the mantle); (2) some pre-Irruptive body of mafic and ultramafic rocks;and (3) ultramafic layers within the Irruptive itself.

2-4. The Country Rocks

Outside the basin, the Nickel Irruptive is surrounded by older rocks. To the north, the basin is bound by Superior Province rocks that consist essentially of granite and quartz-plagioclase-augite gneiss. To the south, a succession of metamorphosed volcanic and sedimentary rocks are overlain by Huronian greywackes and feldspathic quartzites. They are apparently conformable, facing southward, striking east-north-east, and dipping steeply to the north.

Inside the basin is the Whitewater Series with the Chelmsford sandstone occupying the center of the basin. The Chelmsford sandstone, a carbonaceous sub-greywacke, grades downward into the Onwatin slate. The Onwatin slate is a fine-grained, carbonaceous, pyritic argillite with local thinly laminated limestones and cherts. This in turn grades downward into the Onaping Formation which makes up the basal member of the Whitewater Series and rests directly on top of the Nickel Irruptive. The Whitewater rocks show no positive correlation with any rocks outside of the basin.

2-5. The Onaping Formation

The Onaping Formation lies at the base of the Whitewater Series and is about 2000 meters in thickness. It is a massive volume of almost unsorted breccia composed of fragments of various country rocks in a mainly dark, fine-grained matrix characterized by numerous shard-like fragments of devitrified glassy material. Detailed studies on the Onaping Formation can be found in Burrows and Rickaby (1929), Williams (1956), French (1968, 1970), Stevenson (1972), and Peredery (1972). Contact relations between the Onaping Formation and the top of the micropegmatite in the vicinity of Dowling township on the north range have been mapped in detail by Peredery (1972). The map and the localities of the samples used in the present study are shown in Fig. 2-9.

Peredery (1972) subdivided the Onaping Formation into four units: (1) the lowermost basal breccia, (2) the overlying gray Onaping, (3) the uppermost black Onaping, and (4) the melt rocks that occur at the top of the basal breccia and in the gray and black Onaping.

The basal breccia is in sharp contact with the micropegmatite and is intruded by it. It consists of rounded fragments of basement rocks, mainly metasedimentary, granitic, or gneissic, in a medium-grained variable matrix rich in plagioclase and quartz. The rock frag-

Fig. 2-9. Geological Map of the Onaping Formation and Part of

the Upper Micropegmatite in the Vicinity of the High Falls

(after Peredery, 1972)   showing Sample Locations.

LEGEND

+++	MICROPEGMATITE
▓	MELT
▲▲	BASAL BRECCIA
▼▲	GREY ONAPING
	BLACK ONAPING
╱	OBSERVED GEOLOGICAL CONTACT
╌╱	APPROXIMATE GEOL. CONTACT
╱╱	FRAGMENT TRENDS & MUD BODIES
⊥	SWAMP

-N-

1600 FEET

800

0

ONAPING RIVER

HWY 144

←— TO LEVACK

0-2C

0-2 D

0-2F

HIGH FALLS

TO SUDBURY

R R
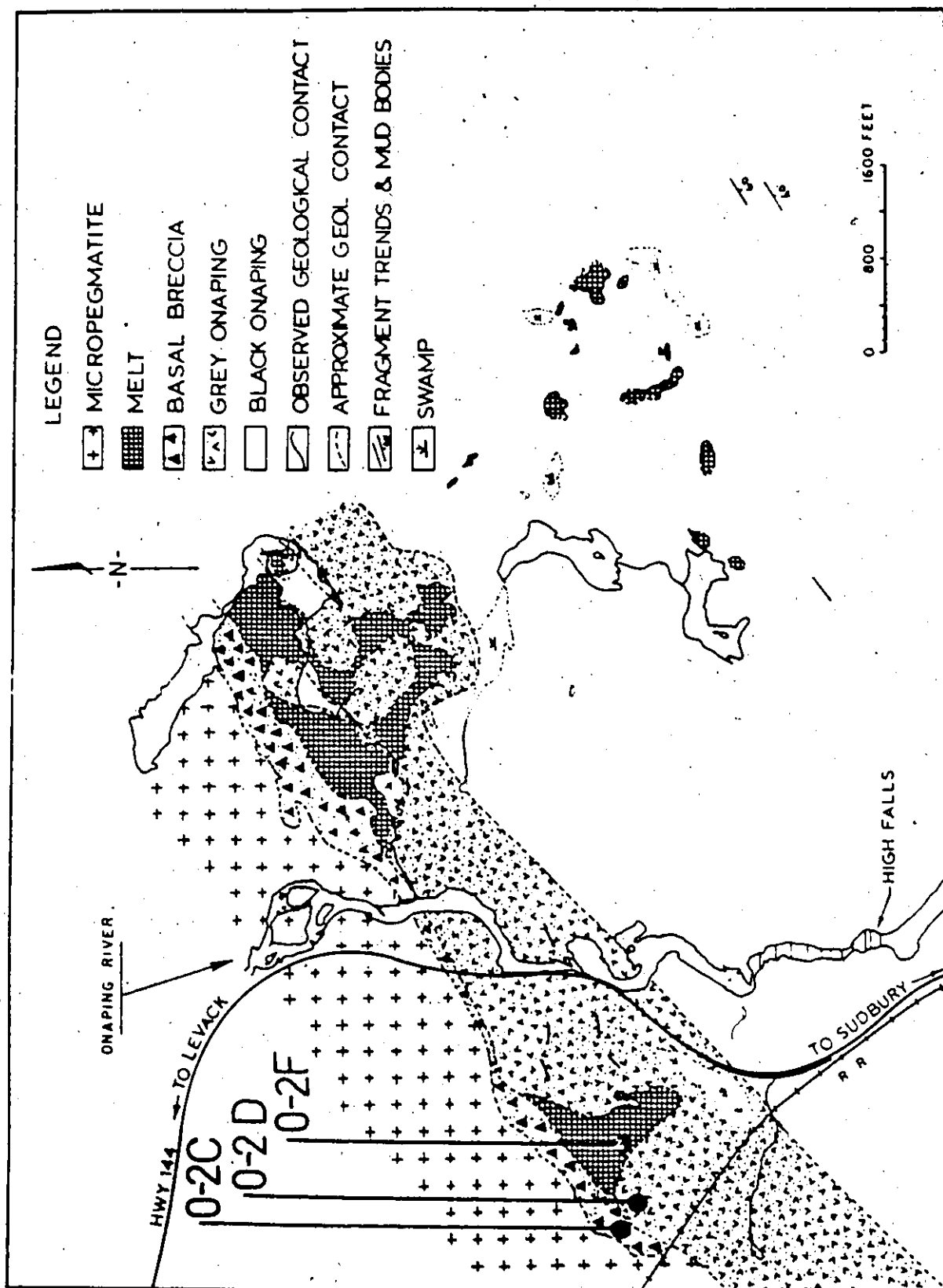
ments range in size from a fraction of an inch to about 100 meters in dimension. Their abundance by area is estimated to vary between 20 to 40 percent.

The gray and black Onaping contain three major components: country rock fragments, a variety of devitrified and recrystallized glasses, and a matrix rich in quartz, feldspar and glass shards. There is no clear evidence of stratification, although the size of the country rock fragments tend to decrease towards the top of the black Onaping. The black Onaping which makes up the majority of the Onaping Formation is characterized by the black color caused by the abundant carbonaceous material within its matrix.

The melt rocks occur as irregular masses on top of the basal breccia and projected into the overlying gray and black Onaping. They commonly show chilled contact relationships with the enclosing rock and contain abundant country rock fragments which are similar to those in the basal breccia and the gray and black Onaping rocks. Chemically they are relatively inhomogeneous and their composition ranges from rhyolite to trachyte.

Shock metamorphic features, such as planar texture in quartz and feldspar, can be found in country rock fragments in all of the above units (French, 1968).

2-5-1. Origin of the Onaping Formation

The origin of the Onaping Formation is critical in inter-

preting the Sudbury structure. Until recently, the Onaping Formation

has always been considered to be an unusual pyroclastic rock and has

been variously described as welded tuff, agglomerate, ash-flow, and

ignimbrite, etc. Dietz's (1964) suggestion that the Sudbury structure

was produced by meteorite impact led to suggestions that the Onaping

Formation is a country rock fallback breccia deposited immediately

after the meteorite impact.

I) Volcanic Ash-Flow Model:

Burrows and Rickaby (1929) concluded that the basal breccia

of the Onaping Formation was a rhyolite breccia and suggested that

fissure-type vents supplied the material because of the great lateral

extent and tremendous volume of the Formation. This model was later

supported by Thomson (1956), Williams (1956), Speers (1957), and

Stevenson (1972). They considered the Onaping Formation as rapidly

accumulated, welded, ash-flow deposits resulting from flowage of

pyroclastic material as a hot, turbulent mixture of gas and suspended

particles of viscous pumice and ash glass during the volcanic activity.

II) Meteorite Impact Model:

This school (Dietz, 1964; French, 1967; Peredery, 1972) suggests that the Onaping Formation represents the fallback breccias following a meteorite impact which created the Sudbury structure. In this view, the basal breccia represents the earliest fallback, or possibly, brecciated country rock in place. The gray Onaping, the true fallback, is as a mixture of shocked country rock and fluidal glass fragments in a matrix of pulverized country rocks. The black Onaping is a latter stage wash-in deposit derived from the impact fallback and the melt rock is the fusion product of country rocks produced during the impact. Their evidence lies in the fact that large chemical variability exists in both the Onaping glasses and the melt rock and in the presence of shock features in the country rock fragments associated with the Onaping Formation. The events that produced the Sudbury structure and the Onaping Formation during the meteorite impact are illustrated in Fig. 2-10 (after Peredery, 1972).

These two models suggest drastically different mechanisms of formation and imply that different parental materials are involved in the make-up of the Onaping Formation. The volcanic ash-flow model would suggest that the entire Onaping Formation is a mixture of essential-ly volcanic material and country rock fragments, whereas the meteorite
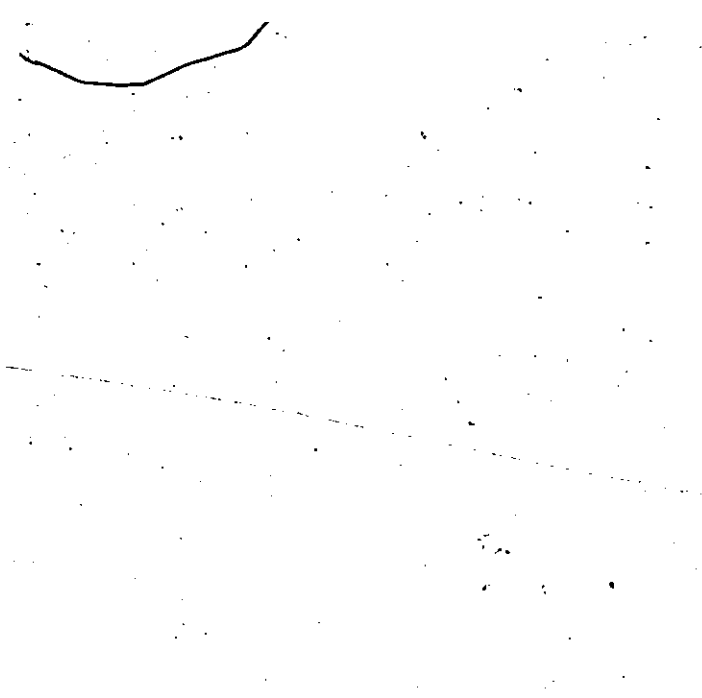
Fig. 2-10. Model for Formation of the Onaping Formation by

Meteorite Impact (after Peredery, 1972).

a. VAPORIZATION SHOCK COMPRESSION

MELT

WATER

ARCHEAN
BASEMENT

shocked
brecciated
fractured

HURONIAN
SEDIMENTS

b. DECOMPRESSION & EJECTION

c. FALL-BACK & WASH-IN

tsunami-like wave

black Onaping

present level
of erosion

basal breccia

melt   grey Onaping
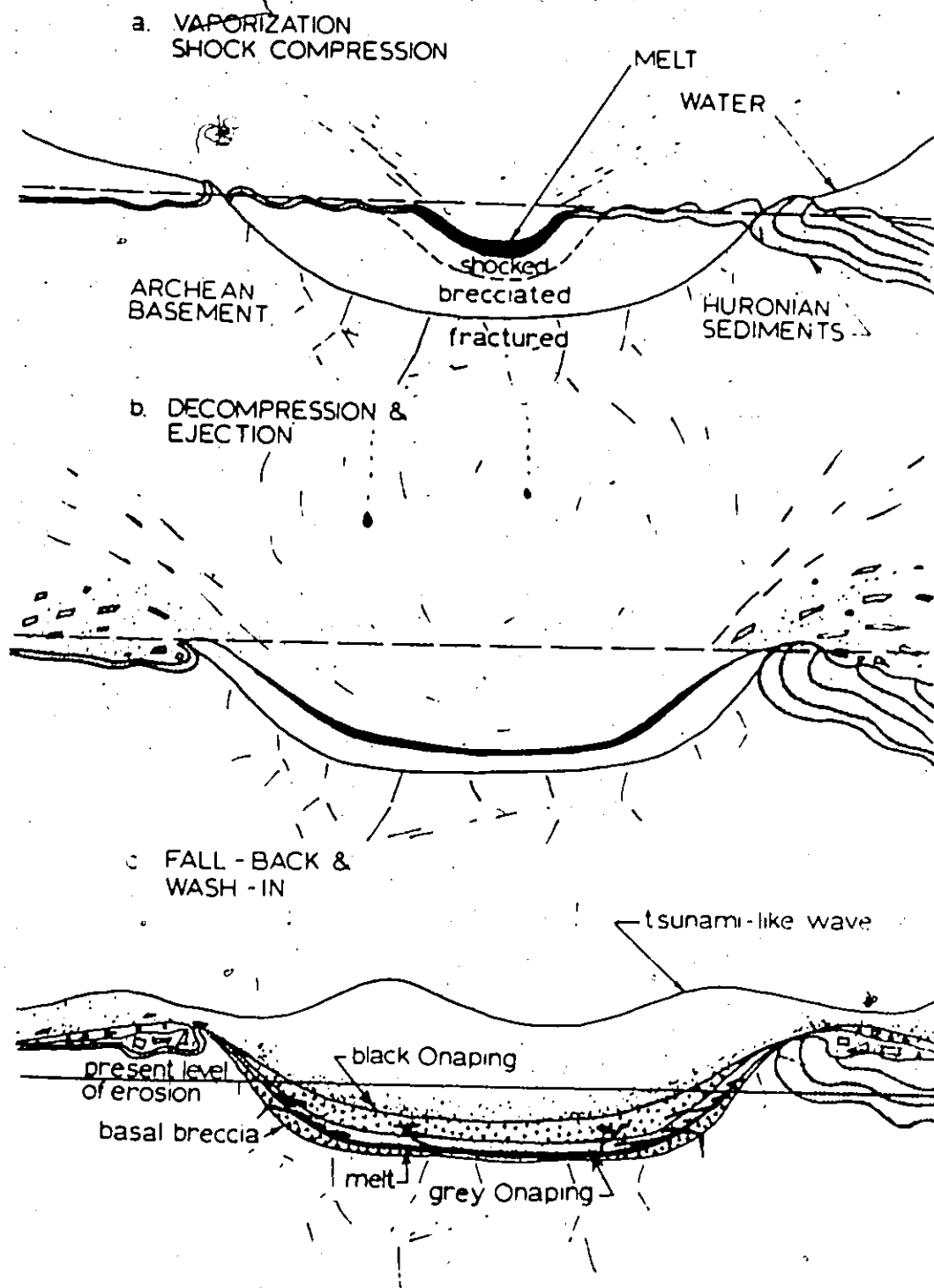
Diagramatic sketch of events producing the Sudbury crater and the Onaping Formation.

a) Hypervelocity impact of meteorite leading to vaporization of meteorite and a certain amount of country rock and water, and compression of the country rocks by shock wave.

b) Decompression and ejection of molten, shocked, and unshocked brecciated country rock. Main mass of the melt is blown along the crater floor and remains inside the crater forming a pool or pools of melt.

c) Fall-back of the ejecta into the crater. Later tsunami-like wave brings the fall-back from outside back into the crater. This latter process, or wash-in, accounts for the black Onaping and its carbonaceous matrix.

impact model would suggest the Onaping Formation as a mixture composed entirely of brecciated and melted country rocks.

2-6. Nature of the Sudbury Nickel Irruptive

The main Irruptive has been variously interpreted as the surface expression of (1) a folded, differentiated sill; (2) a ring-dike complex; and (3) a differentiated, funnel-shaped intrusion.

2-6-1. Folded Differentiated Sill Model

This model was first proposed by Walker (1897) to explain the upward gradation from norite to micropegmatite and was later supported by Coleman (1905, 1913), Collins (1934, 1935, 1936, 1937), and Hawley (1962). They suggested that the original Irruptive magma was intruded along the unconformity between the Whitewater Series and the underlying Archean and Huronian rocks as a single flat-lying sheet which differentiated into norite and micropegmatite by crystallization or liquation (Collins) in situ. The associated offsets are considered to represent fractures formed in the surrounding country rocks and filled with magma which had acquired a quartz diorite composition. The whole Irruptive was later folded into the present basin shape.

The presence of cryptic variation and phase layering in the main Irruptive tends to support this model. However, this model can not satisfactorily explain the contrast in detailed petrography and mineralogy between the north and south range rocks as well as the excessive volume ratio of micropegmatite to norite. According to the folded-sill model, the relative proportion of micropegmatite to norite in the sill as a whole should be similar to the proportions that appear on the surface, 3:1 on the north range and 1:1 on the south range. This is much higher than would have been expected from differentiation of an original gabbroic magma.

2-6-2. Ring-Dike Model

To explain the relative proportion of micropegmatite to norite, Knight (1917, 1923) proposed the multiple intrusion, ring-dike model. This was supported by Phemister (1925), Yates (1938, 1948), and Thomson (1956, 1969). They considered the Irruptive a multiple intrusion of first norite followed quickly by micropegmatite with formation of a hybrid zone between the two magmas. The composite Irruptive was intruded around the edges of a "ring-graben" following subsidence of the central basin, initiated by and subsequent to the Onaping volcanic activity. A genetic relation between the norite and micropegmatite, however, was considered probable as both may have stemmed from a layered magmatic reservoir at depth.

This model explains the relative volume proportion and the abrupt transition between the norite and micropegmatite and is supported by the very steep, even outward, dips of the main Irruptive at the south-west and southeast ends of the basin. The cryptic variation and phase layering in the main Irruptive and the parallelism of phase layering with the lower contact of the main Irruptive, however, provided a major problem for the ring-dike model.

2-6-3. Differentiated Funnel-Shaped Intrusion Model

Wilson (1956) first drew attention to similarities between the Sudbury Nickel Irruptive and the Bushveld complex and other lopoliths. He pointed out that the massive magnetite layers of the Bushveld have their counterpart in a broad but less well-defined magnetite-rich layer at Sudbury. Their inward dipping surfaces and crystal layering that dip inward at a more gentle angle than the footwall suggest a funnel-rather than a lens-shaped body. According to the funnel-shaped model, the presently exposed proportions of micropegmatite to norite are not necessarily a true representation of their actual relative volumes. This proposal accommodates the problem of the relative proportions of the major units of the main Irruptive which is the main argument for the multiple intrusion model.

Wilson (1956) further suggested that layered ultramafic members exist at deeper levels of the Nickel Irruptive. The observation of numerous ultramafic inclusions which occur in the sub-layer tends to support this proposal. Naldrett et al. (1970) studied the mostly olivine-bearing, sub-layer ultramafic inclusions and concluded that the siliceous nature of the main Irruptive could not have been directly responsible for these ultramafic inclusions. They suggested that the inclusions may have been derived from some deep-seated source chamber, where possibly an initial basic magma underwent some fractionation depositing the ultramafic layers before its siliceous residual liquid was intruded into the present site of the Irruptive.

2-7. Origin of the Sudbury Structure

The two main hypotheses on the origin of the Sudbury structure are the tectonic hypothesis and the meteorite impact hypothesis.

2-7-1. The Tectonic Hypothesis

This hypothesis considers the unique location of the Nickel Irruptive relative to the regional geologic setting. According to Speers (1956, 1957), the Irruptive lies at the apex of a broad dome some sixty miles in diameter involving Huronian and older rocks. Uplift of the dome occurred in response to pressure exerted by igneous magma. Successive periods of uplift followed by tensional release gave rise to the numerous

Fig. 2-11. Recent Version of Dietz's Meteorite Impact Model

for Formation of the Sudbury Structure (after

Dietz, 1972).
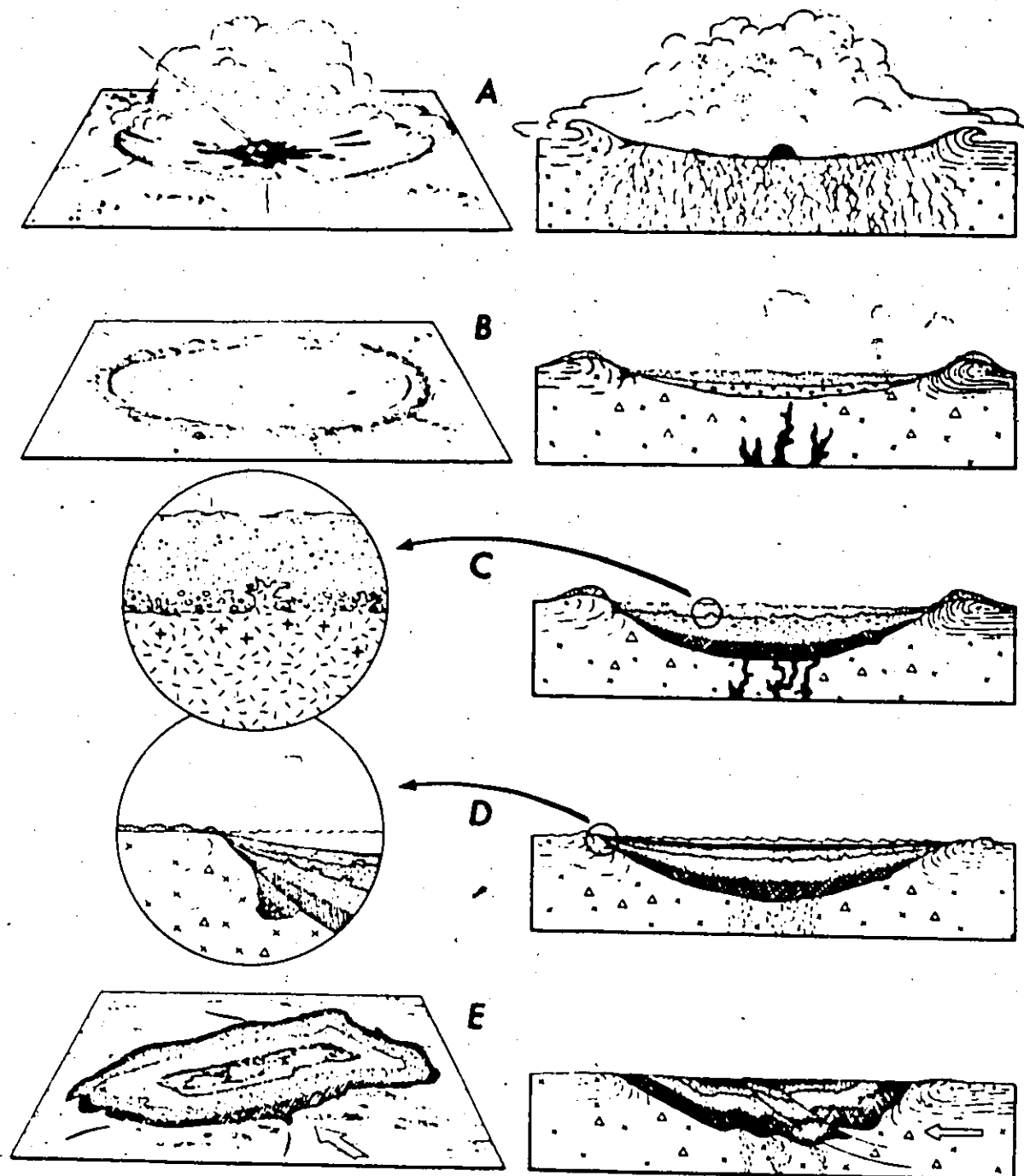
Development of the Sudbury Basin by asteroidal impact, a time-sequence diagram.
A. Asteroidal impact 1720 million years ago, producing a crater and radial tension cracks.
B. Laying down of the Onaping microbreccia as a fallout blanket or suevite. A pool of magma is also generated from the target rocks.
C. Ascent of the Sudbury Irruptive as an impact-triggered magma from the deep crust. The shock-generated melt rock is incorporated into the micropegmatite. The Irruptive differentiates with micropegmatite above and norite below. Apophyses of micropegmatite invade the overlying Onaping suevite. Emplacement of Irruptive is accompanied by foundering.
D. The Whitewater sediments (Chelmsford Formation) are laid down as a greywacke deposit in the Sudbury Basin. Detailed sketch shows sulphide deposit emplaced as an impact splash in footwall along with breccia and noritic matrix.
E. Geologic situation today after distortion by Grenville orogeny and erosional deleveling.

breccias in the area and finally resulted in caldera collapse at the apex

of the dome. Magma escaping around the rim of the caldera flowed

into the center of collapse to produce the Onaping Formation. The

Nickel Irruptive was intruded subsequently along the base of the Onaping

Formation. Thus, the Nickel Irruptive is a later plutonic manifestation

of the igneous activity that gave rise to the extrusive Onaping Formation.

2-7-2. The Meteorite Impact Hypothesis

Dietz (1964) first proposed that the Sudbury structure is the

result of an explosive meteorite impact. Subsequent discoveries of

shatter cones in country rocks by Dietz himself and microscopic shock

metamorphic features in the Onaping Formation and footwall rocks by

French (1967, 1968), both features typical of meteorite impact, add

strong supporting evidence for this hypothesis. The sequence of events

according to the most recent version of Dietz's meteorite impact

hypothesis (1972) are illustrated in Fig. 2-11.

2-8. Model for the History of the Sudbury Nickel Irruptive

Naldrett et al. (1967, 1970, 1972) combined their detailed

petrographic and mineralogical studies with the meteoritic impact theory

and the funnel-shaped intrusion model to derive a relatively complete

emplacement and crystallization history of the Sudbury Nickel Irruptive

in order to explain as many as possible of the characteristics of the /

Irruptive. Their model is illustrated in Fig. 2-12. An outline of the

regional geological history of Sudbury (Brocoum and Dalziel, 1974)

is listed in Appendix B.

Fig. 2-12. Model for Formation of the Sudbury Nickel Irruptive

According to Naldrett et al. (1970).

45

A

S

Quartz-rich Norite

South Range Norite

Felsic Norite Liquid

Accumulation in Progress

N

AFTER INTRUSION
AND ACCUMULATION
OF SOUTH RANGE NORITE

B

S

Granophyric Liquid

Upper Gabbro

Quartz-rich Norite

South Range Norite

Oxide-rich Gabbro

Felsic Norite

N

AFTER CRYSTALLIZATION
OF OXIDE - RICH
AND UPPER GABBROS

C

S

Micropegmatite

Quartz-rich Norite

South Range Norite

Felsic Norite

N

AFTER CRYSTALLIZATION
OF THE WHOLE IRRUPTIVE

D

S

Micropegmatite

present surface

Quartz-rich Norite

South Range Norite

Felsic Norite

N

AFTER FOLDING
AND FAULTING

Chelmsford SST

Onwatin Slate

Onaping Formation

SCALE IN MILES

CHAPTER THREE

NEUTRON ACTIVATION ANALYSIS

3-1. Introduction

Neutron activation analysis for REE in geological samples was first performed by Schmitt et al. (1960), Haskin and Gehl (1962), and Chase et al. (1963). High accuracy and precision can be achieved by separation of the individual REE from each other via an ion exchange procedure prior to beta or gamma radioassay (Mosen et al., 1961; Massart and Hoste, 1967; Haskin et al., 1968). This method can yield results for most or all of the REE. However, the ion-exchange procedure is quite time-consuming. The development of high resolution Ge(Li) detectors allowed group separation of the REE from the rock matrix and radioassay of a single, composite gamma-spectrum. This greatly reduces the time required for chemical processing of the samples.

A number of different procedures for the separation of REE as a group from rock samples have been published recently (Tomura et al., 1968; Morrison et al., 1969; Graber et al., 1970; Melsom, 1970; Denechaud et al., 1970). The procedures used in the present work were mainly based on those of Denechaud et al. (1970) with some modifications.

46

The conventional hydroxide-fluoride precipitation method was adopted to separate and purify the REE as a group. In the final stage the REE were precipitated as a hydroxide paste rather than oxalates.

3-2. Sample Preparation

For whole rock samples, several hundred grams of chips of representative fresh rock were broken off a large handspecimen and cleaned with acetone before crushing. For north range main Irruptive samples, sections of diamond drill core about 10 cm long and 4 cm in diameter were obtained from Strathcona core M-9 at different intervals. These sections were broken into small chips and cleaned with acetone prior to crushing. The cleaned sample chips were pulverized by repeated crushing with a tungsten carbide shatterbox and finally ground in an agate mortar to pass a 200-mesh nylon bolting cloth. The powder was homogenized and stored in a clean polyethylene bottle.

A number of sub-layer handspecimens contain up to 50 percent disseminated sulfide blebs. In these cases, rocks were broken into pieces about 1 cm in each dimension, and chips with no visible sulfide content were handpicked to be pulverized. Although no analytical data are available, sulfide minerals are believed to have RE contents much lower

than silicate minerals because of the very strong lithophile character of the REE. The presence of a small amount of sulfide in a silicate sample will cause a diluting factor on the absolute RE content but will have little effect on the normalized RE fractionation pattern of the sample.

3-3. Standard and Carrier Preparations

Stock solutions of nitrates of each of the REE, except Ce, were made from "specpure" RE oxides of greater than 99.9 percent purity (Johnson Matthey and Company). The concentration is approximately 10 mg of each RE ion per ml. Because of the difficulty in dissolving cerium oxide (CeO_2), cerium ammonium nitrate (primary standard, G. F. Smith Chemical Company) was used to make up the cerium stock solution. Each stock solution was standardized by EDTA titration (Cheng, 1958; Haskin et al., 1968).

Since the majority of the samples analyzed in this study were basic to ultrabasic igneous rocks, a combined standard solution was prepared by mixing appropriately diluted solutions so that the relative abundances of the REE in the standard monitor was similar to that of average basic igneous rocks. A composite REE carrier solution was prepared in the same manner as the standard solution.

The concentrations of REE in the standard and carrier solutions are listed in Table 3-1.

Table 3-1.   Concentrations of REE in the standard and carrier
solutions

Element	Standard Solution (ppm)	Carrier Solution (mg/g)
La	22.9	1.08
Ce	55.8	0.462
Pr	8.53	0.501
Nd	31.7	0.241
Sm	7.22	1.04
Eu	4.22	1.15
Gd	7.25	0.346
Tb	2.82	1.20
Dy	13.9	0.158
Ho	2.32	0.423
Er	4.71	0.605
Tm	1.03	0.315
Yb	7.26	1.19
Lu	0.930	1.41
Y	---	0.522

3-4. Yttrium Tracer Preparation

In this work 106.6 day ^{88}Y was used as a tracer for absolute chemical yield determinations. ^{88}Y was used because it is similar to the REE (especially Dy) in chemical behaviour, has a long half-life, and photopeaks which do not interfere with those of the RE nuclides.

^{88}Y tracer solution was prepared by dilution of a commercially available ^{88}Y concentrate (Amersham/Searle, catalog No. YEY72) with distilled water such that a 200-minute count on a 7.6 cm x 7.6 cm well-type NaI detector gave about 15,000 counts above background in the 1.836 MeV ^{88}Y photopeak area.

3-5. Irradiation

About 200 mg of sample were weighed into a labelled 3 mm O.D. x 2 mm I.D. fused quartz ampoule and heat sealed for irradiations. The ampoules were precleaned by boiling in aqua regia and rinsing with distilled water.

The monitor standard was prepared by weighing 30 to 100 mg of the REE standard solution into a quartz ampoule. The amount of the standard solution used depends on the estimated RE concentration level of the samples. It was chosen such that the induced RE radioactivies in the monitor and samples would be of the same order of magni-

tude. An adequate amount of cleaned, medium-grained quartz powder (prepared by grinding pure quartz tubes in an agate mortar and cleaned with aqua regia) was added into the ampoule to just absorb the solution. Ampoules were then dried in an oven set at 65°C and heat sealed.

Six to eight samples and two standard ampoules were taped together and placed in an aluminum can for each irradiation. Depending on the estimated RE concentration level in the samples, irradiation times of 5 to 20 hours in a high flux position in the McMaster Nuclear Reactor (neutron flux of 4.5 x 10^{13} neutrons/cm^2/sec.) were used, followed by 2 to 3 days cooling before chemical processing.

3-6. Chemical Procedure

The irradiated samples were decomposed by alkaline fusion and the REE were separated and purified as a group in the form of RE hydroxides for radioassay with a Ge(Li) detector. A non-radioactive REE carrier was used. The chemical yield of each REE was determined by re-irradiation of part of the recovered carrier using a ^{88}Y radioactive tracer technique.

3-6-1. Sample Procedure

1) Prior to receiving the irradiated samples, add 3 ml of the REE carrier solution and 3 ml of the ^{88}Y tracer solution to a clean 40 ml zirconium crucible. Add identical amounts of the carrier and tracer solutions to a 150 ml beaker, which will receive the standard monitor.

2) Add about 50 mg of reagent grade NaCl to the crubible
Evaporate the solution in the crucible to dryness under a heat
lamp and then heat to about 150°C on a hot plate and allow to cool
about one hour before the start of the fusion. Spattering occurs
during the fusion if water is retained in the NaCl. The addition
of NaCl helps mechanical mixing of sample and carrier before
fusion.

3) Cover the bottom of the crucible with about 5 g of sodium
peroxide.

4) Wipe the outside wall of the quartz ampoule containing
the sample, clean with 2M HCl. Carefully open the ampoule and
transfer the irradiated sample into the crucible and cover with
another 5 g of sodium peroxide.

5) Mix the contents of the crucible by careful stirring with
a nickel steel spatula. Then melt slowly over a Meeker burner.
When complete melting is obtained, increase the flame to keep
completely molten (cherry red) for about two minutes. Swirl
occasionally to ensure complete mixing of the melt.

6) Allow the crucible to cool to near room temperature,
then place the crucible on its side in a 400 ml beaker. Put the
crucible lid and the spatula in the same beaker.

7) Slowly add about 80 ml H_2O to the beaker to digest the fusion cake. Cover the beaker quickly with a watch glass to contain the vigorous reaction.

8) When reaction ceases, slowly add about 30 ml of conc. HCl to the beaker and cover again with the watch glass. Stir occasionally until all the fusion cake is dissolved. Add more conc. HCl if necessary.

9) Heat the solution to boiling on a hot plate until clear. Remove the crucible, lid and spatula from the beaker and rinse the adhering solution into the beaker with 6M HCl. The final volume should be around 150 ml.

10) Cool the beaker to room temperature by placing in an ice bath. Dissolve about 15 g of solid NH_4Cl in the solution and add conc. NH_4OH with constant stirring to adjust the pH to 9 or greater to precipitate the hydroxides. One can usually achieve this pH by measuring the volume of the solution when permanent traces of the precipitate first appear and then adding an additional amount of NH_4OH equal to 10 percent of this volume.

11) Allow the contents to age for two minutes and then centrifuge the hydroxides into a 50 ml polycarbonate centrifuge tube. Discard the supernate into the radioactive waste.

12) Wash the precipitate with 40 ml diluted NH_4OH, centrifuge and discard the supernate.

13) Dissolve the hydroxides in 15 ml 6M HCl and precipitate the fluorides by adding 5 ml conc. HF. Centrifuge and discard the supernate.

14) Wash the fluorides with 20 ml water, centrifuge and discard the supernate.

15) Dissolve the fluorides in 10 ml of 2M HCl saturated with boric acid. Stir the contents and warm the tube in a water bath to hasten dissolution.

16) Add sufficient 16M NaOH with constant stirring to adjust the pH to 10-11 and precipitate the hydroxides. Centrifuge out the hydroxides and discard the supernate which contains mostly Al.

17) Wash the precipitate twice with 30 ml water and discard the washings.

18) Repeat steps 13, 14, and 15.

19) Add conc. NH_4OH with stirring until the pH is 9 or greater in order to precipitate the RE hydroxides.

20) Centrifuge and discard the supernate. Wash with 30 ml water and discard the washing.

21) Dissolve the RE hydroxides with 5 ml 6M HCl. Pre-
cipitate the RE fluorides by adding about 10 ml saturated ammonium
fluoride solution and 5 ml conc. HF. Adjust the pH of the solution
to about 5 by adding the conc. HF drop by drop with constant
stirring. This removes most of the scandium remaining up to
this stage. As in a buffered NH_3 solution at pH 5, RE fluorides
will precipitate quantitatively while most of the Sc will form
ScF_6^{-3} complex and remains in the solution (Moeller and Kremers, 1945).

22) Centrifuge out the RE fluorides and discard the supernate.

23) Repeat steps 14, 15, 19, and 20.

24) Transfer the RE hydroxides to a 50 ml glass centrifuge
tube. Wash with 30 ml water, centrifuge and discard the supernate.

25) Wash the precipitate with 30 ml methyl alcohol. Use a
capillary pipette to break up the precipitate, centrifuge and discard
the supernatant.

26) Add 2 ml methyl alcohol. Use a capillary pipette to
break up and transfer the precipitate to a 4 dram glass vial.

27) Cap the vial and carefully transfer to a 50 ml poly-
carbonate centrifuge tube. Use a wool plug at the bottom of the tube
to ensure that the vial sits vertically inside the tube.

28) Centrifuge for one minute, remove the vial from the tube and carefully remove the supernate in the vial with a capillary pipet.

29) Dry the RE hydroxide precipitate under a heat lamp until the precipitate hardens. Do not overdry, otherwise the hydroxide cake will easily crack. ,

30) Steps 28 and 29 should be carefully controlled in order to achieve identical counting geometry for all samples.

31) After drying, the vial should be capped and sealed with masking tape to prevent evaporation and cracking of the hydroxide cake over the counting period.

3-6-2. <u>Standard Procedure</u>

1) Carefully clean the outside wall of the standard ampoule with acetone and 2M HCl.

2) Open the ampoule and transfer the contents into a 150 ml beaker. Break the ampoule in half and add to the beaker.

3) Add 10 ml 2M HCl, cover the beaker with a watch glass and warm on a hot plate for about 15 minutes to equilibrate the carrier and tracer solutions with the standard. Occasionally wash the inside of the ampoule with the carrier and tracer solutions.

4) Filter the solution in a 50 ml glass centrifuge tube.

5) Repeat step 3.

6) Filter the contents of the beaker in the same tube as in step 4. Rinse the filter paper several times with 2M HCl.

7) Add sufficient conc. NH_4OH to bring the pH to 9 or greater and to precipitate the RE hydroxides. Centrifuge and discard the supernate.

8) Use a capillary pipette to break up the precipitate, wash twice with 30 ml water, once with 30 ml methyl alcohol, centrifuge and discard the supernate.

9) Add 2 ml methyl alcohol. Using a capillary pipette to break up and transfer the precipitate to a 4 dram glass vial.

10) Centrifuge and dry the RE hydroxide precipitate to form a cake of uniform thickness in the same manner as in steps 27 to 31 of the sample procedure.

3-7. Gamma-Ray Activity Measurement

3-7-1. Instrumentation

The gamma spectrometer system used in this study consists of:

1) A Canberra model 7245, 130 gm coaxial Ge(Li) detector with 7.2 cm^2 active area facing the window;

2) a Canberra model 3002 high voltage supply for the detector;

3) a Canberra model 14081C FET low noise preamplifier;

4) a Canberra model 1416 spectroscopy amplifier;

5) a 1600 channel RIDL pulse height analyzer (analog to digital

converter and memory unit);

6) a Hewlett-Packard display oscilloscope and a Telex teletype

print-out.

The energy resolution of the system is 3.4 KeV for the

1.333 MeV photopeak of ^{60}Co at FWHM (Full Width at Half Maximum).

A 7.6 cm x 7.6 cm well-type NaI detector connected to the

above system was used for measuring the 1.836 MeV photopeak activity

of the ^{88}Y tracer.

3-7-2. Counting Procedure and Gamma-Ray Spectrometry

Because of the different half-lives of the individual RE

isotopes, three counting periods at intervals of 3, 10 and 40 days after

the irradiation are required to obtain optimum results. The counting

sequence, the starting time following irradiation, the isotope observed,

the energies of the gamma-rays and other information pertaining to radio-

assay are summarized in Table 3-2. Nuclear parameters are taken from

the General Electric Chart of the Nuclides, 11th edition, 1973.

The photopeaks used in calculation of elemental concentrations are underlined in Table 3-2. Essentially the same photopeaks are used in chemical yield determinations on the re-irradiated carriers. They were chosen on a basis of optimum counting statistics and/or minimum interference from other RE nuclides. Mutual interferences among individual RE photopeaks are noted in the comments included in Table 3-2.

The counting vials were placed on a sample holder rack mounted above the Ge(Li) detector, and the distance between the vial and the detector was adjusted in each count set to optimize counting statistics and counting time. Usually, 30 minutes at 10 cm in count set I and 1 to 3 hours at about 1 cm above the detector in count sets II and III were satisfactory. Following count set III samples and standards were counted in a 7.6 x 7.6 cm well-type NaI(Tl) detector for a sufficient time to obtain about 15,000 counts above background for the 1.836 MeV photopeak of ^{88}Y. Usually, 200 minutes were sufficient. The dead time for all counting sets was kept below 20%.

The RE nuclides listed in Table 3-2 are those determined in the majority of samples, and counting periods at intervals of 3, 10 and 40 days following irradiation were routinely used in their determinations. In the initial phases of the study the feasibility of measuring 2.35 ^{165}Dy and 7.52 hr ^{171}Er by counting within half-a-day after the end of irradiation was investigated. In the case of Dy the rather short half-life was un-

favourable.   Rapid processing of samples and the handling of rather high radiation levels were required to obtain adequate counting statistics. In general, the intensity of ^{165}Dy photopeaks was too low to permit quantitative measurement and Dy was not determined in this study. In the case of Er the 0.3084 MeV photopeak of 7.52 hr ^{171}Er is observed by counting within one day after the end of irradiation. However, its intensity is low and it is located on the relatively high Compton tail from 9.3 hr ^{152m}Eu. The weak intensity, short half-life and high base-line uncertainty rendered the determination of Er too unreliable for routine measurement.

In count set III the 0.08426 MeV photopeak of ^{170}Tm usually appears as a shoulder on the ^{160}Tb peak at 0.08679 MeV. An approximate value for Tm can be obtained by stripping the ^{160}Tb peak. Due to the high uncertainty involved, Tm is not reported.

It should be noted that other REE appear in the various count sets in addition to those noted in Table 3-2. In count set II ^{140}La, ^{160}Tb and ^{177}Lu are present in addition to ^{147}Nd and ^{175}Yb which are the two nuclides measured. In count set III ^{169}Yb is also present as well as the four other REE measured.

Table 3-2. Counting Procedure and Nuclear Properties Pertaining to Activation Analysis of Rare Earth Elements

Count Set	Decay Time (days)	Nuclide Counted	Half-Life	Isotopic Abundance of Target Nuclide, %	Cross-Section (barns)	Principal Gamma Rays, MeV	Interferences, Sensitivities, Comments
I	3	^{140}La	40.23 h	99.91	9.6	0.3288, 0.4870, 0.8158, 1.5962	The 0.4870 MeV peak is free of interference and gives the best counting statistics in this set.
		^{153}Sm	46.5 h	26.72	210	0.06968, 0.1032	241.5 day ^{153}Gd also has a photopeak at 0.1032 MeV, but its intensity is negligible compared with ^{153}Sm in count set II.
II	10	^{177}Lu	6.71 d	2.59	2100	0.1130, 0.2084	Both the 0.1982 MeV peak of 31 day ^{169}Yb and the 0.2156 MeV peak of 72.3 day ^{160}Tb contribute to uncertainty in the baseline of ^{177}Lu.
		^{147}Nd	10.99 d	17.22	1.3	0.0911, 0.5310	The 0.5310 MeV peak is free from interference but is usually of weak intensity. High statistical uncertainty is often inherent in Nd determination.
		^{175}Yb	4.19 d	31.84	65	0.1138, 0.2825, 0.3963	The 0.3963 MeV peak is free of interference from other REE.
III	40	^{141}Ce	32.53 d	88.48	0.54	0.1454	Some interference from the 0.1488 NeV peak of ^{175}Yb occurs. It is minimal in count set III.
		^{152}Eu	12.7 y	47.82	5700	0.1218, 0.2446, 0.7789, 0.3443, 0.9642, 1.0860	This peak is free of interference and provides the best sensitivity of the various Eu photopeaks.
		^{153}Gd	241.5 d	0.200	125	0.06968, 0.09743, 0.1032	There is interference from the 0.0936 MeV peak of ^{169}Yb which causes uncertainty in baseline assignment. Analytical uncertainty for Gd is high.
		^{160}Tb	72.3 d	100	30	0.08679, 0.2986, 0.8794, 0.9662	May suffer interference from the 0.2958 MeV peak of 12.7 year ^{152}Eu.
IV	50	^{88}Y	106.6 d			0.8980, 1.8360	

Gamma photopeak used for abundance calculations.

61

3-8. Calculations

3-8-1. Net Peak Area Calculation

The intensity of the radioactivity of a nuclide can be re-presented by the net peak area corresponding to one of its gamma-ray peaks, where the net peak area is the total peak area minus the back-ground area. In a complex RE spectrum, the photopeak baseline which is largely generated by the Compton effects from gamma-rays at higher energies must be determined accurately.

To establish the baseline, a smooth curve was first drawn through the data points (counts per channel versus channel number) from the region of the spectrum containing the photopeak of interest. A straight line was then drawn between the bottom of the valleys on either side of the peak. Approximately ten channels on each side of the photopeak were used to define the bottom of the valleys. The value of the baseline at the photopeak maximum was thus determined graphical-ly.

The net peak area was calculated by summing a selected number of channels on either side of the photopeak maximum and sub-tracting the background area calculated as the product of the counts in the median baseline channel times the number of channels summed. In most instances, the number of channels integrated was that corres-ponding to the FWHM. However, if the peak to background ratio was

low channels in the full peak area were summed. Alternatively, if interference from an adjacent photopeak was prominent, only a few channels about the photopeak maximum were summed to minimize the effects of uncertainties in the baseline and photopeak overlapping. Whichever method was used, samples and standards were always treated in the same manner.

3-8-2. Chemical Yield Calculation

As demonstrated by Denechaud et al. (1970), the fractional re-coveries of individual REE are not always equal. Therefore, chemical yields for individual REE in all samples and standards were determined. The calculation of the absolute chemical yield for each REE required deter-mination of the relative chemical yield for the element and the ^{88}Y yield for the sample.

The relative chemical yields for the REE were determined by re-irradiation of a portion of the recovered RE carrier. After completion of all the counting sets, the recovered carrier was re-irradiated according to the following procedure:

1) Take the RE hydroxide cake into solution by addition of 5 ml 2M HCl to each sample and standard counting vial.

2) Transfer an aliquot of approximately 200 mg into a quartz ampoule.

3) Place the ampoule in an oven and evaporate to dryness at 65°C; then heat seal the ampoule.

4) Irradiate fractions of sample and standard carrier, prepared as above, at a total neutron flux equal to that received by the sample in the original irradiation. The residual activities from the first irradiation will be negligible compared to the radioactivities induced in the second irradiation.

5) After seven to eight days decay, transfer the irradiated carrier from the ampoule into a one-dram vial with 2M HCl.

6) Count on a Ge(Li) detector for about two hours.

The aliquots of carrier solution used for yield determination were not weighed nor were their counting geometries made identical, because the purpose of this re-irradiation was to obtain the relative activities of individual REE in each sample. The photopeaks used for the relative chemical yield determinations are given in Table 3-2.

The relative chemical yield (Y') for an individual REE (R) is defined as:

$$Y'(R) = A'_s / A'_m \cdot \left((G'_c + G'_m) / (G'_c + G'_s) \right) \quad \ldots \qquad 3\text{-}1$$

where A'_s = activity of the re-irradiated R carrier in the sample,

A'_m = activity of the re-irradiated R carrier in the standard monitor

G'_c = weight of R in the carrier added to the sample and standard

G'_s = weight of R in the sample

G'_m = weight of R in the standard monitor.

As long as the weight difference between R in the sample and in the standard is small, the second ratio in equation 3-1 can be taken as unity. Thus,

$$Y'(R) = A'_s / A'_m \qquad 3\text{-}2$$

The relative chemical yields for La, Sm, Eu, Tb, Yb and Lu were obtained in this way by comparing their activities in irradiated sample and standard carrier aliquots. The relative chemical yields for other REE were obtained by interpolation from a graph of relative chemical yield versus REE atomic number for La, Sm, Eu, Tb, Yb and Lu.

The absolute chemical yield for each REE was then calculated as follows:

1) Assume that the absolute chemical yield for Dy is identical to that for the ^{88}Y tracer of the same sample.

2) Calculate a conversion factor by dividing the absolute chemical yield for Dy by the relative chemical yield for Dy.

3) Calculate the absolute chemical yield for each of the other REE by multiplying the relative chemical yields by the conversion factor derived in step (2).

This calculation assumes that the absolute chemical yield of Dy is identical to that of the ^{88}Y tracer because the ionic radius of Y is similar to that of Dy and its chemical behaviour is very close to that of the heavy REE. The use of ^{88}Y tracer greatly simplifies the carrier re-irradiation procedure but introduces a systematic un- certainty of up to one percent for each REE. This uncertainty can be ignored when relative RE abundances, for example chondrite normalized abundances, are compared from sample to sample (Denechaud et al., 1970).

If an ^{88}Y tracer technique is not used, one can obtain absolute chemical yields by weighing the re-dissolved carrier solution and the aliquot of solution taken for re-irradiation and applying a simple algebraic mass conversion.

3-8-3. Elemental Concentration Calculation

The activity of an element in the sample, after correction for counting duration and radioactive decay, was compared with that in the standard monitor and the concentration of the element calculated as follows:

$$C_s = (A_s/A_m) \cdot (W_m/W_s) \cdot (C_m/Y) \qquad \dots \qquad 3\text{-}3$$

where C_s = concentration of the element in the sample in ppm

C_m = concentration of the element in the standard monitor in ppm,

A_s = activity in counts per unit time for the sample

A_m = activity in counts per unit time for the standard monitor

W_s = weight of the sample in grams

W_m = weight of the standard monitor in grams

Y = absolute chemical yield for the element.

3-9. Precision and Accuracy

The major factors that affect the precision and accuracy of REE activation analysis are variation in neutron flux, counting geometry, sample inhomogeneity, uncertainty in employing ^{88}Y tracer, and uncertainty in photopeak integration. The first two factors impose similar degrees of uncertainty on all REE. The last three factors, however, may impose different degrees of uncertainty on individual REE.

In this work, the precision was governed largely by photopeak integration uncertainty; that is, error due to counting statistics and baseline placement. Thus, the elements with poorer precision (Nd, Gd in Table 3-3) are those with which poor counting statistics and high baseline uncertainty are normally associated. The total uncertainty due to counting statistics in most of the Sudbury samples is at least ±3% for Ce, Sm, Eu and Tb and ±5% for La, Yb and Lu.

The precision and accuracy of the analytical procedure used in this study can be evaluated by replicate analyses of the U.S.G.S. standard rock BCR-1. The results (Dostal, 1973 and this work) are shown in Table 3-3.

3-10. Sensitivity

Sensitivity is the minimum amount of an element that can be detected by a given analytical method. Theoretically, for neutron activation analysis, one can achieve very high sensitivity by adjusting the irradiation, analytical and counting parameters to optimum conditions for each experiment. Practically, however, there are various limitations to these adjustments and often a minimum precision is required for quantitative determinations. Therefore, "detection limit" is a more practical concept. A detection limit is defined in this work as the minimum concentration of an element that will produce, during a specific

Table 3-3. Comparison of Rare Earth Abundances (ppm) for U.S.G.S. Standard Rock BCR-1 Determined by Different Methods

	Dostal (1973) and this Work		RNAA[2,3,4,5,6]	INAA[7,8]	IDMS[9,10]	U.S.G.S. Recommended Value[11]
	Average[1]	% standard deviation (1)				
La	26.7	8.2	25.0	23.4	26.1	26
Ce	54.5	5.1	52.8	46	54.4	53.9
Nd	32.0	15	28.7	33	30.5	29
Sm	7.21	4.7	6.8	6.7	7.09	6.6
Eu	2.06	4.4	1.94	1.89	1.95	1.94
Gd	7.2	21	7.7	-	6.47	6.6
Tb	1.08	4.6	1.03	1.0	-	1.0
Yb	3.38	6.2	3.2	3.3	3.53	3.36
Lu	0.514	8.8	0.41	0.60	0.56	0.55

RNAA: Radiochemical Neutron Activation Analysis. INAA: Instrumental Neutron Activation Analysis.
IDMS: Isotope Dilution Mass Spectrometry.

1: average of 10 samples except for Nd and Gd which are averages of 3 samples (Dostal, 1973 and this Work).
2: average of data of 6 different analysts from Dr. Haskin's laboratory (Kosiewicz, 1973).

3: Rey et al., 1970.
4: Ragland et al., 1971.
5: Green et al., 1972.
6: Culler et al., 1974.
7: Gordon et al., 1968.
8: Randle, 1974.
9: Philpotts and Schnetzler, 1970.
10: Gast et al., 1970.
11: Flanagan, 1973.

counting period and under specific experimental conditions, a net

photopeak activity twice the square root of the background activity.

The detection limit of an element can therefore be expressed

as:

$$C = \frac{A \cdot e^{\lambda d} \cdot M}{\phi \cdot \delta \cdot (1-e^{-\lambda T}) \cdot W \cdot N \cdot f \cdot \delta \cdot Y \cdot 10^9} \qquad \cdots \qquad 3\text{-}4$$

where   C = detection limit (ppb)

A = minimum detectable activity at time of counting

$e^{\lambda d}$ = decay from end of irradiation

M = atomic weight of the target element

ϕ = thermal neutron flux (neutrons/cm^2/sec)

δ = (n, γ) reaction cross section of the target nucleus (barns)

$(1-e^{-\lambda T})$ = saturation factor for an irradiation time T

W = sample weight (gm)

N = Avogadro's Number (6. 023 x 10^{23} atoms/mole)

f = isotopic abundance of the target nucleus

δ = overall counting efficiency of the detector

Y = chemical yield of the element

Under normal experimental conditions all these parameters

are fixed except W, d and T (sample weight, decay time and irradiation

time, respectively), which may vary within limited ranges. Thus, if

one suspects that the element concentration is low, it is generally
possible to improve the detection limit somewhat by increasing the
sample weight (W), the irradiation time (T), and decreasing the decay
time (d).

The situation is further complicated because the REE are
counted as a group so that photopeaks from more than one RE isotope
occur in the same spectrum. High Compton background from high
energy gamma-rays will be imposed upon photopeaks in the low energy
region thereby increasing the background in this region. This, in turn,
decreases the detection limit of the REE with low energy photopeaks.
When overlapping of two photopeaks occurs, the detection limit is further
decreased by mutual interferences between the two photopeaks. Some
of the more significant interferences were noted in Table 3-2. For
nuclides such as ^{165}Dy, ^{171}Er, and ^{166}Ho, which were not determined
in this study, reduced detection limits due to interferences of this
nature were serious.

Therefore, the relative RE abundances in a sample are
also an important factor in determining the detection limit of individual
REE. Because of variable relative RE abundances in different samples,
it is very difficult to define a detection limit common to all samples.

However, the neutron activation detection limit for most REE

determined by wet chemical, group-separation method is generally in

the ppb range (Higuchi et al., 1970; Haskin et al., 1970), which is

sensitive enough for RE determination in most terrestrial rocks.

3-11. Analytical Results

The results of RE activation analyses for samples from the

Sdubury district are presented in Tables 3-4, 3-5, 3-6, 3-7 and 3-8.

Table 3-4. Rare Earth Abundances (ppm) of North Range Main Irruptive Rocks

Sample No.	La	Ce	Nd	Sm	Eu	Gd	Tb	Yb	Lu	(Eu/Eu*)[1]	(La/Yb)$_N$[2]	ΣREE[3]
Strathcona Section												
(micropegmatite)												
M-9-195	42.0	81.4	-	5.63	1.45	4.26	0.54	1.88	0.30	0.91	13.5	133
M-9-995	44.7	116	-	9.38	2.15	-	1.12	1.73	0.29	0.78	15.7	175
M-9-3605	56.2	138	-	8.22	1.73	-	0.83	2.48	0.37	0.76	13.8	208
M-9-4405	56.7	133	51.0	8.52	1.64	6.53	0.93	1.57	0.26	0.66	21.9	203
Average	49.9	117	-	7.94	1.74	-	0.86	1.92	0.31	0.78	16.2	180
(oxide-rich gabbro)												
M-9-5205	43.2	101	36.0	8.16	2.24	-	0.96	2.94	0.35	0.94	8.91	159
(felsic norite)												
M-9-6405	20.3	43.1	-	3.32	1.31	-	0.39	1.06	0.15	1.35	11.6	69.6
M-9-7520	24.0	46.7	-	3.77	1.78	-	0.55	1.53	0.25	1.49	9.48	78.6
Average	22.2	44.9	-	3.55	1.55	-	0.47	1.30	0.20	1.42	10.5	74.1
(mafic norite)												
S-27-5	26.9	57.2	-	3.89	1.14	-	0.42	1.19	0.14	1.02	13.7	90.9
S-27-6	28.8	62.8	-	4.43	1.19	-	0.44	1.40	0.21	0.98	11.3	99.3
Average	27.9	60.0	-	4.16	1.17	-	0.43	1.30	0.18	1.00	12.5	95.1

Notes: 1. Eu/Eu* is the ratio of Eu concentration in the sample to the interpolated value, Eu*, between Sm and Tb from the chondrite-normalized R.E. fractionation pattern of the sample.
2. (La/Yb)$_N$ is the chondrite-normalized ratio of La concentration to Yb concentration.
3. ΣREE is the sum of La+Ce+Sm+Eu+Tb+Yb+Lu in ppm.
- not determined.

73

Table 3-5. Rare Earth Abundances (ppm) of South Range Main Irruptive Rocks

Sample No.	La	Ce	Nd	Sm	Eu	Gd	Tb	Yb	Lu	(Eu/Eu*)	(La/Yb)$_N$	ΣREE
Blezard Section												
(micropegmatite)												
W-155	64.4	109	46.8	8.71	1.72	-	0.99	3.19	0.48	0.68	12.2	189
W-150	47.9	97.1	36.1	7.16	1.60	-	0.74	2.57	0.41	0.81	11.3	158
Average	56.2	103	41.5	7.94	1.66	-	0.87	2.88	0.45	0.75	11.8	174
(upper gabbro)												
W-153	61.7	123	-	9.79	2.42	-	0.96	2.27	0.32	0.90	16.5	200
(south range norite)												
W-126	18.9	30.2	-	3.15	1.12	-	0.36	1.07	0.14	1.23	10.7	54.9
W-120	15.3	25.3	-	1.86	0.74	-	0.27	0.97	0.14	1.24	9.60	44.6
W-116	24.0	47.4	17.3	3.42	1.45	-	0.60	1.82	0.28	1.25	7.98	79.0
Average	19.4	34.3	-	2.81	1.10	-	0.41	1.29	0.19	1.24	8.79	59.5
(quartz-rich norite)												
W-110	30.1	51.9	-	4.33	1.25	-	0.52	1.51	0.20	0.99	12.1	89.8
W-104	36.7	63.3	26.8	4.71	1.27	4.13	0.60	2.24	0.34	0.91	9.93	109
Average	33.4	57.6	-	4.52	1.26	-	0.56	1.88	0.27	0.95	11.0	99.4

Table 3-6.   Rare Earth Abundances (ppm) of Sub-Layer Rocks

Sample No.	La	Ce	Nd	Sm	Eu	Gd	Tb	Yb	Lu	(Eu/Eu*)	(La/Yb)$_N$	Σ REE
North Range												
Strathcona mafic sub-layer												
S-27-27-A (norite)	26.6	51.7	-	6.18	2.11	-	0.73	2.83	0.40	1.17	5.70	90.6
S-29-125-1675 (norite)	23.2	33.1	17.2	3.90	1.08	-	0.51	1.08	0.16	0.91	13.0	63.0
Whistle mafic sub-layer												
WHL-A (gabbro)	12.0	24.7	-	3.78	1.20	-	0.57	1.76	0.25	1.01	4.13	44.3
Foy offset												
E-2-70 (quartz diorite)	45.8	84.4	-	6.38	1.63	-	0.67	1.70	0.24	0.91	16.4	141
South Range												
Sultana sub-layer												
MS-776-E-70	41.1	95.9	-	6.25	1.81	-	0.67	1.43	0.20	1.05	17.4	147
Little Stobie mine sub-layer												
L-71-3 (gabbro inclusion ore)	22.0	44.3	-	3.37	0.85	-	0.43	1.37	0.23	0.83	9.74	72.5
Frood offset												
F-2 (sulfide spotted quartz diorite)	18.1	33.9	-	3.59	0.90	-	0.40	1.25	0.17	0.88	8.78	58.3
Copper Cliff offset												
C-71-1 (quartz diorite)	52.6	95.0	42.0	8.53	1.90	7.48	1.18	2.55	0.35	0.74	12.5	162

Table 3-7. Rare Earth Abundances (ppm) of Sub-Layer Inclusions

Sample No.	La	Ce	Nd	Sm	Eu	Gd	Tb	Yb	Lu	(Eu/Eu*)	(La/Yb)$_N$	ΣREE
North Range												
Strathcona Inclusions												
S-23-32-A (pyroxenite)	14.0	30.8	–	3.59	0.99	–	0.41	2.13	0.35	0.98	3.98	50.3
S-23-32-B (pyroxenite)	13.2	34.6	–	4.73	0.98	–	0.51	2.52	0.38	0.76	3.18	56.9
S-23-32-D (pyroxenite)	31.2	62.5	–	5.56	1.49	–	0.50	2.11	0.17	0.94	5.32	104
S-29-139-1804 (pyroxenite)	10.1	21.9	–	1.59	0.54	–	0.23	0.86	0.13	1.08	7.11	25.4
S-20-40-A (norite)	15.6	29.2	–	4.57	1.39	–	0.42	1.66	0.28	1.12	5.70	53.1
S-20-40-B (pyroxenite)	8.63	17.2	–	3.33	0.79	–	0.32	0.95	0.17	0.91	5.53	31.4
S-20-40-C (pyroxenite)	9.32	20.1	–	2.96	0.83	–	0.34	1.18	0.16	0.99	4.79	34.9
S-20-40-D (peridotite)	10.7	22.3	–	2.92	0.79	–	0.34	1.22	0.17	0.94	5.32	38.4
S-27-27-C (peridotite)	8.28	19.7	–	2.06	0.53	–	0.24	0.88	0.13	0.89	5.68	31.8
Whistle Inclusions												
W-9 (olivine gabbro)	18.9	44.0	22.6	5.03	1.31	–	0.61	1.26	0.20	0.91	9.11	71.3
W-23 (olivine gabbro)	15.0	32.4	–	4.94	2.04	–	0.79	2.50	0.41	1.28	3.64	58.1
South Range												
Murray Inclusions												
M-1580-4 (norite)	17.2	40.5	–	4.00	1.28	–	0.56	1.80	0.31	1.04	5.78	65.7
M-1650-16 (peridotite)	12.7	27.9	14.3	2.53	0.63	–	0.39	1.58	0.24	0.81	4.89	46.0
Little Stobie Inclusions												
L-71-2 (pyroxenite)	1.72	4.41	–	0.59	0.25	–	0.18	0.60	0.10	1.06	1.39	7.86

Table 3-8.   Rare Earth Abundances (ppm) of Onaping Formation and Superior Province Country Rocks

Sample No.	La	Ce	Nd	Sm	Eu	Gd	Tb	Yb	Lu	(Eu/Eu*)	(La/Yb)$_N$	Σ REE
Onaping Formation												
O-2F (melt rock)	25.4	51.3	23.5	4.78	0.89	4.01	0.53	1.68	0.25	0.66	9.18	84.8
O-2D (grey Onaping)	23.7	40.9	-	3.11	0.74	2.32	0.35	1.26	0.20	0.84	11.4	70.3
O-2C (basal breccia)	20.8	43.8	-	3.24	0.93	-	0.45	1.43	0.23	0.92	8.85	70.9
Superior Province Gneiss												
SG-1	15.8	30.5	13.0	2.50	0.83	-	0.33	0.55	0.08	1.13	17.5	50.6

CHAPTER FOUR

RARE EARTH PATTERNS OF SUDBURY NICKEL IRRUPTIVE ROCKS

4-1. General Geochemistry of Rare Earth Elements

REE (atomic number 57 to 71) are members of the IIIB group elements. Geochemically, they are strictly lithophile elements. The metals and their oxides are non-volatile. Their ions are strongly electro-positive and RE compounds are predominantly ionic. The ionic radius of the RE ions decrease regularly with increasing atomic number, a phenomenon known as "the lanthanide contraction". In nature, the most stable oxidation state for all members of the RE group is +3. Only Ce and Eu are known to undergo changes in oxidation state in the natural environment (trivalent Ce may be oxidized to the +4 state and trivalent Eu reduced to the +2 state). Some of the important physical and chemical parameters of the REE are listed in Table 4-1.

Because of their very similar chemical properties, a con-sequence of similar electronic configurations, REE are highly coherent in nature. Analytical separation of an individual REE from other members of the group is difficult. This led geochemists such as Rankama and Sahama

Table 4-1. Physical and Chemical Parameters of Rare Earth Elements (Topp, 1965; Whittaker and Muntus, 1970)

Element	Symbol & Stable Valence State(s)	Atomic Number	Ionic Radius (Å)		Melting Point of the Metal (^{o}C)	Heat of Formation of R_2O_3 ($-\Delta H$, 25°C, Kcal/mole)
			6-fold Coordination	8-fold		
Lanthanum	La^{+3}	57	1.13	1.26	920	428.6
Cerium	Ce^{+3}	58	1.09	1.22	795	435.0
	Ce^{+4}		0.88	1.05		
Praseodymium	Pr^{+3}	59	1.08	1.22	935	436.8
Neodymium	Nd^{+3}	60	1.06	1.20	1024	432.1
Promethium	Pm	61				
Samarium	Sm^{+3}	62	1.04	1.17	1072	433.9
Europium	Eu^{+3}	63	1.03	1.15	826	392.3
	Eu^{+2}		1.25	1.33		
Gadolinium	Gd^{+3}	64	1.02	1.14	1312	433.9
Terbium	Tb^{+3}	65	1.00	1.12	1356	436.8
Dysprosium	Dy^{+3}	66	0.99	1.11	1407	445.8
Holmium	Ho^{+3}	67	0.98	1.10	1461	449.5
Erbium	Er^{+3}	68	0.97	1.08	1497	453.6
Thulium	Tm^{+3}	69	0.96	1.07	1545	451.8
Ytterbium	Yb^{+3}	70	0.95	1.06	824	433.7
Lutetium	Lu^{+3}	71	0.94	1.05	1652	452.8

(1950) and Goldschmidt (1954) to conclude that no relative fractionation of the REE would occur in nature. Only in recent years has improvement of technique made accurate measurement of individual REE possible and revealed that fractionation in nature does occur.

The fractionation of these chemically similar elements provides a useful tool for attack of petrogenetic problems, especially those pertaining to igneous rocks (Gast, 1968; Philpotts and Schnetzler, 1968; Schilling and Winchester, 1969; Kay et al., 1970; Arth and Hanson, 1975; etc.). The future use of the REE as indicators of the physical-chemical conditions of formation of rocks and minerals is promising, particularly as more experimental information on REE partition between minerals is obtained (Masuda and Kushiro, 1970; Cullers et al., 1973; Zielinski and Frey, 1974; Drake, 1975).

The absolute abundances of the REE in nature follows the Oddo-Harkins rule; that is, a plot of abundance versus atomic number shows a zig-zag pattern caused by low abundance of odd-Z elements relative to nearest-neighbour even-Z elements. This effect tends to mask RE fractionation trends so that it is accepted practice to divide each RE value in the sample by its abundance in some primitive material, such as chondritic meteorites. A plot of the logarithm of such normalized values

against atomic number usually yields a smooth curve showing the RE fractionation of the sample relative to the primitive material (Masuda, 1962; Coryell et al., 1963).

Many geochemists normalize against chondrites because the primitive earth is often assumed to approximate chondritic composition with respect to RE fractionation pattern and because no large RE fractionations have been observed in individual chondrites (Schmitt et al., 1963; Haskin et al., 1966a). In this work, unless otherwise stated, all RE patterns are normalized against chondrites. The term "RE fractionation pattern" refers to such a normalized RE pattern. The values used for normalization are the absolute RE contents of a composite of nine chondrite samples reported by Haskin et al. (1968b) and listed in Appendix D.

For the chondrite normalized RE fractionation patterns, the La/Yb ratio appears to be an appropriate index of the degree of RE fractionation. In this work, unless otherwise stated, all the La/Yb ratios are normalized against chondrites. A La/Yb ratio of one indicates a flat chondrite normalized RE pattern; a La/Yb ratio larger than one indicates a RE fractionation pattern with a negative slope (that is, enrichment in light REE relative to heavy REE) and a La/Yb ratio less than one indicates a RE fractionation pattern with a positive slope (that is, depleted in light REE relative to heavy REE).

4-2. Rare Earth Patterns in the Main Irruptive

    4-2-1. North Range Rocks

The chondrite normalized RE patterns in four micropegmatite, one oxide-rich gabbro, and two felsic norite samples from drill core M-9 together with two mafic norite samples collected at the 2700 level in the Strathcona mine are presented in Figs. 4-1-A and 4-1-B. The location of diamond drill hole M-9 and sample locations are shown in Fig. 2-5.

The overall RE fractionation patterns of these rock units on the north range do not differ greatly from each other. All of the samples are strongly enriched in total RE content with respect to chondrites. The ΣREE (sum of La + Ce + Sm + Eu + Tb + Yb + Lu in ppm) ranges from 69.6 in felsic norite (M-9-6405) to 208 in micropegmatite (M-9-3605) as compared to 1.74 in chondrites. The north range samples have absolute Yb content ranging from about 5 to 15 times, and La content ranging from about 60 to 180 times, that of the chondrite. They exhibit light RE enrichment as shown by the high chondrite normalized La/Yb ratios (Table 3-4). The La/Yb ratios range from 8.91 in M-9-5205 to 21.9 in M-9-4405.

Within this general pattern each rock unit exhibits distinctive characteristics in detailed RE features. In general, ΣREE and the degree of light to heavy REE fractionation (La/Yb ratio) increase from norite to micropegmatite. The oxide-rich gabbro has ΣREE falling between the norites and the micropegmatites. The mafic norite, although similar to the felsic norite mineralogically, has higher ΣREE and La/Yb ratios than the felsic norite.

Fig. 4-1-A. Rare Earth Fractionation Patterns of North Range

Main Irruptive Rocks: Micropegmatites (M-9-195,

M-9-995, M-9-3605 and M-9-4405) and Oxide-Rich

Gabbro (M-9-5205).

ROCK / CHONDRITES

La Ce Pr Nd Pm Sm Eu Gd Tb Dy Ho Er Tm Yb Lu

o M-9-195
△ M-9-995
□ M-9-3605
▽ M-9-4405
◇ M-9-5205
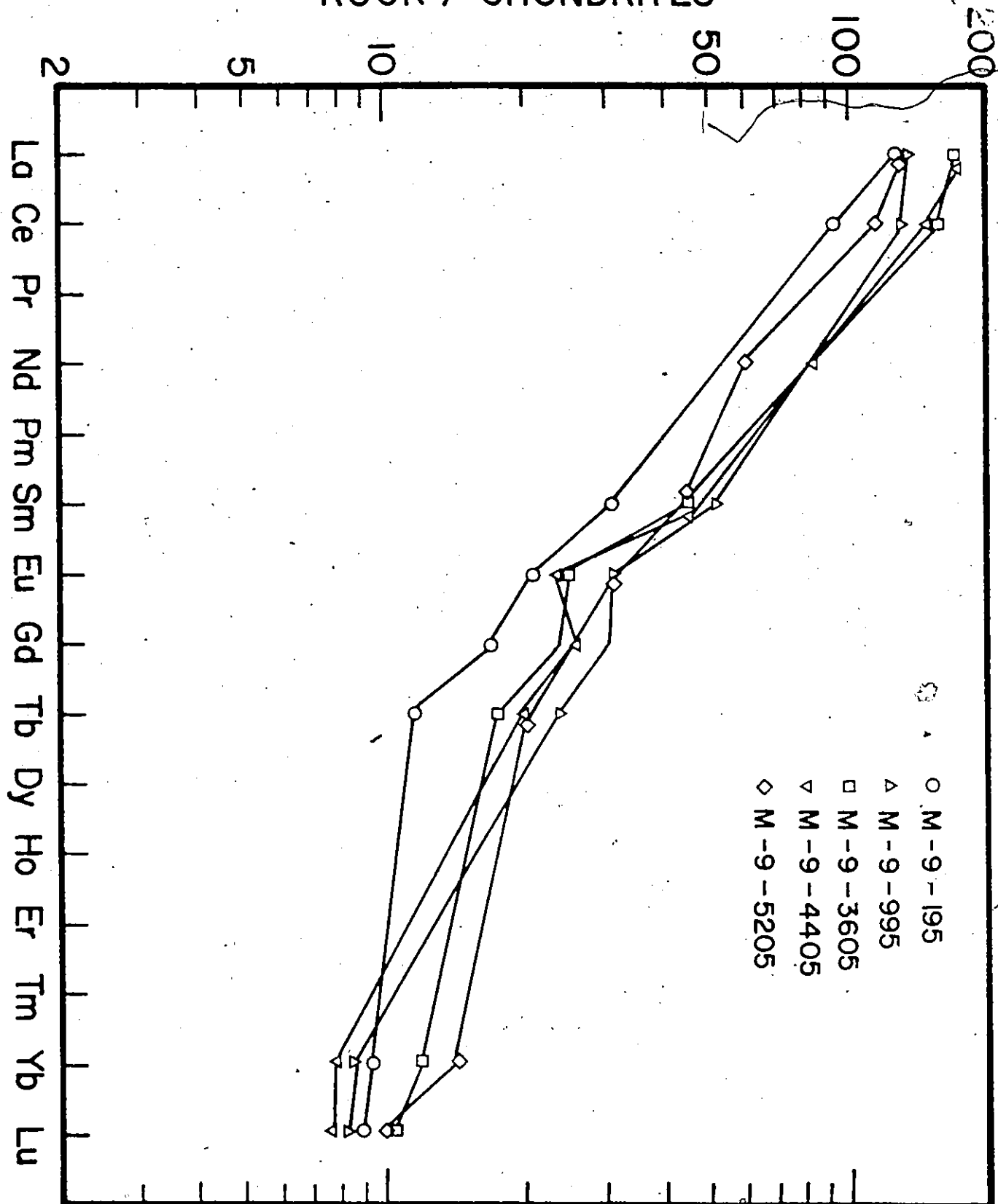
Fig. 4-1-B. Rare Earth Fractionation Patterns of North Range

Main Irruptive Rocks: Felsic Norites (M-9-6405 and

M-9-7520) and Mafic Norites (S-27-6 and S-27-5).
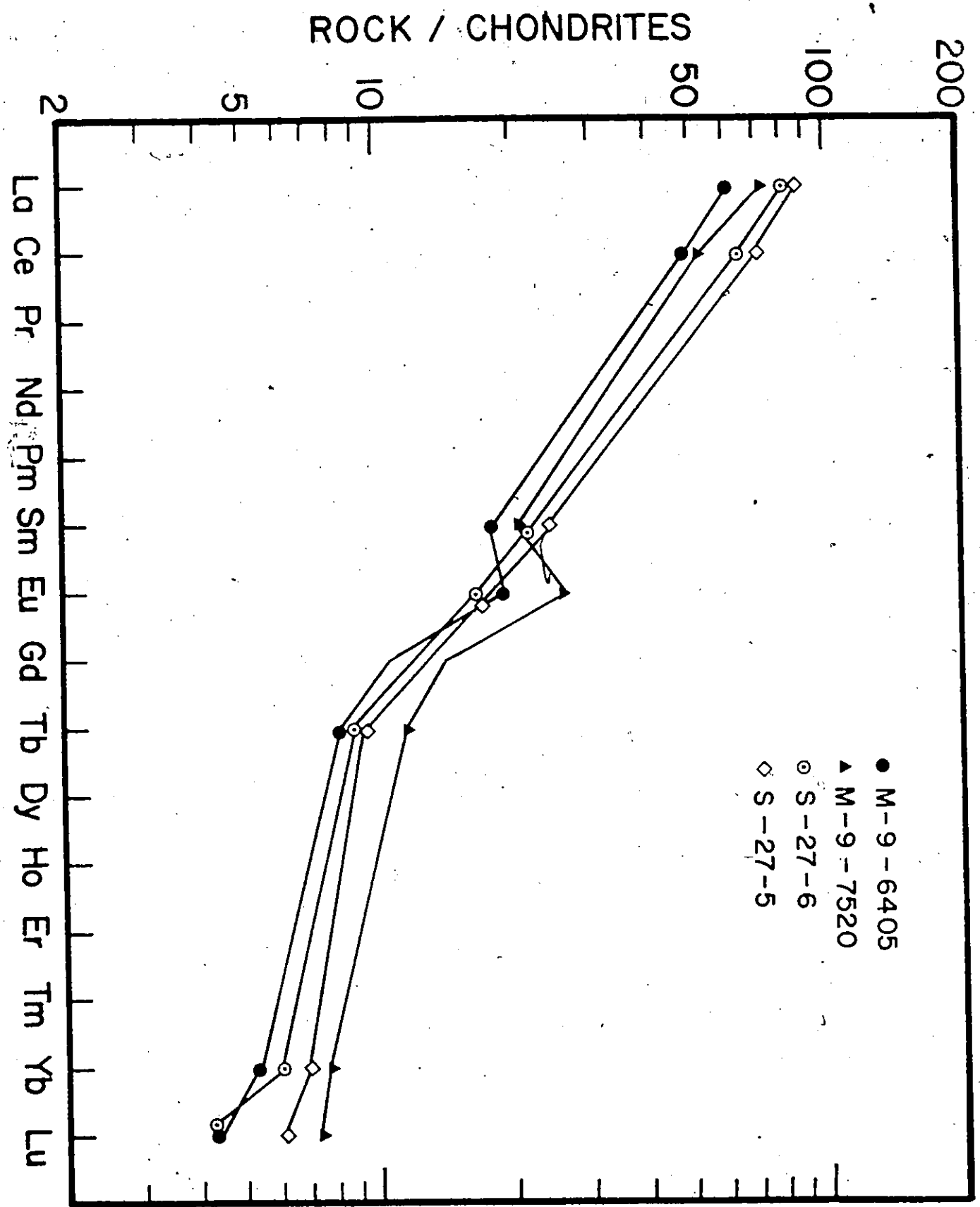
The most distinctive feature of the north range rocks is the nature of their Eu anomalies. An anomalous Eu concentration is usually expressed by the Eu/Eu* ratio which is the ratio of the measured Eu abundance to the expected value (Eu*) if Eu behaved as an adjacent REE. In this work the Eu* value is obtained by interpolation between Sm and Tb on a smooth chondrite normalized RE fractionation pattern. An Eu/Eu* ratio greater than one indicates a positive Eu anomaly and a ratio less than one indicates a negative Eu anomaly.

The north range micropegmatites invariably show negative Eu anomalies with an average Eu/Eu* value of 0.78, whereas the two felsic norites show strong positive Eu anomalies with an average Eu/Eu* value of 1.42. The single oxide-rich gabbro has a very weak negative Eu anomaly (Eu/Eu* = 0.94). The mafic norites again differ from the felsic norites showing no significant Eu anomalies.

4-2-2. South Range Rocks

The chondrite normalized RE patterns in two micropegmatite, one upper gabbro, three norite and two quartz-rich norite samples from the Blezard traverse on the south range are presented in Figs. 4-2-A and 4-2-B. Sample locations are shown in Fig. 2-6.

In general, the south range rocks have RE patterns similar to the corresponding rock units on the north range. Σ REE and La/Yb ratio increase from norite to micropegmatite and the characteristic Eu anomaly features (negative Eu anomaly in micropegmatites and positive Eu anomaly in norites) found in the north range rocks are also observed in the south range rocks. The south range upper gabbro (W-153) has higher Σ REE and La/Yb ratio than the north range oxide-rich gabbro (M-9-5205). The difference may be caused by different amounts of apatite and sphene contained in these samples as both minerals, which occur in the transition zone gabbros (Naldrett et al., 1970), may contain large amounts of REE.

The absolute Yb content ranges from about 4 to 16 times, and La content from about 45 to 200 times, that of the chondrites. As is the case on the north range the two border norites, the quartz-rich norites, have higher Σ REE and higher average La/Yb ratios than the overlying south range norite. The Eu anomalies in the border norites are weakly negative (W-104) to insignificant (W-110).

Fig. 4-2-A. Rare Earth Fractionation Patterns of South Range

Main Irruptive Rocks: Micropegmatites (W-155 and W-150)

and Upper Gabbro (W-153).
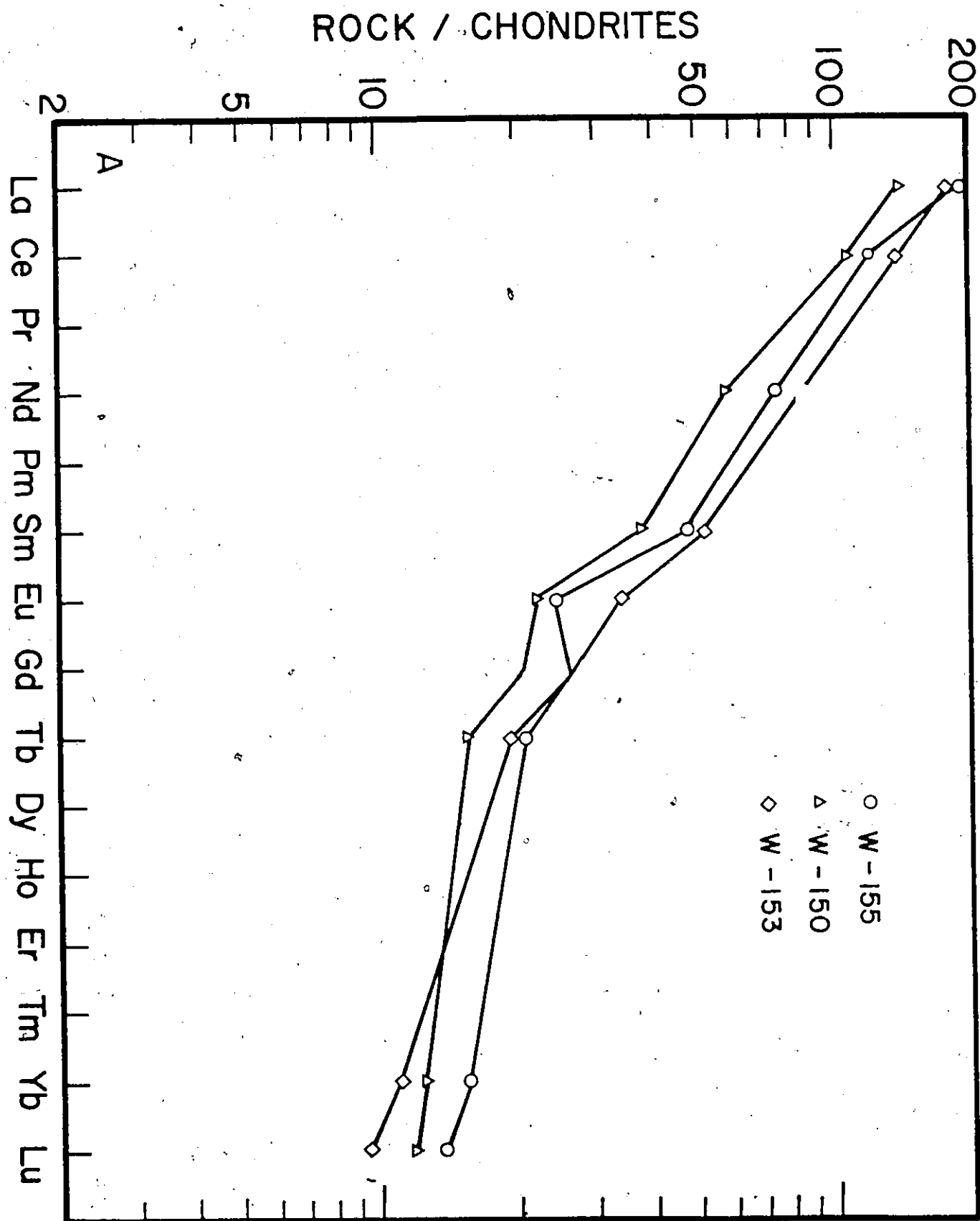
Fig. 4-2-B. Rare Earth Fractionation Patterns of South Range

Main Irruptive Rocks: Norites (W-126, W-120 and

W-116) and Quartz-Rich Norites (W-110 and W-104).
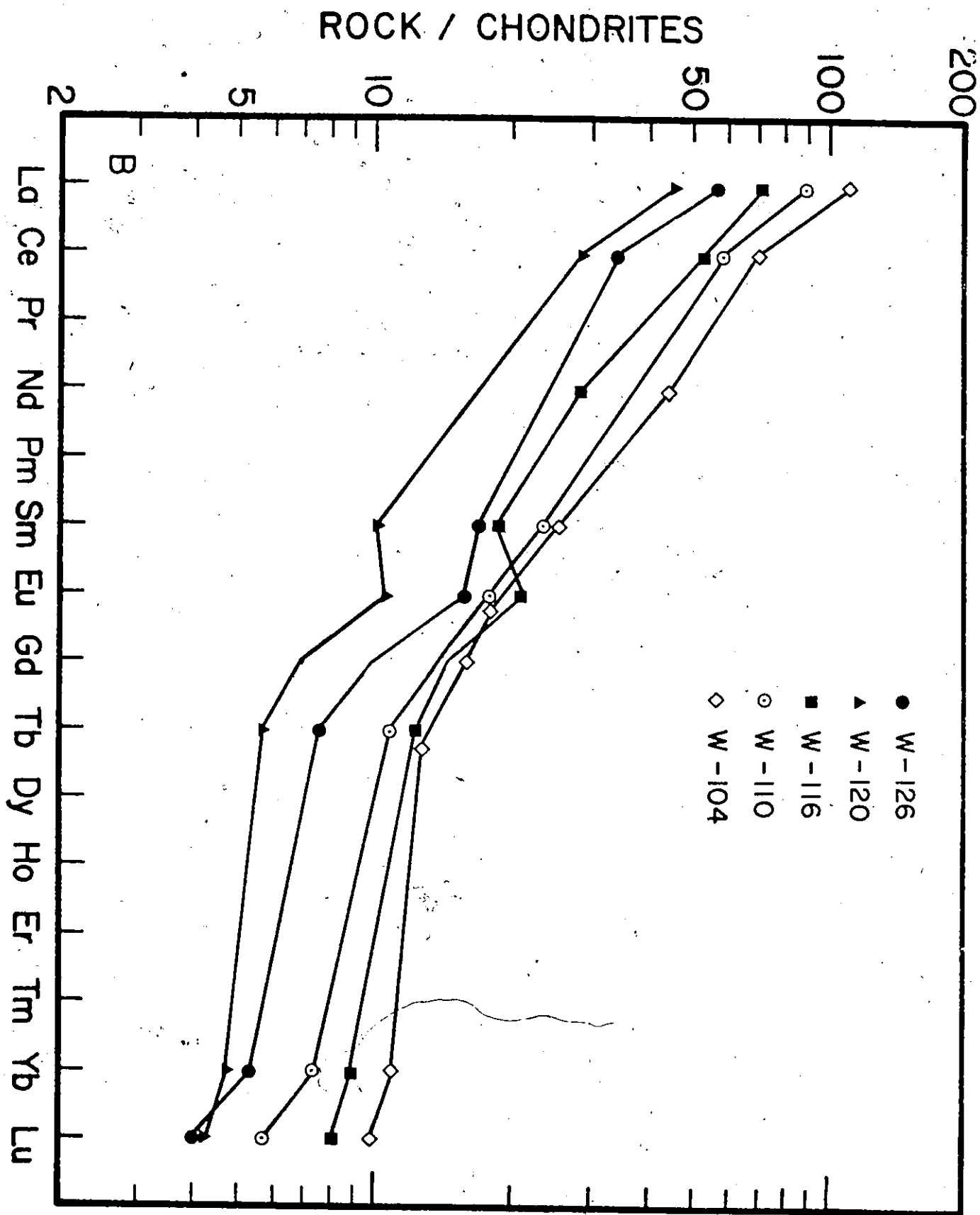
4-3. Rare Earth Patterns in the Sub-Layer

4-3-1. Mafic Sub-Layer and Offset Rocks

The RE patterns of north range sub-layer rocks including two Strathcona mafic sub-layers, one Whistle mafic sub-layer and one Foy offset sample are presented in Fig. 4-3-A. Patterns for one Sultana sub-layer, one Little Stobie gabbro inclusion ore and two offset (Copper Cliff offset and Frood gabbro inclusion ore) samples from the south range are presented in Fig. 4-3-B. The RE pattern of average border norite (average of two north range mafic norites and two south range quartz-rich norites) are also shown for comparison.

The Frood (F-2) and Little Stobie (L-71-2) gabbro inclusion ore samples contain about 40% and 20% respectively of fine-grained inter-stitial sulfide blebs. The sulfides were not separated from the silicate during sample preparation. Therefore, the absolute RE contents of the silicate portion of these two samples may be 40% and 20% respectively higher than the values reported in Table 3-6. However, as discussed in the previous chapter the RE fractionation patterns shown in Fig. 4-3-B are essentially those of the silicate portion of these samples.

When compared with the main Irruptive rocks the RE frac-tionation patterns of the sub-layer rocks are similar to the border norites but show a wider range of variation from sample to sample. Overall average ΣREE for border norites and sub-layer rocks are 97 ± 9 and

Fig. 4-3-A. Rare Earth Fractionation Patterns of Sub-Layer Rocks:
North Range --- Strathcona (S-27-27-A and S-29-125-1675),
Whitle (WHL-A) Mafic Sub-Layer and the Foy Offset
(E-2-70).

REE chondrite-normalized diagram. ROCK / CHONDRITES versus La Ce Pr Nd Pm Sm Eu Gd Tb Dy Ho Er Tm Yb Lu.

Legend:
○ S-27-27-A
△ S-29-125-1675
□ WHI-A
◇ E-2-70
⊙ Average border norite
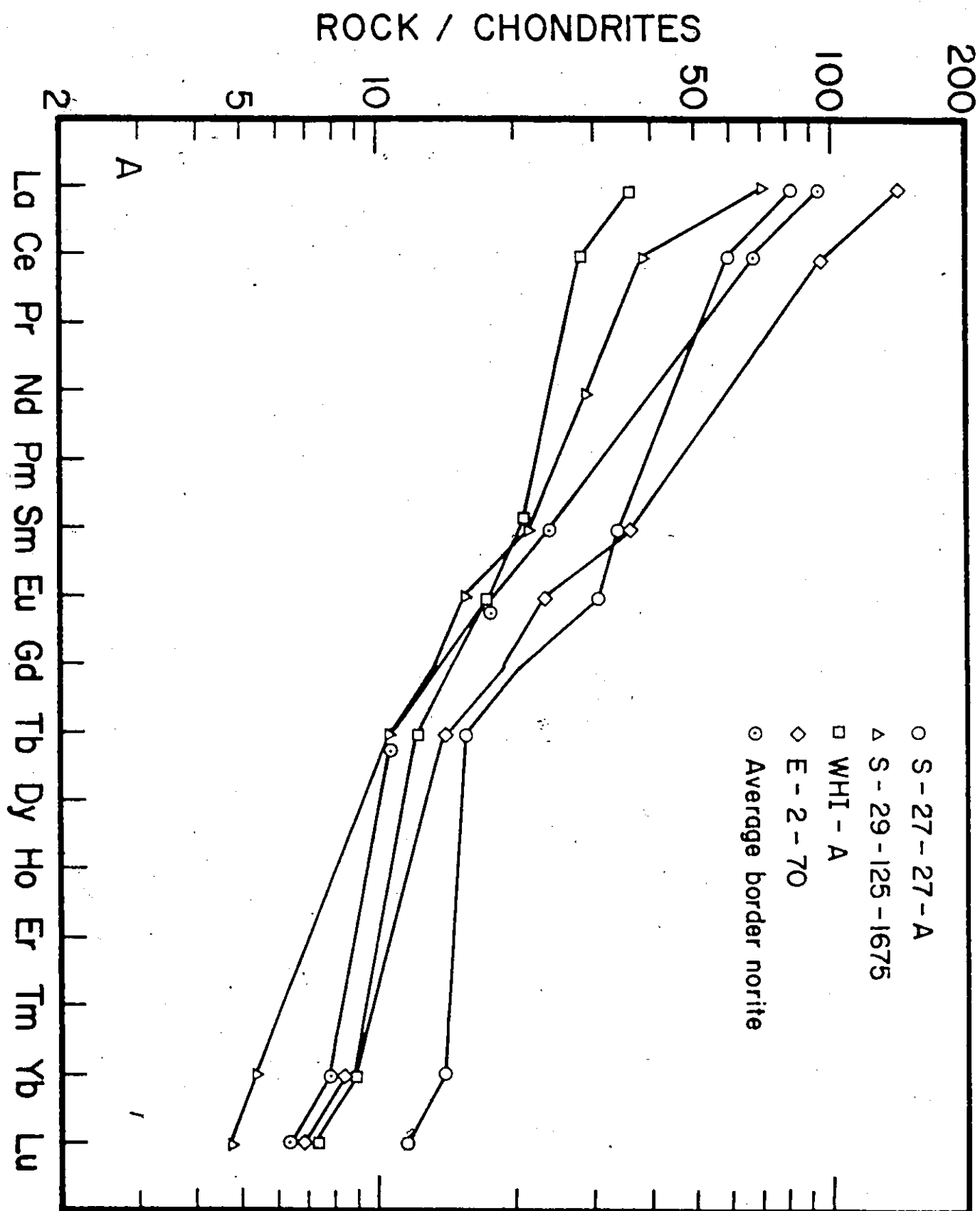
Fig. 4-3-B. Rare Earth Fractionation Patterns of Sub-Layer Rocks:

South Range --- Sultana (MS-776-E-70) and Little Stobie

Mine (L-71-3) Sub-Layer, and Frood Mine (F-2) and

Copper Cliff (C-71-1) Offset

REE chondrite-normalized diagram (ROCK / CHONDRITES vs La Ce Pr Nd Pm Sm Eu Gd Tb Dy Ho Er Tm Yb Lu), labeled B. Legend: ● F-2; ▲ L-71-3; ■ MS-776-E-70; ◇ C-71-r'; ⊙ Average border norite.
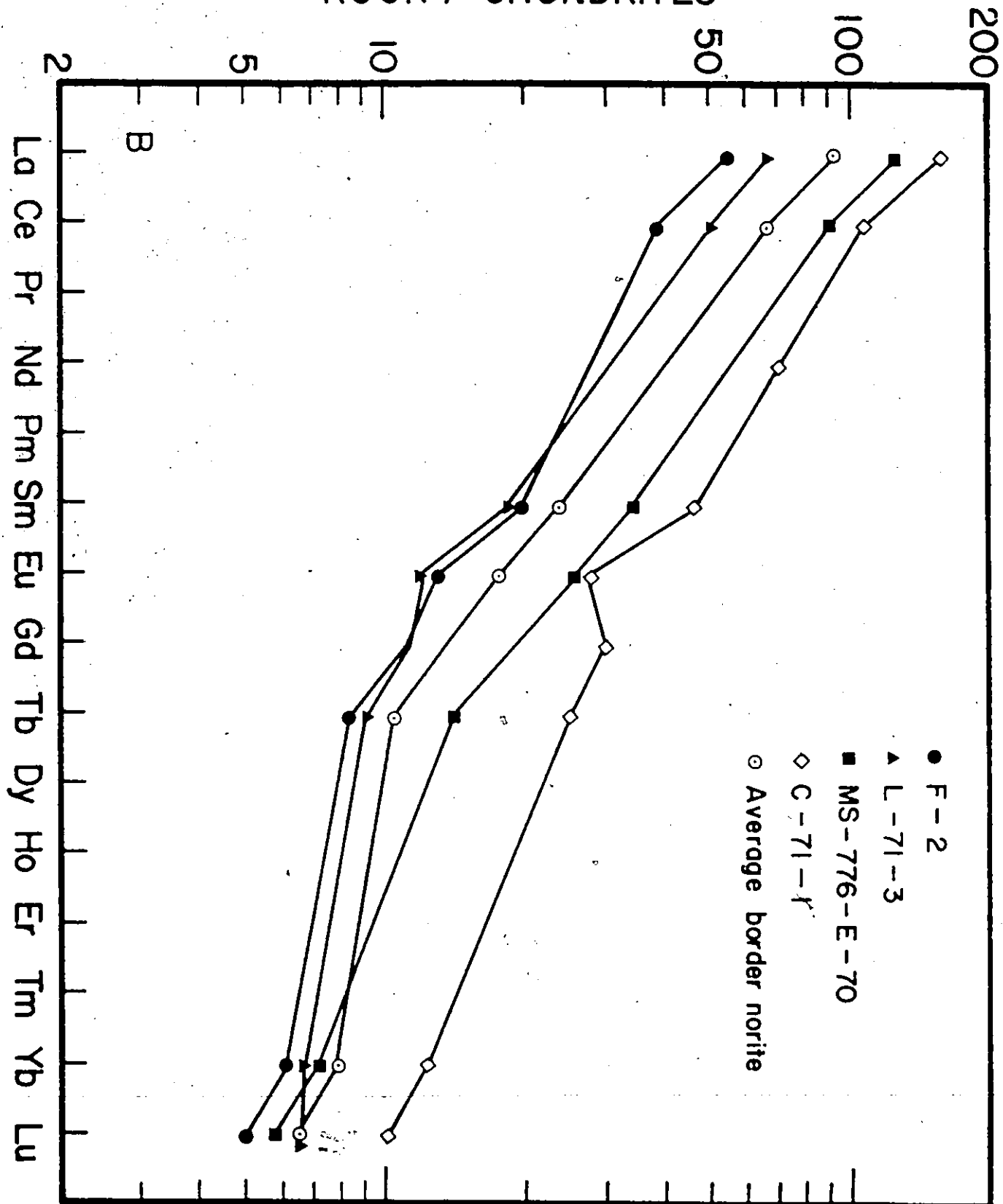
97 ± 46 respectively. Average La/Yb for border norites and sub-layer rocks are 11.8 ± 1.5 and 11.0 ± 4.9 respectively.

Two groups of sub-layer rocks may be distinguished - one with lower Σ REE and La/Yb ratios (Strathcona sub-layer and Whistle sub-layer) and the other with higher Σ REE and La/Yb ratios (Foy offset, Copper Cliff offset, Sultana sub-layer) than the main Irruptive border norites. The Whistle sub-layer (WHL-A) has a lower Σ REE (44.3) and La/Yb ratio (4.13) than other noritic rocks. The Sultana sub-layer (MS-776-E-70) has high Σ REE (147) and La/Yb ratio (17.4). The Copper Cliff offset has the highest Σ REE (162) of all the sub-layer rocks and has a strong negative Eu anomaly (Eu/Eu* = 0.74).

Sub-layer and offset rocks are characterized generally by weak to distinct negative Eu anomalies. The Copper Cliff offset quartz diorite has the strongest negative Eu anomaly while quartz diorite and gabbro from Frood and Little Stobie have weak negative anomalies. With one exception all other samples are characterized by very weak Eu anomalies, either negative or positive, and of low analytical significance. The one exception is a Strathcona sub-layer sample having a distinct positive Eu anomaly possibly caused by somewhat open system solidification with respect to plagioclase.

4-3-2. Sub-Layer Mafic and Ultramafic Inclusions

The chondrite normalized RE patterns of nine Strathcona,

two Whistle, two Murray and one Little Stobie mafic and ultramafic

inclusions are presented in Figs. 4-4-A, 4-4-B and 4-4-C. In this

study, only those inclusions not represented by the main rock types of the

Nickel Irruptive and by immediately adjacent country rocks are discussed.

Average Σ REE and La/Yb ratio for all sub-layer inclusions

are 48 ± 23 ppm and 5.1 ± 1.8 respectively. These rocks are therefore

much lower in Σ REE and La/Yb ratio than the main Irruptive border

norites and the sub-layers norites and quartz diorites.

Unlike certain types of ultramafic rocks every inclusion is

characterized by light RE enrichment, as are the main Irruptive norites.

In general, the entire suite is characterized by rather consistent Σ REE

and La/Yb ratios. The concentrations of La and Yb are 25 to 60 and

4 to 12 times higher respectively than in chondrites. Exceptions are the

pyroxenite L-71-2 from the Little Stobie sub-layer which has significantly

lower Σ REE (7.86) and a relatively flat RE fractionation pattern (La/Yb =

1.39), and a peridotite inclusion, S-23-32-D, from the Strathcona sub-layer

which is characterized by high Σ REE (104) compared with other inclusions.

Two gabbroic sub-layer inclusions (S-20-40-A and W-23) have

positive Eu anomalies, and samples S-23-32-B, S-27-27-C and M-1650-16

have weak negative Eu anomalies. Other inclusions do not show significant

Eu anomalies.

Fig. 4-4-A. Rare Earth Fractionation Patterns of Sub-Layer

Inclusions: Strathcona Mine

ROCK / CHONDRITES

A

La Ce Pr Nd Pm Sm Eu Gd Tb Dy Ho Er Tm Yb Lu

○ S – 23 – 32 – A
△ S – 23 – 32 – B
▽ S – 29 – 139 – 1804
◆ S – 23 – 32 – D
◇ S – 20 – 40 – B
□ S – 20 – 40 – C
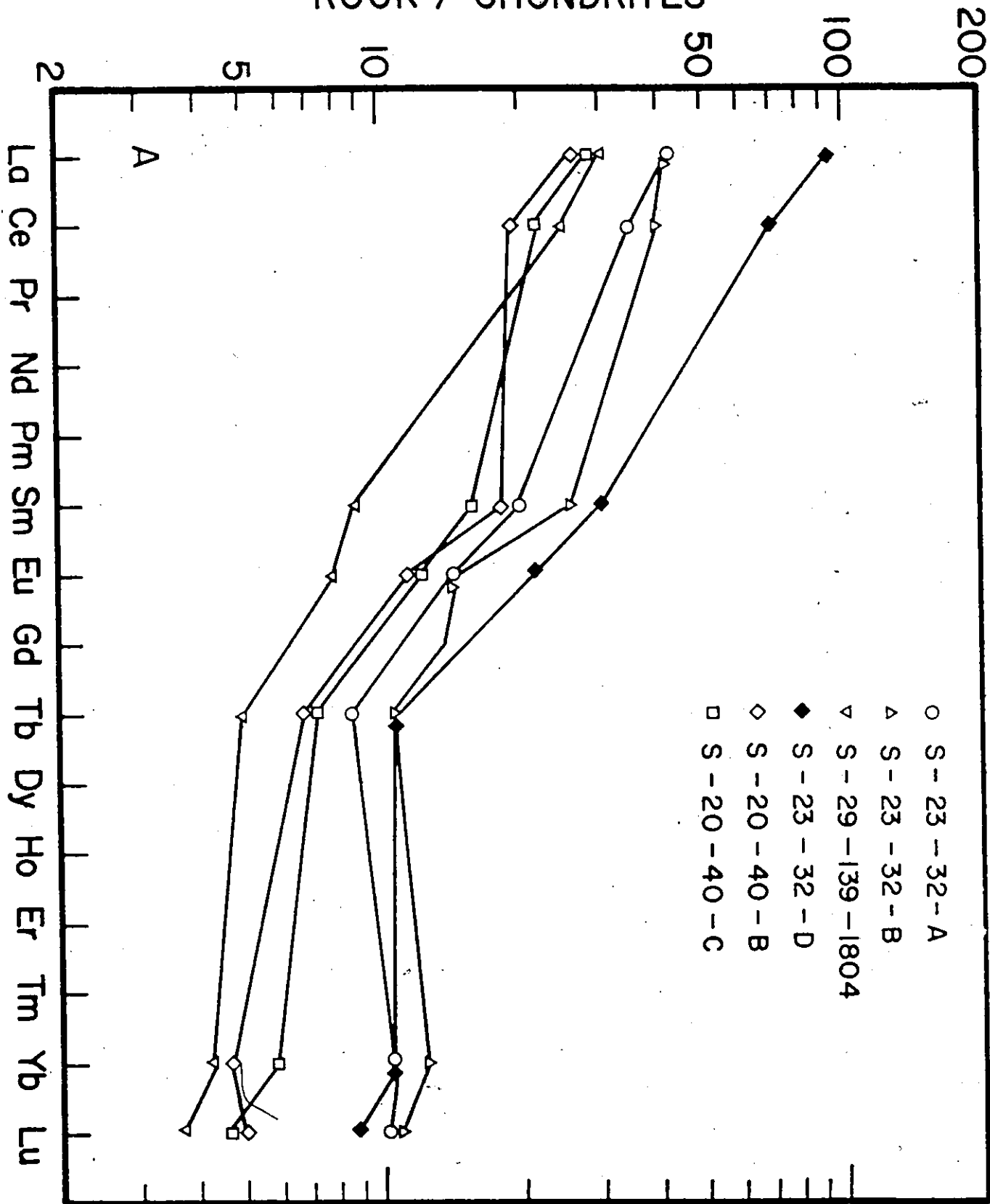
Fig. 4-4-B. Rare Earth Fractionation Patterns of Sub-Layer

Inclusions: Strathcona Mine (S-27-27-C,

S-20-40-D and S-20-40-A) and Whistle (W-9 and

W-23).
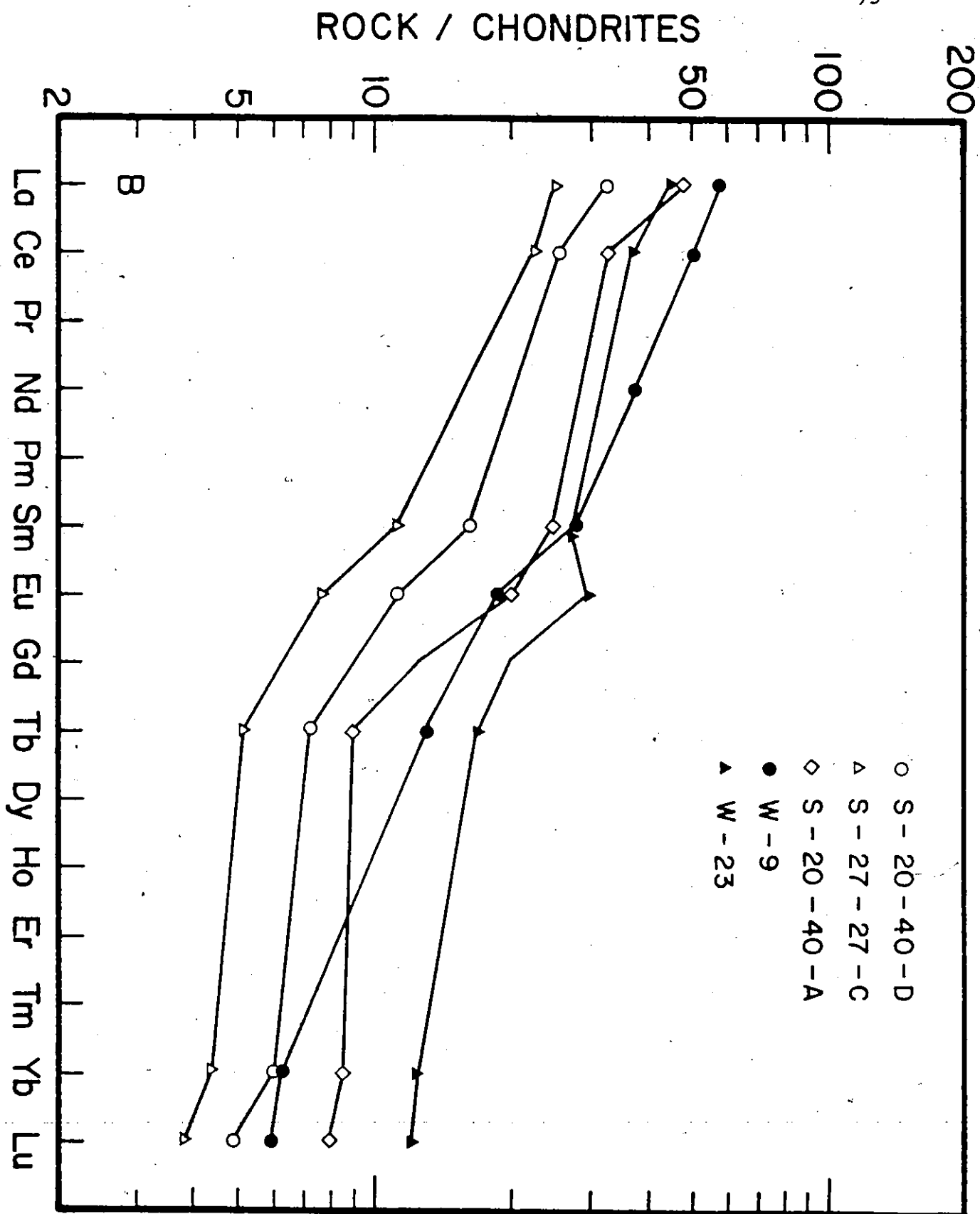
Fig. 4-4-C. Rare Earth Fractionation Patterns of Sub-Layer

Inclusions: Murray (M-1650-16 and M-1580-4)

and Little Stobie (L-71-2) Mines.

ROCK / CHONDRITES

C

○ M – 1650 – 16
△ M – 1580 – 4
◇ L – 71 – 2

La Ce Pr Nd Pm Sm Eu Gd Tb Dy Ho Er Tm Yb Lu
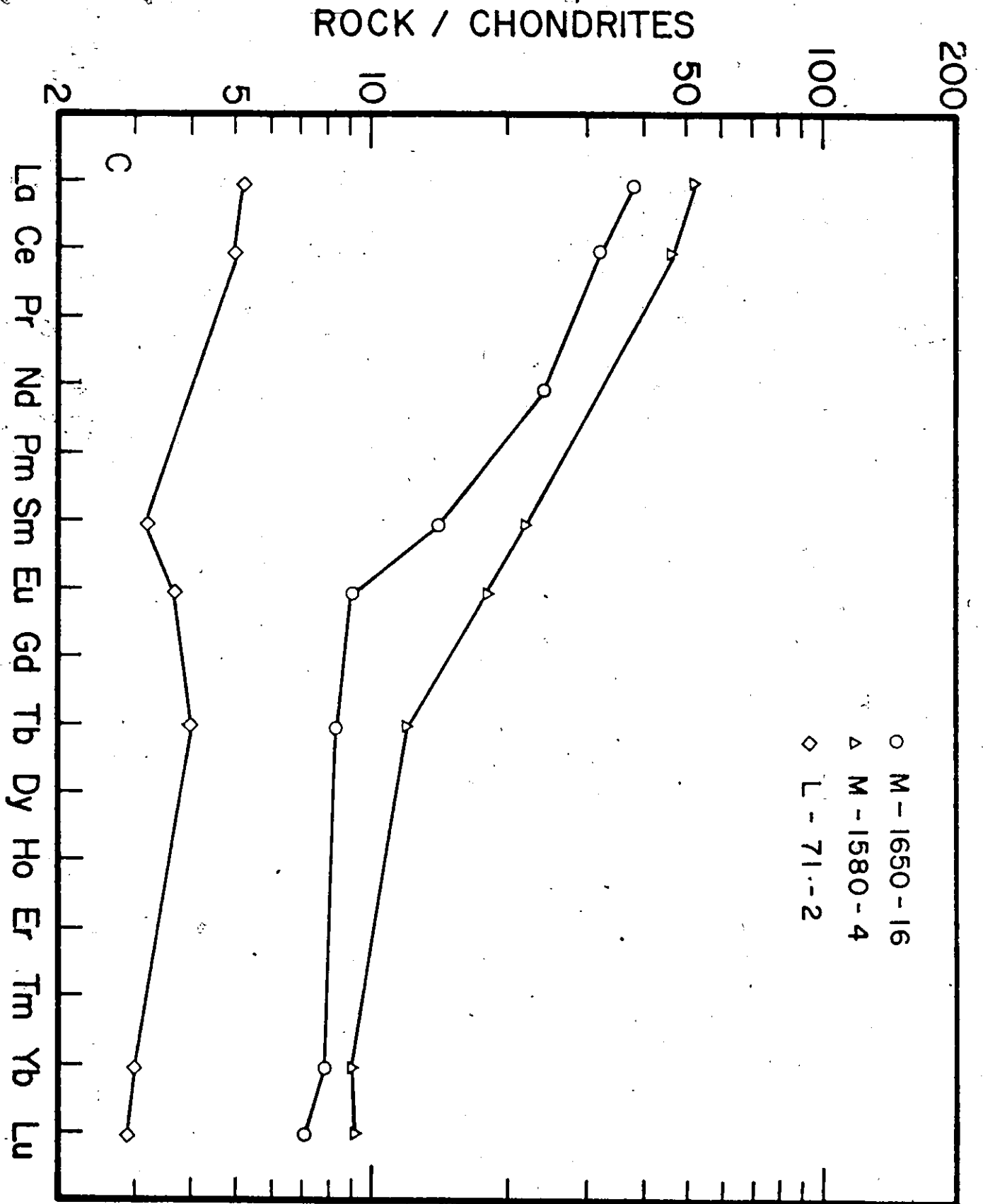
4-4. Rare Earth Patterns of Onaping Formation and Superior
Province Country Rocks

4-4-1. Onaping Formation Rocks

Three Onaping Formation rocks were collected from the
vicinity of the High Falls on the north range (Fig. 2-9). Sample O-2C is
from basal breccia near the contact with the main Irruptive. O-2D is
a sample of grey Onaping, and O-2F is melt rock from within the grey
Onaping. Each represents a different facies of the Onaping Formation.

The basal breccia and grey Onaping are not homogeneous
rocks. These units contain a variety of rock and glass fragments within
a medium-grained matrix. When preparing samples O-2C and O-2D large
pieces of handspecimen were first broken into small chips. Chips containing
breccia fragments larger than 1/2 cm in diameter were removed so that the
analyzed samples represent the matrix portion of the basal breccia and
grey Onaping respectively.

The RE-patterns of O-2C, O-2D and O-2F are presented in
Fig. 4-5. The Σ REE and La/Yb ratios of the Onaping Formation samples
are similar to those of main Irruptive norites. The RE patterns of basal
breccia and grey Onaping are very similar to each other. The basal
breccia has a weak negative Eu anomaly whereas the grey Onaping and
melt samples have significant and strong negative Eu anomalies of 0.84
and 0.66 respectively. The melt rock has higher ΣREE than either basal
breccia or grey Onaping whose ΣREE contents are nearly identical.

Fig. 4-5. Rare Earth Fractionation Patterns of Onaping

Formation and Country Rocks (data for Onwatin Slate

and Metagreywacke from Wildeman and Haskin, 1973).

REE chondrite-normalized diagram (ROCK / CHONDRITES vs. La Ce Pr Nd Pm Sm Eu Gd Tb Dy Ho Er Tm Yb Lu) with the following legend:

- ○ Average micropegmatite
- △ O - 2F (melt rock)
- ■ O - 2C (basal breccia)
- ◆ O - 2D (grey Onaping)
- □ SG - I (Superior Province granite)
- ▽ Onwatin slate
- ● Metagreywacke
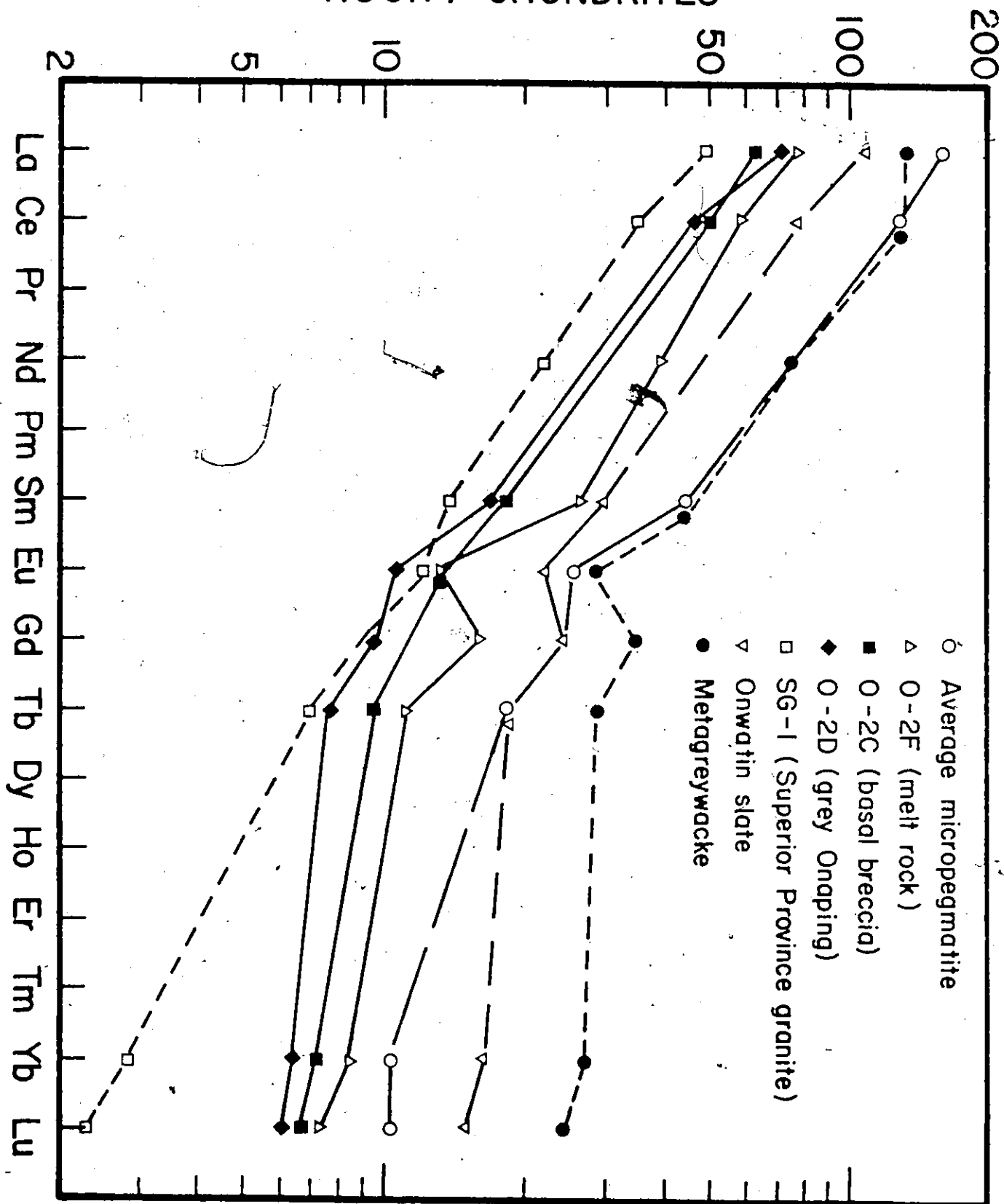
4-4-2. North Range Superior Province Rock

Sample SG-1 from the Superior Province granite-gneiss

terrane north of the Irruptive was collected from the basal contact of

the main Irruptive in the vicinity of the Strathcona mine.   In this area,

the felsic gneiss is tonalite in composition (Naldrett and Kullerud, 1967;

Cowan, 1968).   The RE pattern of SG-1 is presented in Fig. 4-5.   RE

patterns of Onwatin slate and average Canadian Shield metagreywacke

(from Wildeman and Haskin, 1973) and average main Irruptive micro-

pegmatite are also shown in Fig. 4-5 for comparison (see discussion in

Chapter 5).

The sample is low in Σ REE and highly depleted in heavy

REE.   It has a very high La/Yb ratio (17.5) and has a Eu/Eu* ratio of

1.13.   Its general RE pattern is similar to the Minnesota Precambrian

granitic rocks (Haskin et al., 1968b; Arth and Hanson, 1972; Jahn et al.,

1974).

CHAPTER FIVE

DISCUSSION

5-1. Rare Earth Elements in Igneous Rock Systems

5-1-1. Rare Earth Patterns in Rock Forming Minerals

Partition of REE between rock forming minerals is one of

the major mechanisms responsible for various RE patterns in whole

rocks. The RE pattern of a particular mineral phase depends on both

the pattern of the liquid phase from which this mineral crystallized,

and the distribution coefficients for REE partition between the mineral

and the liquid.

The distribution coefficient is defined in this study as the

ratio of the concentration of a trace element in the solid phase to that in

the coexisting liquid under equilibrium conditions. Distribution coefficients

vary with temperature, pressure, major element composition of the

phases, and the kinetics of the system. For example, in minerals of

solid-solution series, the RE distribution coefficient values appear to

depend on the major element composition of the minerals, and it has been

shown that Eu/Eu* ratio of feldspars increases with increasing alkali

content of the feldspar (Schnetzler and Philpotts, 1970; Dundas et al.,

1971). The influence of all these variables is probably reflected in the

large variations reported by different authors for the absolute values of

RE distribution coefficients, although differing experimental technique

is also a contributing factor.

Distribution coefficients have been determined for RE partition

between phenocrysts and host lavas, minerals and chilled marginal zones

of layered intrusions, minerals and plutonic whole rock values and from

experimental synthetic systems. The variation of RE distribution co-

efficients with changing pressure, temperature, and composition of

the mineral phases is so far incompletely understood, and there is some

uncertainty in the general applicability of RE distribution coefficients

obtained from one rock system to another rock which may have crystallized

under different environmental conditions.

Although reported RE distribution coefficients range over

a factor of ten or more, the relative values of RE distribution coefficients

within a given mineral phase are quite uniform. Therefore, the use of

relative RE distribution coefficients is more meaningful than the use of

individual distribution coefficients. Because elements with similar geo-

chemical properties, such as the REE, are often affected in the same

sense by many variables, their relative ratios are usually more constant

than their individual values. In this work, values of RE distribution co-
efficients for several pertinent common rock forming minerals (Fig. 5-1)
as compiled by Helmke and Haskin (1973) are adopted in discussions in-
volving RE behaviour in basic rock systems. The values are taken from
original papers of Schnetzler and Philpotts (1968; 1970), Onuma et al. (1968),
Frey (1969), Culler et al. (1973) and Paster et al. (1974), and are listed in
Appendix C. The clinopyroxene values are for Ca-rich clinopyroxene
and the plagioclase values are for anorthite-rich plagioclase.

Fig. 5-1 shows that plagioclase is relatively enriched in light
REE and exhibits a strong positive Eu anomaly. All the mafic rock forming
minerals have RE distribution coefficient patterns characterized by en-
richment in heavy REE relative to light REE. This is especially the case
in garnet which has high heavy RE distribution coefficients. Except for
the heavy REE in garnet and occasionally in clinopyroxene, these mafic
minerals, in general, have absolute RE distribution coefficient values
less than unity. RE distribution coefficients are very small for ortho-
pyroxene and olivine and are about a factor of ten lower than for co-
existing clinopyroxene.

Data on RE distribution cofficients in acid rock systems are not
as abundant as in basic rock systems. In general, minerals in acid rocks
have higher RE distribution coefficients than corresponding minerals in

Fig. 5-1. Rare Earth Distribution Coefficients for Several Rock

Forming Minerals in Basic Rock Systems (after Helmke

and Haskin, 1973).
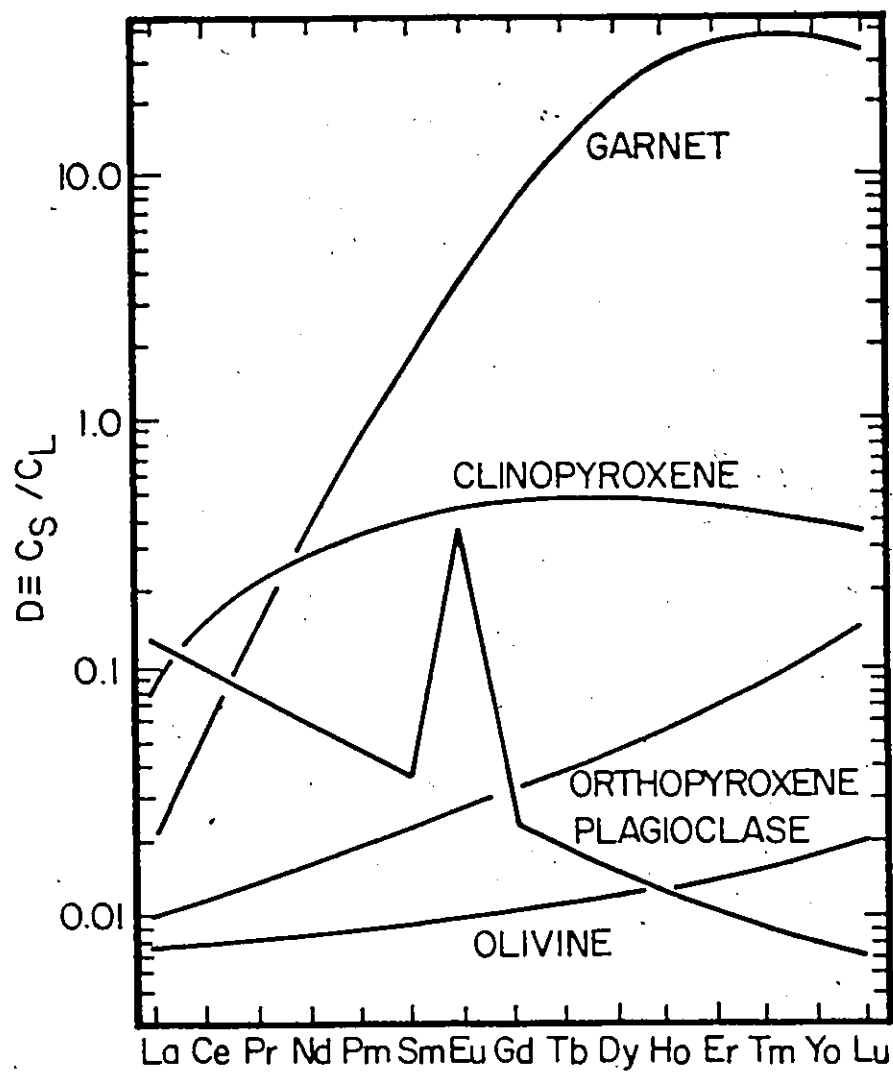
basic rocks (Nagasawa and Schnetzler, 1971).   Biotite and amphibole

have RE distribution coefficient patterns similar to the clinopyroxene

shown in Fig. 5-1.   The RE distribution coefficients for amphibole

sometimes have values greater than unity.   The RE distribution coefficient

pattern for K-feldspar is similar to that of plagioclase but with smaller

values and often with a higher Eu/Eu* ratio than the coexisting plagioclase

(Nagasawa, 1971).   RE distribution coefficients for several common rock

forming minerals in acid rock systems used in this study are compiled

from Higuchi and Nagasawa (1969), Schnetzler and Philpotts (1970) and

Nagasawa and Schnetzler (1971) and are listed in Appendix C.

5-1-2. Rare Earth Patterns in Igneous Rocks

During fractional crystallization, selective RE partition into

crystals may affect the RE pattern of a magma in the following ways:

1) crystallization of garnet will strongly deplete heavy REE in the melt

   and result in a very high La/Yb ratio in the melt;

2) crystallization of clinopyroxene will moderately increase the absolute

   total RE content of the remaining melt.   The increase is more pro-

   nounced for the light REE producing an increase in the La/Yb ratio

   of the melt;

3) crystallization of orthopyroxene and olivine will increase the La/Yb

   ratio and strongly increase the absolute total RE content of the melt;

4) feldspar crystallization will slightly decrease the La/Yb ratio, increase

the absolute total RE content and strongly deplete the Eu content

of the melt.

The reverse of the above effects is expected in the cumulates

precipitated in fractional crystallization and in the unmelted solid phases

in the case of partial melting. The magnitude of these effects depends on

the relative amount of each mineral phase removed from the system.

Owing to the very strong enrichment of Eu in feldspars,

removal of feldspar from a melt may cause a negative Eu anomaly in the

melt and a positive Eu anomaly in early cumulus feldspar-bearing rocks

relative to the initial system. Since feldspars are the only common rock

forming minerals that preferentially concentrate Eu relative to other REE,

they are the most important phases in producing significant Eu anomalies

in a differentiating system.

In summary, in igneous rock systems, olivine, orthopyroxene

and feldspar are the major rock forming minerals that may substantially

change the absolute total RE content of the system. As far as RE frac-

tionation patterns are concerned, garnet and clinopyroxene are the major

rock forming minerals that may appreciably change the La/Yb ratio and

the overall fractionation pattern. Feldspars are the only major rock

forming minerals that may alter the Eu/Eu* ratio of the system.

5-2. Rare Earth Patterns in Differentiated Intrusions

Determination of RE abundances in several differentiated intrusions have been reported. The only systematic discussions of RE behaviour in layered intrusion are those of Haskin and Haskin (1968) and Paster et al. (1974) on the Skaergaard. In this section RE fractionation patterns of layered intrusions are compared in order to illustrate the common features of RE behaviour.

5-2-1. The Skaergaard Intrusion

Detailed RE studies have been made on Skaergaard rocks by Haskin and Haskin (1968) and Paster et al. (1974). The chondrite normalized RE patterns of the Skaergaard rocks are shown in Fig. 5-2.

Haskin and Haskin (1968) found no simple variation between the REE and the major elements in these rocks. All rocks except the late transgressive acid granophyres have RE abundances similar to the chilled marginal gabbro.. The cumulates remained essentially constant in their absolute RE abundances and their RE fractionation patterns fluctuated only slightly from that of the chilled marginal gabbro through solidification of some 97% of the magma. They concluded that the REE became increasingly concentrated in the residual liquid with little change in the RE fractionation pattern as solidification progressed.

Fig. 5-2. Rare Earth Fractionation Patterns in the Skaergaard

Intrusion (from Haskin and Haskin, 1968).
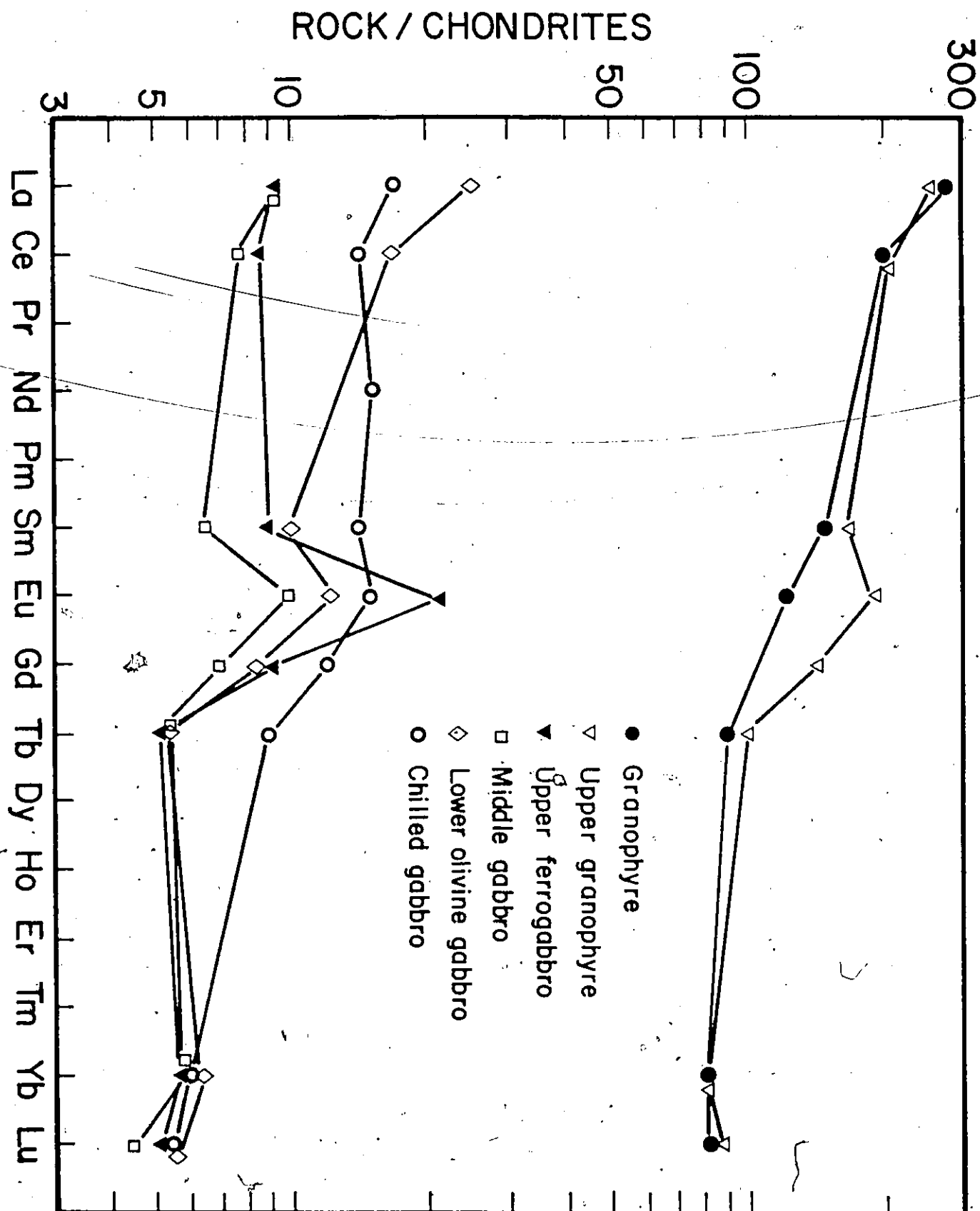
Paster et al. (1974) analysed additional Skaergaard rocks
and mineral separates and found that the RE distribution coefficients
for pyroxene and plagioclase appear to decrease markedly with increasing
solidification of the magma. They attributed this effect to closed-system
crystallization of trapped intercumulus liquid. Because the intercumulus
liquid is high in REE, very high RE concentrations accumulate in the
margins of the cumulus minerals. As the amount of trapped liquid de-
creases towards the top of the Layered Series, the apparent RE distribution
coefficients of the minerals decrease as well.

All the Skaergaard gabbroic cumulates have positive Eu
anomalies due to the presence of cumulus plagioclase in these rocks. The
RE content of the final granophyre is more than ten times that of the
gabbros and is characterized by a negative Eu anomaly relative to the
chilled marginal gabbro.

5-2-2. The Stillwater Intrusion

Frey et al. (1968) reported RE abundances in a chilled
gabbro from the Stillwater intrusion (Fig. 5-13) with very low total REE,
strongly depleted light REE (La/Yb = 0.40), and strong positive Eu
anomaly (Eu/Eu = 3.9). These parameters are drastically different
from the RE fractionation patterns of other continental basic rocks. If
the RE fractionation pattern of this rock represents the original magma,
then its strong positive Eu anomaly indicates a high degree of selective

assimilation of plagioclase by the magma prior to intrusion, which is
unlikely.

A new analysis of the same chilled gabbro sample by Kosiewicz
(1973) confirmed this RE pattern, but another chilled gabbro analyzed by
Kosiewicz (see Fig. 5-3) had a flat RE pattern with higher total RE
abundances and no significant Eu anomaly. This sample was considered
by Kosiewicz to be more representative of the composition of the Still-
water chilled gabbro. He also analyzed other rocks from different zones
in the Stillwater intrusion. The data are presented in Fig. 5-3.

No systematic study of RE variation in the intrusion as a
whole was attempted by Kosiewicz. Instead, he considered each rock
sample on an individual basis. The RE abundances of the intercumulus
material were obtained by subtracting the estimated amount of REE in
the cumulus minerals from the RE abundances in the whole rock. Unlike
the Skaergaard, the RE fractionation patterns of the intercumulus
materials in the Stillwater rocks do not appear to represent unfrac-
tionated frozen parent liquid. Kosiewicz suggested that this was due to
partial solidification of the trapped liquid in situ followed by migration
of the final dregs of liquid over short distances and out of the system re-
presented by the analysed sample.

Fig. 5-3. Rare Earth Fractionation Patterns in the Stillwater Intrusion

(from Frey et al., 1971 and Kosiewicz, 1973).
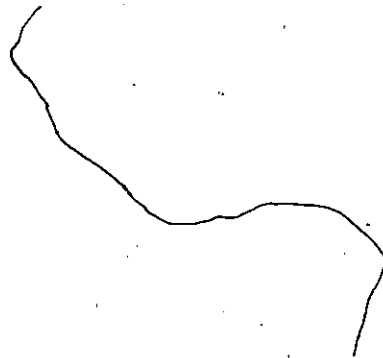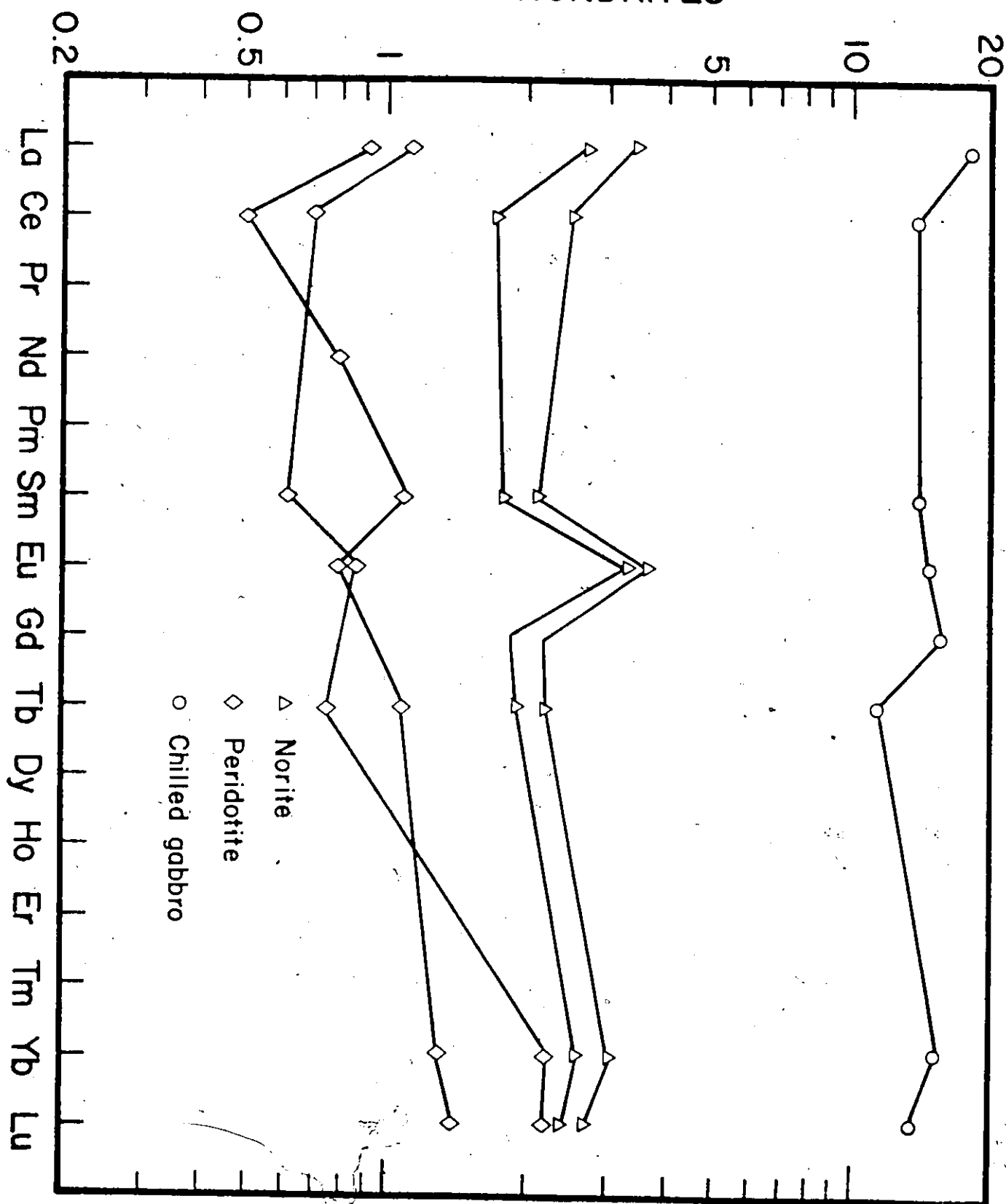
Fig. 5-3 shows that the Stillwater cumulates have total RE contents much lower than the chilled gabbro. All the rocks have relatively flat RE fractionation patterns. There are distinct positive Eu anomalies in the Stillwater norites, probably due to cumulus plagioclase in these rocks.

5-2-3. The Bushveld and Muskox Intrusions

Neither the Bushveld nor Muskox intrusions have been systematically studied with regard to REE. Available data for the Bushveld from Frey et al. (1968; 1971) and Hunter (1974) and for the Muskox from Kosiewicz (1973) are shown in Figs. 5-4 and 5-5, respectively.

The norite and pyroxenite from the Bushveld intrusion have similar RE fractionation patterns. Both are enriched in light REE and the norite has a distinct positive Eu anomaly due to cumulus plagioclase. Its total RE content is about ten times higher than the pyroxenite. The Bushveld granite and felsite have almost identical RE patterns with the granite having higher absolute RE abundances. Both are enriched in light REE and have strong negative Eu anomalies. Their total RE contents are a factor of ten higher than the norite.

Fig. 5-4. Rare Earth Fractionation Patterns in the Bushveld

Intrusion (from Frey et al. , 1968, 1971 and Hunter,

1974).
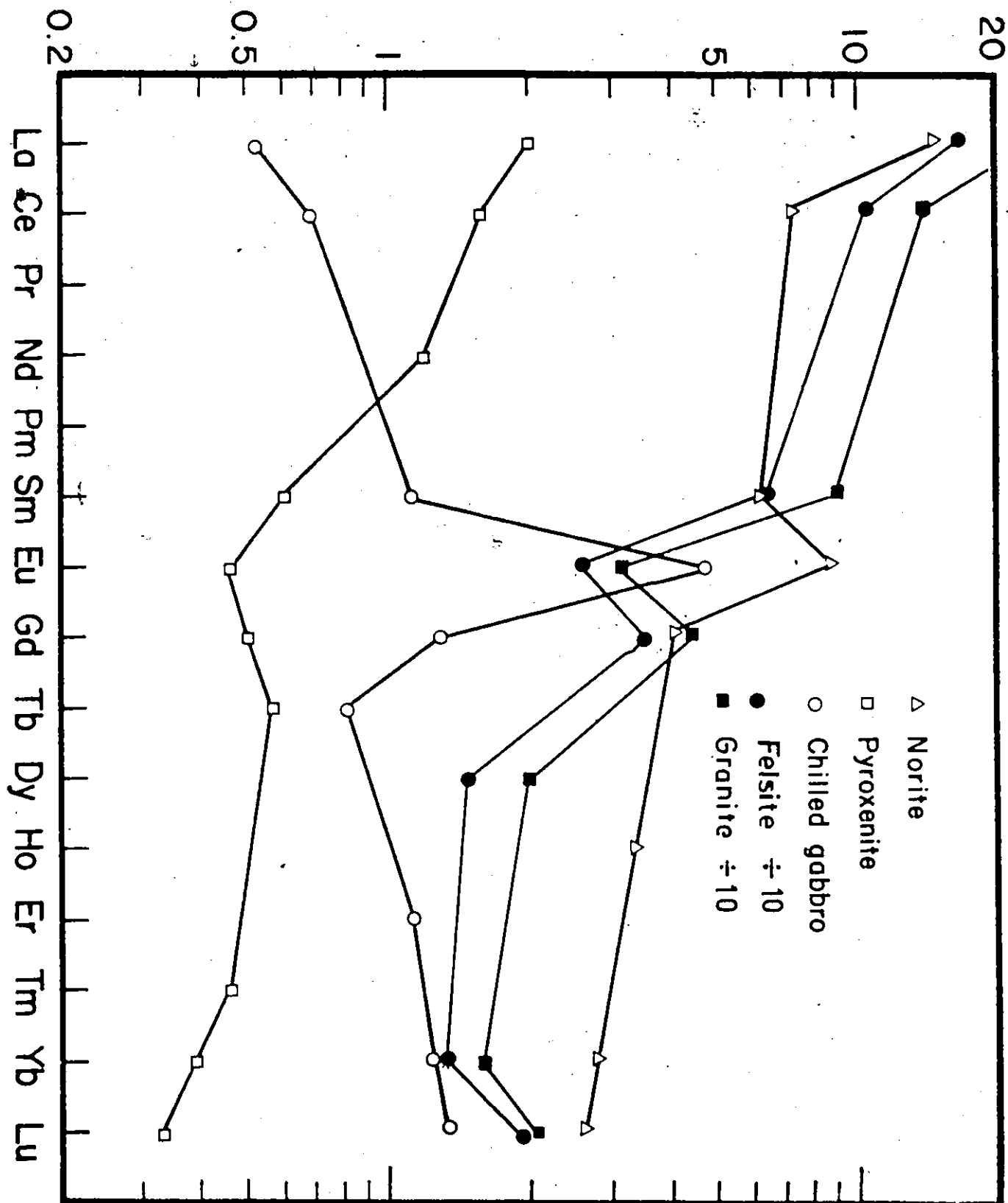
The Bushveld chilled gabbro analysed by Frey et al. (1968) has a peculiar RE fractionation pattern similar to the Stillwater chilled gabbro reported by Frey et al. (1968); that is, very low total RE abundances, depletion in light REE (La/Yb = 0.31), and a very strong positive Eu anomaly (Eu/Eu* = 2.4). Other Bushveld rocks, however, have light REE enrichment and much lower Eu/Eu* ratios. No reasonable mechanism has been proposed to derive the RE fractionation patterns observed in the Bushveld cumulates from a magma with a RE pattern similar to the chilled gabbro. Therefore, one may suspect that this particular sample does not represent the RE fractionation pattern of the original Bushveld magma. The magma probably had a RE fractionation pattern similar to that of the norite shown in Fig. 5-4, but with a much lower Eu/Eu* ratio. Future analyses on other chilled gabbro samples may clarify this problem.

Gabbroic and pyroxenitic cumulates from the Muskox intrusion have RE fractionation patterns compatible to similar cumulates in other layered intrusions. The mafic rocks are enriched in light REE and have higher total RE contents and La/Yb ratios than the ultramafic rocks. The granophyre has an even higher La/Yb ratio and much higher total RE content than any other rocks in the intrusion. One gabbroic cumulate has a positive Eu anomaly due to plagioclase accumulation whereas the granophyre has a very strong negative Eu anomaly. Unfortunately, no RE fractionation pattern for the Muskox chilled gabbro is available.

Fig. 5-5. Rare Earth Fractionation Patterns in the Muskox

Intrusion (from Kosiewicz, 1973).
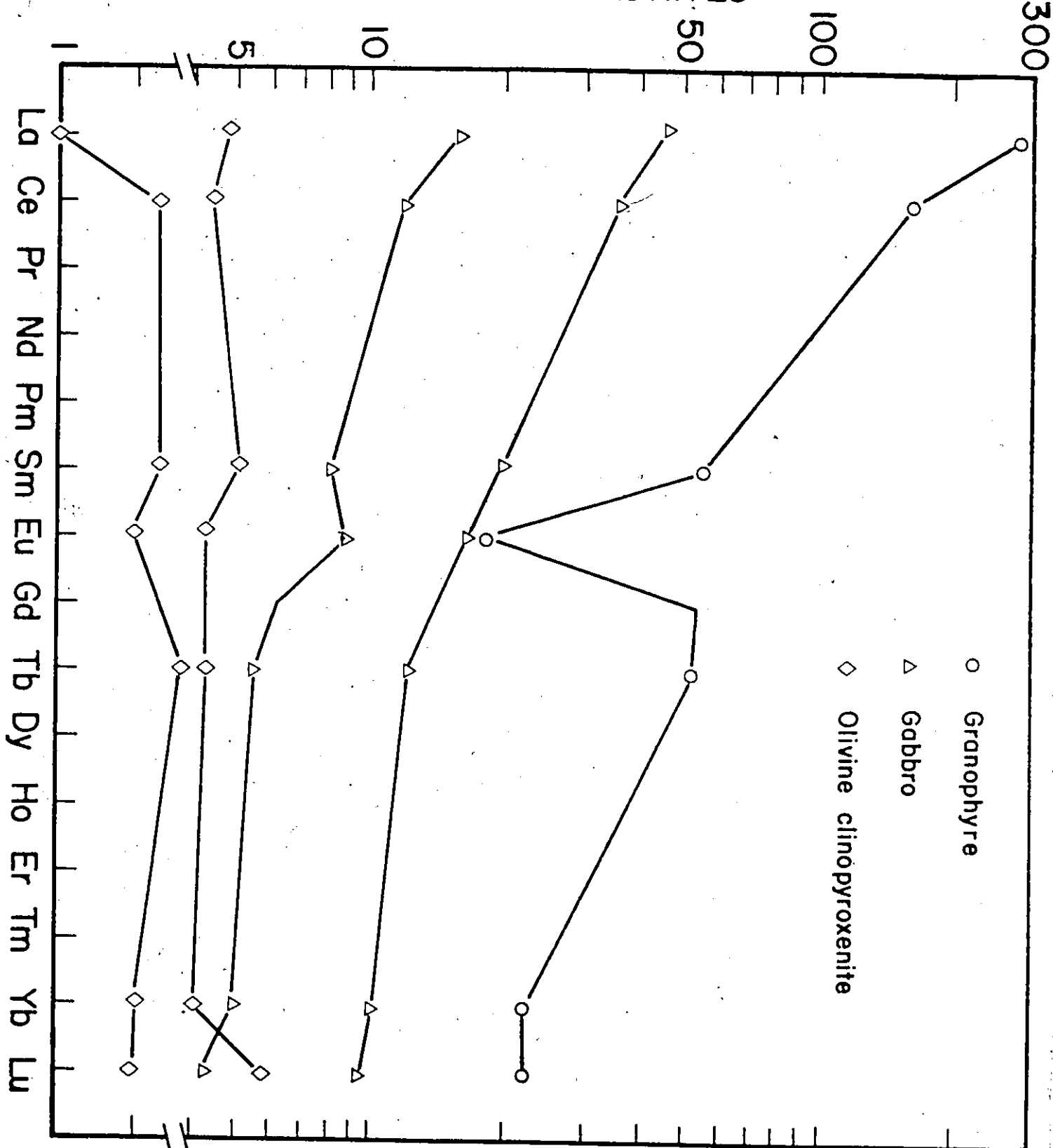
5-2-4. The Southern California Batholith

Towell et al. (1965) studied the RE fractionation patterns in several plutons of the Southern California Batholith. Their results are presented in Fig. 5-6.

They attributed the increase in absolute total RE content, the increase in fractionation favouring the light REE and the decrease in Eu/Eu* ratio with increasing acidity of the rocks to magmatic differentiation of gabbroic magma at depth. They also suggested that the anomalous behaviour of Eu was due to partial reduction of the element to Eu^{+2} which followed Sr^{+2} in feldspars.

5-3. Rare Earth Behaviour in Layered Basic Intrusions

5-3-1. Features of Rare Earth Behaviour in Layered Basic Intrusions

From the observed RE fractionation patterns of rocks in different layered intrusions discussed in section 5-2, several general features of RE behaviour in layered basic intrusions can be recognized:

1) There is a trend of increasing total RE abundances in rocks from stratigraphic bottom to top of layered intrusions, with the final acid rocks having total RE contents which are often much higher than rocks formed at early stages;

Fig. 5-6. Rare Earth Fractionation Patterns in the Southern

California Batholith (after Towell et al. , 1965).
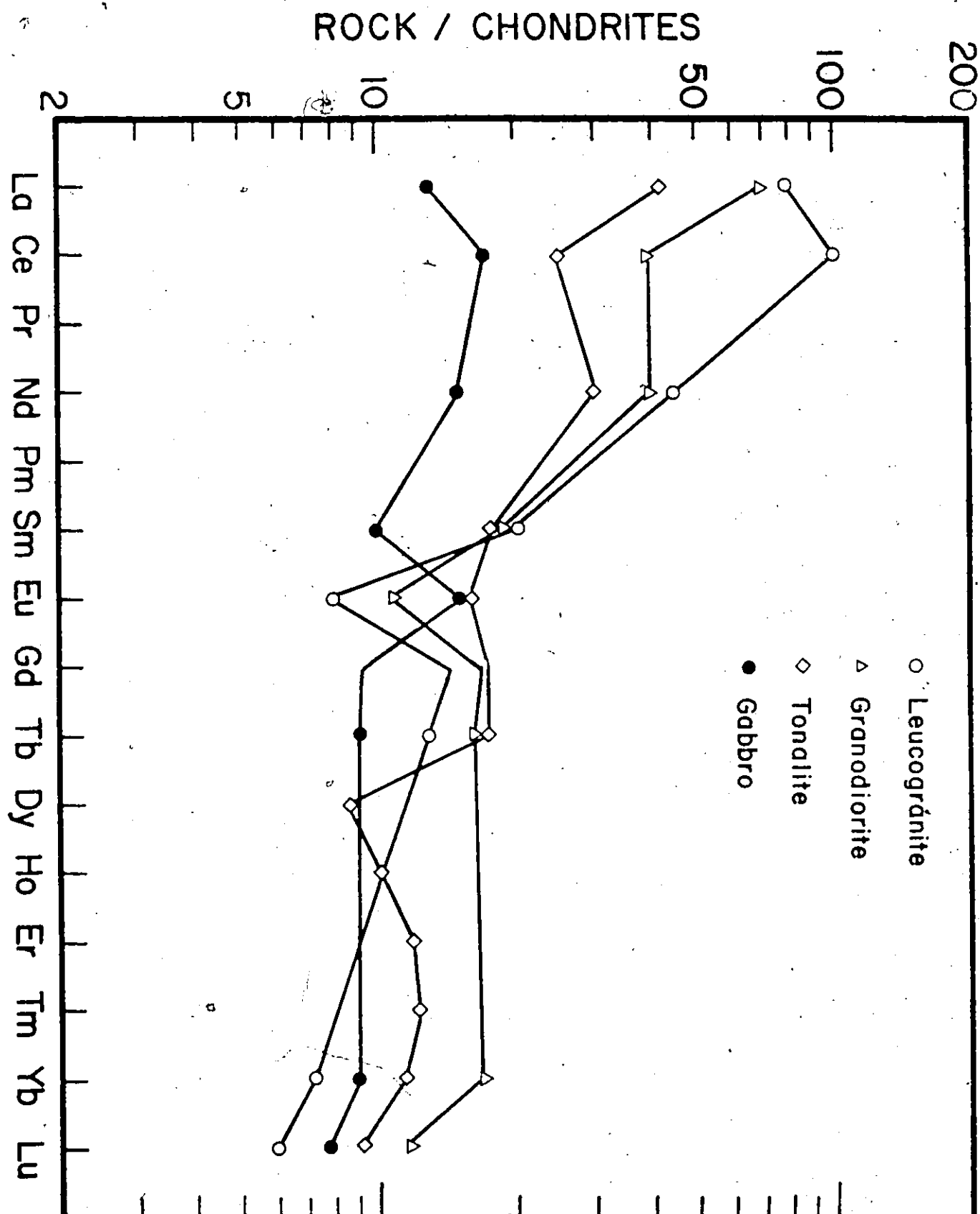
2) Rocks formed at an early stage tend to have total RE contents lower than the chilled marginal gabbro, while rocks formed at later stages tend to have total RE contents higher than the chilled gabbro;

3) There is a general trend of increasing La/Yb ratio from stratigraphic bottom towards the top of the intrusion with a tendency of early stage rocks to have lower La/Yb ratios and late stage rocks higher La/Yb ratio with respect to the chilled gabbro;

4) Gabbroic rocks often show positive Eu anomalies and late stage acid rocks show negative Eu anomalies with respect to their chilled border gabbros;

5) Except for Eu, rocks from a particular layered intrusion generally have RE fractionation patterns similar to their chilled gabbros. Deviations from the RE fractionation pattern of the chilled gabbro are sometimes observed in early stage ultramafic rocks.

5-3-2. Theoretical Considerations on Rare Earth Behaviour in Layered Basic Intrusions

The behaviour of trace elements during magmatic differentiation has been described by mathematical models in many papers (McIntire, 1963; Schilling and Winchester, 1967; Gas t, 1968; Greenland, 1970; Shaw, 1970, 1972). When a trace element (such as a REE) is partitioned between two phases such that thermodynamic equilibrium is reached in a closed system, its distribution between coexisting phases can be described by the Nernst

distribution law:

$$D = a_x^s \ / \ a_x^\ell \qquad \qquad \cdots \qquad 5\text{-}1$$

where D = distribution coefficient,

a_x^s = activity of component x in phase s, say in the solid phase,

a_x^ℓ = activity of component x in phase ℓ, say in the liquid phase.

If we assume that a magma undergoes fractional crystallization in a closed system and that during the crystallization only the surface of the crystals is in equilibrium with the coexisting liquid phase, or that as soon as crystals are formed they are removed from the liquid phase, then an expression based on the Doerner-Hoskins distribution law (see McIntire, 1963) is usually more applicable. Greenland (1970) has developed a general equation that describes the trace element distribution in rocks for different crystallization models which takes into account the variations of mineral proportions and distribution coefficients during the crystallization. However, for general purposes, the simpler Rayleigh fractionation law which is actually a particular case of Greenland's (1970) equation (6), is often adopted. The main assumptions are that minerals crystallize in constant proportions and have constant trace element distribution coefficients.

In such a system, the average concentration of a trace element in all the solid phases ($\overline{C}^s$) formed after a fraction X of the initial system has crystallized, is given by

$$\overline{C}^s = C^o (1 - (1-X)^D) / X \qquad \dots \quad 5\text{-}2$$

where C^o = trace element concentration in the initial system,

D = combined distribution coefficient of the trace element

for all the solid phases.

The trace element concentration in the residual liquid phase (C^ℓ) after a fraction X of the initial melt has crystallized is given by

$$C^\ell = C^o (1-X)^{D-1} \qquad \dots \quad 5\text{-}3$$

Similar equations can be used to describe trace element behaviour during fractional melting (Shaw, 1970).

Most cumulates in layered intrusions contain intercumulus liquid (Wager et al., 1960). If we assume that the intercumulus liquid has the same trace element concentration as the magma which is in equilibrium with the cumulus crystals and that all intercumulus liquid is trapped and solidifies as intercumulus material, the concentration of a trace element in the final rock can then be expressed as

$$C^c = F\,C^s + (1-F)\,C^\ell \qquad \dots \qquad 5\text{-}4$$

or

$$C^c = C^\ell(1 + F(D-1)) \qquad \dots \qquad 5\text{-}5$$

On the other hand, the intercumulus liquid may experience _in situ_ fractional crystallization under partially closed system conditions whereby the final dregs of the liquid are squeezed out of the rock. In this case the average trace element concentration in the solid phase formed from the intercumulus liquid can be expressed by equation 5-2:

$$\overline{C^s} = C^\ell(1 - (1-X_t)^{D_t})\,/\,X_t \qquad \dots \qquad 5\text{-}6$$

and the trace element concentration in the final rock becomes

$$C^c = F\,C^s + (1-F)\,\overline{C^s} \qquad \dots \qquad 5\text{-}7$$

or

$$C^c = C^\ell(FD + (1-F)(1-(1-X_t)^{D_t})\,/\,X_t \qquad \dots \qquad 5\text{-}8$$

In these equations

C^c = concentration in the final rock,

C^ℓ = concentration in the liquid phase (intercumulus liquid) which is in equilibrium with the cumulus phase,

F = weight fraction of the cumulus phase in the final rock,

$1-F$ = weight fraction of the intercumulus material in the final rock,

D = distribution coefficient for the cumulus phase,

X_t = weight fraction of the intercumulus liquid that has crystallized,

D_t = distribution coefficient for the solid phase formed from the intercumulus liquid.

In this study intercumulus material is defined as material formed from trapped intercumulus liquid by closed system crystallization. Adcumulus overgrowth formed under open system conditions is considered to have RE composition similar to the cumulus phase.

From Fig. 5-1, it is clear that most major rock forming minerals in basic layered intrusions, at least at an early stage of crystallization, have RE distribution coefficients which are less than unity (excluding garnet which is not observed in the layered intrusions discussed in section 5-2). Therefore, the values of (1-X), $(1-X_t)$, F, (1-F), D and D_t in the above equations are likely to be less than unity. In this case then $C^c < C^{\ell}$ and $C^{\ell} > C^o$; that is, the cumulate will have lower total RE content than the coexisting liquid phase and the total RE content of the residual liquid will become progressively greater as the process of fractionation continues. These relationships provide the basic reasons for observation (1) in section 5-3-1.

It is clear that at the outset of magma crystallization the values of C^{ℓ} in the above equations approach C^o. Thus, the trace element concentration in the original magma is usually closely approximated by the chilled border rock in layered intrusions. This is the basis of observation (2) in section 5-3-1.

When considering the distribution of La or Yb in layered intrusions equation 5-1 can be written as

$$C_s^{La} = C_{\ell}^{La}\, D^{La} \qquad \ldots\ldots \quad \text{5-9}$$

or

$$C_s^{Yb} = C_{\ell}^{Yb}\, D^{Yb} \qquad \ldots\ldots \quad \text{5-10}$$

Division of equations 5-9 by 5-10 gives

$$(La/Yb)^s = (La/Yb)^{\ell}(D^{La}/D^{Yb}) \qquad \ldots\ldots \quad \text{5-11}$$

Similarly, equation 5-3 gives

$$(La/Yb)^{\ell} = (La/Yb)^o\,(1-X)^{D^{La}-D^{Yb}} \qquad \ldots\ldots \quad \text{5-12}$$

Similar types of equation can be derived for equations 5-5 and 5-8. In basic layered intrusions in which early stage cumulates are dominated by mafic minerals D^{La} will be smaller than D^{Yb} (see Fig. 5-1). Therefore, $(La/Yb)^s < (La/Yb)$ and $(La/Yb)^{\ell} > (La/Yb)^o$. These considerations provide the basic reasons for observation (3) in section 5-3-1.

Basic reasons for observation (4) in section 5-3-1,

that is, the behaviour of Eu in layered intrusions will be discussed in

section 5-7.

Equation 5-5 indicates that the RE composition of a rock

containing both cumulate and intercumulus material is, in part, a

function of the amount of intercumulus liquid in the rock. The contri-

butions of varying amounts of intercumulus material to the whole rock

RE content can be estimated from the RE distribution coefficients for

the cumulus minerals. Fig. 5-1 shows that clinopyroxene has the largest

RE distribution coefficient for common rock forming minerals in basic

rock systems (excluding garnet). Therefore, the contribution of inter-

cumulus material will be a minimum for a clinopyroxene cumulate.

By assuming that all of the intercumulus liquid solidifies

in situ and using equation 5-4, one can calculate the contributions of vary-

ing amounts of intercumulus material to the RE contents of clinopyroxene

cumulates formed at the beginning of magma crystallization. Similar

calculations can be carried out for the ratios of La/Yb from the relation-

ship

$$(La/Yb)^c = \frac{FC_s^{La} + (1-F)\,C_{\ell}^{La}}{FC_s^{Yb} + (1-F)\,C_{\ell}^{Yb}} \qquad \ldots \qquad 5\text{-}13$$

which is derived from equation 5-4. Results of such calculations
are listed in Table 5-1.

Similarly, the RE fractionation patterns of cumulates
crystallizing in the presence of varying amounts of intercumulus
liquid can also be estimated. Again, because clinopyroxene has the
largest distribution coefficients, this effect will be minimum for a
clinopyroxene cumulate. Using the same equations and making the same
assumptions as above, the calculated RE fractionation patterns of clino-
pyroxene cumulates containing varying amounts of intercumulus material
are as shown in Fig. 5-7.

These calculations indicate that at an early stage of cry-
stallization the effects of intercumulus material on the RE contents and
RE fractionation patterns of the cumulates, and the deviation of these
parameters from that of the original magma, will depend on the amount
of trapped liquid and the type of cumulus mineral that crystallizes.
However, as fractionation proceeds, an increase in RE content of the
residual liquid will generally occur. The importance of this effect may
be considered for a hypothetical case in which solidification of a magma

Table 5-1. Rare Earth Contributions of Varying Amounts of Intercumulus Material to Clinopyroxene Cumulates and the La/Yb Ratios of the Cumulates Relative to the Parent Magma

Amount of intercumulus material in rock	Contribution by intercumulus material (%)							(La/Yb) Rock/Parent Magma
	La	Ce	Sm	Eu	Tb	Yb	Lu	
60%	95	90	79	77	75	78	79	0.82
50%	93	85	71	69	66	70	71	0.76
40%	91	80	63	59	56	62	64	0.68
30%	86	71	52	48	46	51	53	0.59
20%	77	59	39	35	33	37	39	0.48
10%	59.	40	22	20	18	21	22	0.35
5%	42	24	12	10	9	11	12	0.27

(C^o) has reached the mid-point (X=0.5). Clinopyroxene is considered the only phase to separate from the system prior to this point (D = distribution coefficient for clinopyroxene). From the relation $C^{\ell} = C^o (1-X)^{D-1}$ the RE pattern of the residual liquid (line L) can be calculated relative to the original magma (line A) at this time. The result is shown in Fig. 5-8.

The RE content in this residual liquid (L) is higher than the original magma but the RE fractionation pattern deviates little from the original magma (A). At this stage it is assumed that clinopyroxene and plagioclase start to crystallize simultaneously in a ratio of one-to-one. The contributions of varying amounts of intercumulus material, which now has the composition of liquid L, to the RE contents, La/Yb ratios and RE fractionation patterns of 1:1 clinopyroxene-plagioclase cumulates formed at this stage can be calculated. The results are listed in Table 5-2 and shown in Fig. 5-8 respectively.

These calculations show that intercumulus material contributes significantly to the RE contents as well as the RE fractionation patterns of the cumulates. Due to the very small values of RE distribution coefficients of olivine, plagioclase (except Eu), and pyroxene, extensive crystallization of these minerals is required to substantially change the RE fractionation pattern of the original magma.

Fig. 5-7. Comparison of Calculated Rare Earth Patterns of

Clinopyroxene Cumulates containing Varying

Amounts of Intercumulus Material with the Parent Magma.

CLINOPYROXENE / PARENT MAGMA

Table 5-2. Rare Earth Contributions of Varying Amounts of Intercumulus Material to a 1:1 Clinopyroxene-Plagioclase Cumulate, and the La/Yb Ratios of these Cumulates Relative to the Original Magma after Half of the Original Magma has Crystallized as Clinopyroxene

Amount of intercumulus material in rock	Contribution by Intercumulus Material (%)							(La/Yb) Rock/ Original magma
	La	Ce	Sm	Eu	Tb	Yb	Ln	
60%	95	89	87	79	86	88	88	1.2
50%	90	89	82	73	78	82	83	1.2
40%	85	83	75	61	71	76	77	1.1
30%	79	76	66	51	61	67	68	1.1
20%	69	64	53	37	48	54	56	0.98
10%	50	45	34	21	29	34	36	0.86
5%	32	27	20	11	16	20	21	0.79

Fig. 5-8. Comparison of Rare Earth Patterns of Residual
Liquid L and 1:1 Clinopyroxene-Plagioclase
Cumulates with Original Magma A. Formation of
Clinopyroxene-Plagioclase Cumulates begins After
Half the Original Magma has Crystallized as Clino-
pyroxene. Patterns Calculated for Cumulates
containing 5 to 60% Intercumulus Material.
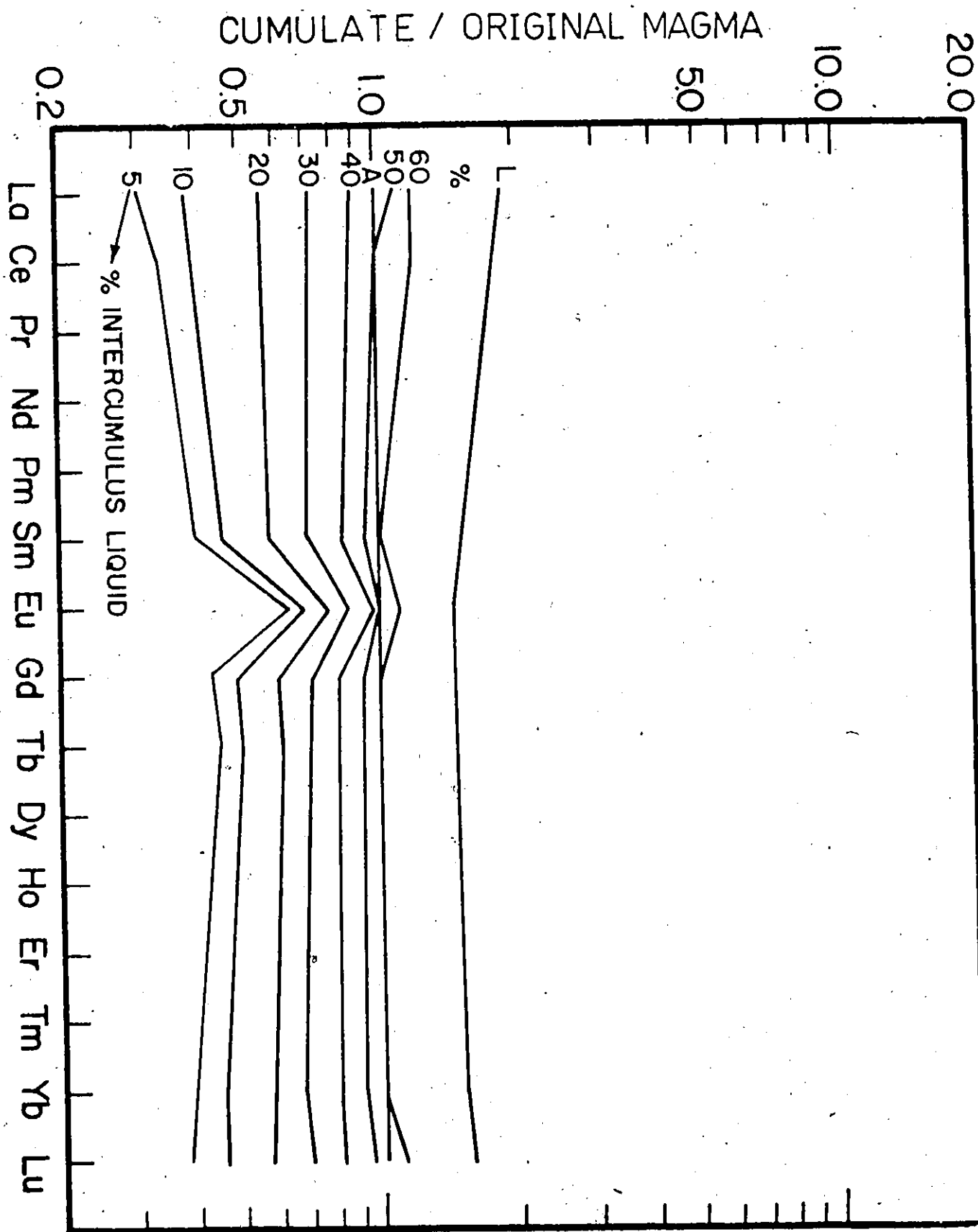
These calculations also show that deviations of RE fractionation patterns of cumulates from the original magma will be minimized if plagioclase and mafic minerals precipitate simultaneously. Thus, the preferential incorporation of heavy REE into the mafic minerals will be compensated by the preferential incorporation of light REE into plagioclase. Deviations from the RE pattern of the original basic magma will be further minimized if these cumulates form at a middle stage of differentiation (as calculated in Fig. 5-8). Thus, the light REE enrichment of the magma prior to precipitation of mafic minerals will also compensate for the preferential incorporation of heavy REE into the mafic minerals. Hence, gabbroic rocks from a middle section of a layered basic intrusion often have RE fractionation patterns (except for Eu) similar to the original magma.

Similar calculations can be performed for cumulates described by equation 5-8; that is, where the intercumulus liquid undergoes in situ fractional crystallization in a partially crystallized closed system with loss of the final dregs of liquid. As many variables are involved calculations have not been pursued. However, by comparing equations 5-8 and 5-6 with equation 5-4, it appears that results similar to those shown in Tables 5-1 and 5-2 and Figs. 5-7 and 5-8 but with less pronounced fractionation effects would be obtained.

In an orthocumulate, most of the intercumulus liquid is trapped and solidifies _in situ_ and the rock has a high content of intercumulus material. In an adcumulate, adcumulus growth will gradually push out the intercumulus liquid and thus reduce the amount of the intercumulus material in the final rock. Therefore, in layered intrusions, early stage orthocumulates have RE contents slightly less than the original magma and RE fractionation patterns similar to the original magma. Early stage adcumulates have RE contents somewhat less than the original magma and RE fractionation patterns reflecting the combined RE patterns of the constituent minerals in the rocks. These patterns may deviate somewhat from that of the original magma.

Wager _et al._ (1960) considered rocks of the Skaergaard intrusion to be largely orthocumulates. Rocks of the Stillwater intrusion are largely adcumulates. The amounts of intercumulus material in the Stillwater cumulates are estimated to be between 0 to 28 percent by Koniewicz (1973) as compared to 28 to 52 percent in the Skaergaard cumulates according to Pastor _et al._ (1974). The different amount of intercumulus material in the Stillwater adcumulates and Skaergaard orthocumulates may explain the fact that the early Stillwater cumulates have total RE contents a factor of ten less than that of its chilled gabbro and RE fractionation patterns deviating somewhat from its chilled gabbro, whereas the Skaergaard cumulates are only slightly lower in REE than the chilled gabbro and have RE fractionation patterns similar to the chilled gabbro.

Wager and Brown (1967) established experimentally that most cumulates contain intercumulus liquid and estimated that as much as 50% intercumulus liquid may coexist with the cumulus minerals in some layered intrusions. The fact that some layered intrusions show little change in RE fractionation patterns and have patterns that are similar to the chilled marginal facies, indicates that trapped intercumulus liquid played an important role in the RE behaviour of these layered intrusions. Calculations and discussions performed above are the basic reasons for observation (5) in section 5-3-1.

In the case of continued equilibrium crystallization, that is, where crystals remain at all times in complete equilibrium with the liquid, then the trace element concentration in the residual liquid (C^L) after a fraction X of the initial system (C^O) has crystallized is given (Shaw, 1970; 1972) as

$$C^L = \frac{C^O}{(1-X) + D X}.$$

.... 5-14

and the equilibrium trace element concentration of the crystal (C^B) is given by

$$C^B = C^L D$$

.... 5-15

Equations 5-14 and 5-15 correspond to equations 5-3 and 5-1 in the

Rayleigh fractionation model. Based on these two equations, the same

conclusions as obtained from the Rayleigh model can be derived. The

main difference in the two cases is that in the continuous equilibrium

model the REE will not be as highly concentrated in the final residual

liquid phase (and therefore the final stage rocks) as in the case of the

Rayleigh fractionation model.

In summary, the calculations and accompanying discussions

outlined in this section, although based on simplified ideal cases, appear

to provide basic explanations for the general features of RE behaviour

in layered basic intrusions.

5-4. <u>Rare Earth Behaviour in the Sudbury Main Irruptive</u>

5-4-1. <u>Comparison of the North and South Range Rocks</u>

The number of main Irruptive rocks analyzed is not sufficient

to make a detailed correlation of north and south range rocks similar to

the modal and cryptic layering correlations of Naldrett <u>et al</u>. (1970;

1972, see fig. 2-2). Examination of Figs. 4-1 and 4-2 suggests that

micropegmatite on the north range has a slightly wider range of RE

patterns than micropegmatite on the south range. In contrast, norite

on the south range appears to have a wider range of RE patterns than

norite on the north range. These differences may reflect minor petro-

graphic differences between the north and south range rocks, or they

may reflect differing sample populations of the corresponding

rock units on the north and south ranges. In any case, north and

south range RE fractionation patterns are characterized more by their

similarities than their differences.

A comparison of average RE patterns and RE ratios for

various units of the north and south ranges shows the marked similarities

between the corresponding rock units. Overall averages for REE,

Eu/Eu* and La/Yb were calculated for the principal rock units for the

entire Irruptive and the results are presented in Table 5-3. Chondrite

normalized fractionation patterns representing averages for various rock

units are shown in Figs. 5-9 and 5-10.

5-4-2. Border Norite of the Main Irruptive

The Sudbury Nickel Irruptive does not have an obvious

chilled border facies as do many other layered intrusions. However,

Naldrett et al. (1970) recognized certain systematic trends in mineralogy,

texture and chemical composition in the south range quartz-rich norite.

These include decreasing quartz content, decreasing Fe/(Fe+Mg) ratio of

pyroxene and increasing grain size of plagioclase away from the country

rock contact (that is, structurally upwards). They interpreted the

quartz-rich norite as a rather rapidly cooled border facies of the south

range rocks. Subsequently, Hewins (1971) observed similar trends in

the north range mafic norite and suggested that this unit was the rapidly

cooled border facies on the north range.

Table 5-3. Comparison of Average Rare Earth Properties of North and South Range Main

Irruptive Rocks

Rock Unit	Average ΣREE			Average Eu/Eu*			Average $(La/Yb)_N$		
	North Range	South Range	Main Irruptive	North Range	South Range	Main Irruptive	North Range	South Range	Main Irruptive
Micropegmatite	180	174	178	0.78	0.75	0.76	16.2	11.8	14.7
Oxide-rich gabbro	159	200	180	0.94	0.90	0.92	8.91	16.5	12.7
Norite	74.1	59.6	65.3	1.42	1.24	1.31	10.5	8.79	9.87
Border Norite	95.1	99.4	97.3	1.00	0.95	0.98	12.5	11.0	11.8

Fig. 5-9. Average Rare Earth Fractionation Patterns of North

Range (N. R.) and South Range (S. R.) Main

Irruptive Rocks

REE diagram. X-axis: La Ce Pr Nd Pm Sm Eu Gd Tb Dy Ho Er Tm Yb Lu. Y-axis: ROCK / CHONDRITES (2, 5, 10, 50, 100, 200).

Legend:
- ○ N.R. micropegmatite
- ● S.R. micropegmatite
- ▼ N.R. oxide-rich gabbro
- □ N.R. felsic norite
- △ S.R. upper gabbro
- ■ S.R. norite
- ⊙ N.R. mafic norite
- ◇ S.R. quartz-rich norite
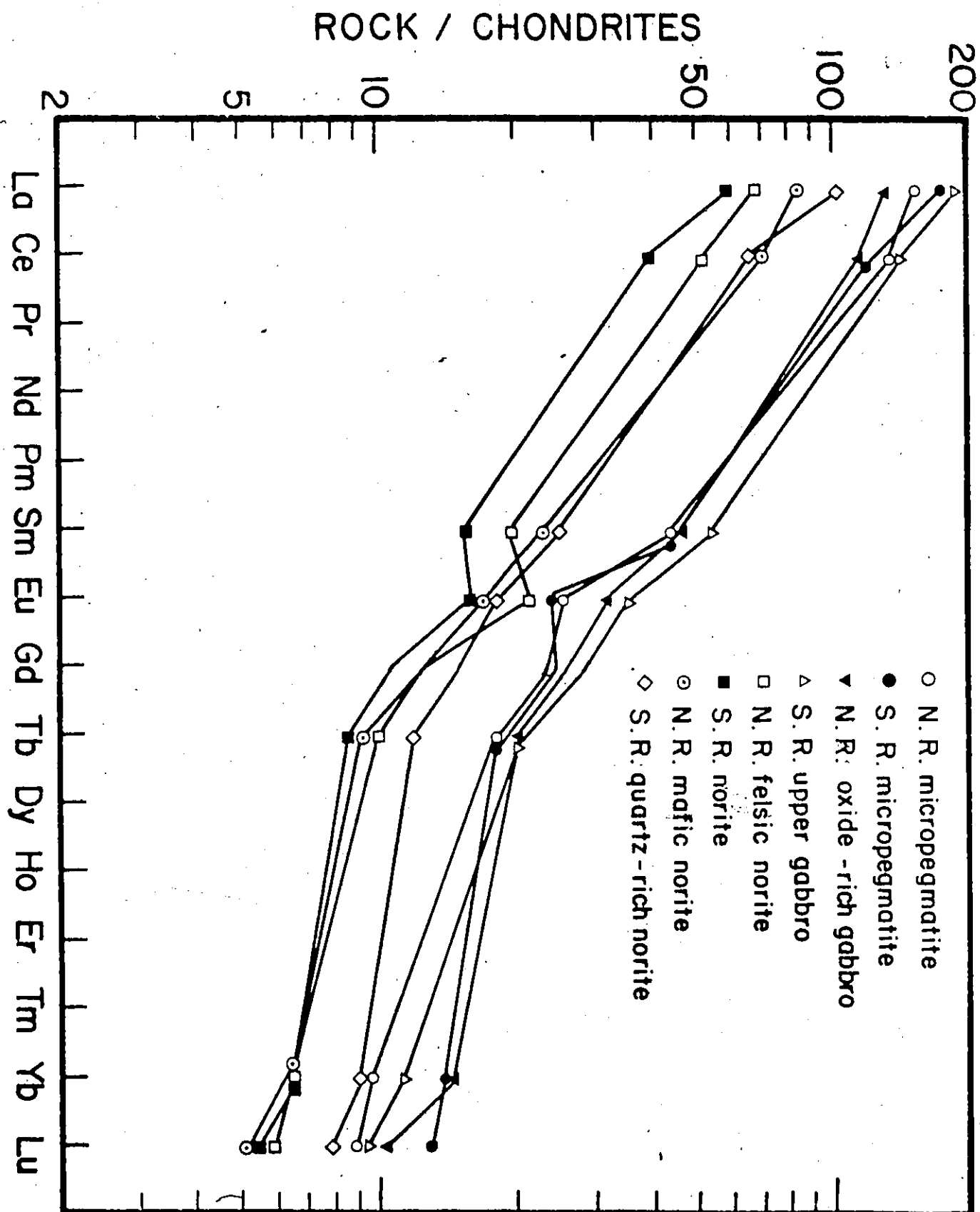
Fig. 5-10. Rare Earth Fractionation Patterns of Average

Sudbury Main Irruptive Rocks
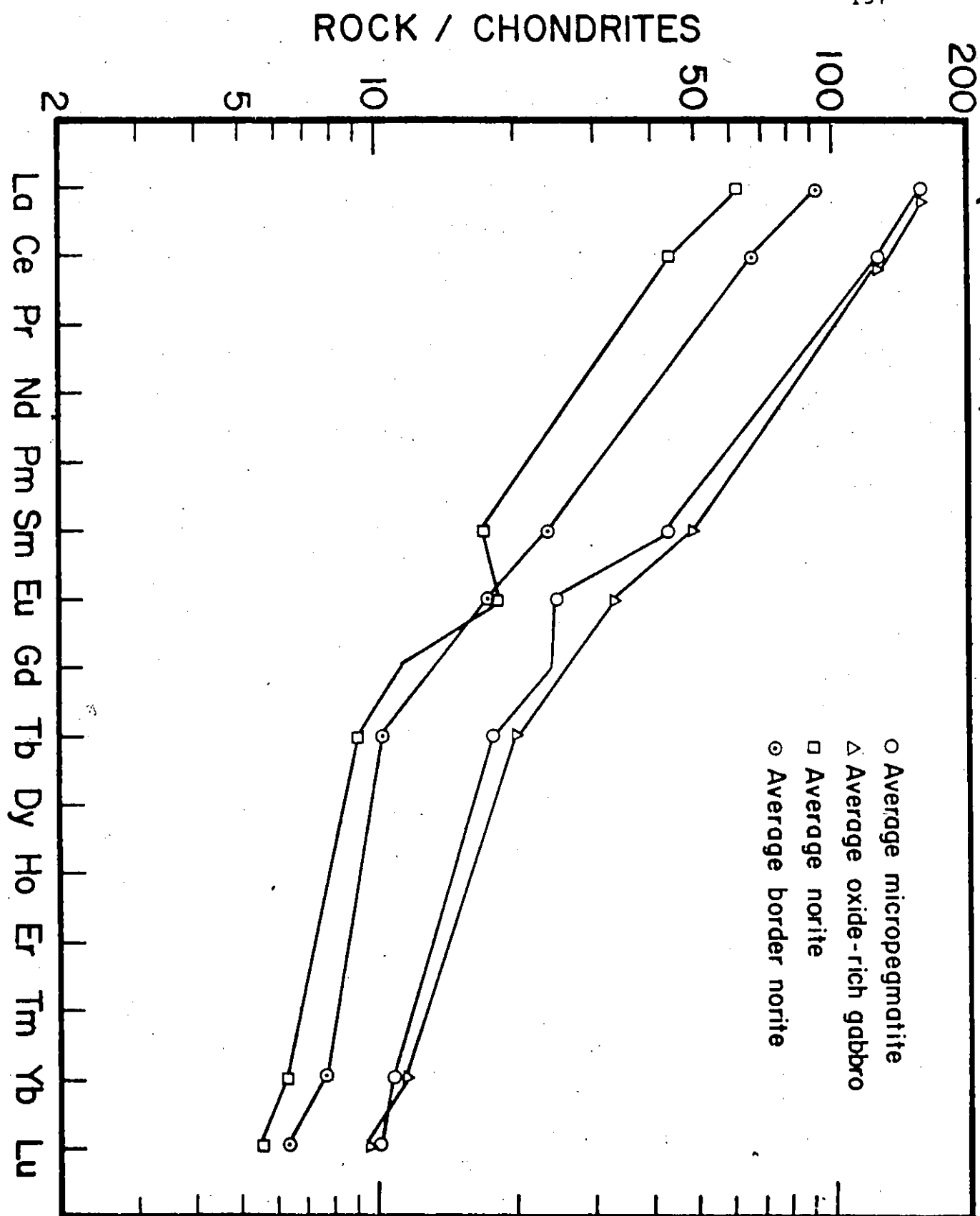
These border norites, if rapidly cooled, should retain the RE properties of the original main Irruptive magma, especially with respect to RE fractionation patterns. Thus, in a rapidly cooled border rock cumulus crystals do not have sufficient time to settle, and little interchange is expected between the intercumulus liquid and the main body of magma. Crystallization from a rapidly freezing border liquid which solidifies as a relatively closed system should preserve the composition of the coexisting liquid. This situation is approximated by the effect of increasing proportions of intercumulus material as shown in Table 5-1 and Fig. 5-7. From these calculations it is apparent that the faster the border rock cools, the larger the amount of intercumulus material and therefore, the closer its RE fractionation pattern to that of the coexisting liquid.

When the temperature of the magma drops, cumulus minerals start to settle. As shown in section 5-3-2, a true cumulate consisting of plagioclase and pyroxene will have lower total RE content than the co-existing magma. Even when some trapped intercumulus liquid is present, an early stage cumulate will still have lower total RE content than the original magma because at an early stage of differentiation the RE content of the magma has not yet increased significantly by fractional crystal-lization. This appears to be the case in the Skaergaard and Stillwater intrusions.

In the Sudbury Irruptive, norite overlying the border rocks has hypersthene, plagioclase and augite as the main cumulus minerals (Naldrett et al., 1970). The norite immediately overlying the border norite should, therefore, have lower total RE content than the original main Irruptive magma. As both north and south range border norites have higher total RE contents and La/Yb ratios than the overlying norites and as this difference cannot be satisfactorily explained by differences in their modal compositions, it follows that the border norites very probably have RE compositions more similar to the original magma than the overlying noritic cumulates.

The norites overlying the border norite have strong positive Eu anomalies, whereas the border norite shows no significant Eu anomaly. The lack of a significant Eu anomaly in the border norite may have been caused by two mechanisms:

1) the original main Irruptive magma had no Eu anomaly and the border norite crystallized as a closed system with respect to cumulus feldspar;

2) the original magma had a negative Eu anomaly but the border norite contains cumulus plagioclase which compensates for the negative Eu anomaly in the original magma.

In the case of exclusion of cumulus plagioclase from the border norite, crystallization of plagioclase will cause a negative Eu anomaly in the border norite magma itself. However, because of rapid cooling, this depletion of Eu in the interprecipitate liquid is not removed by diffusion between the main body of the magma and the interprecipitate liquid. Consequently, the whole rock will show no net change in Eu.

In the Irruptive, the plagioclase contents of the border norites and overlying norites are similar. If the presence of cumulus plagioclase in the border norite is the cause of the lack of an Eu anomaly, then the plagioclase content of the immediately overlying norite will be insufficient to explain their strong positive Eu anomalies. The second mechanism appears unsatisfactory as an explanation for the lack of significant Eu anomaly in the border norite.

Thus, mechanism (1) is believed to be the cause of the absence of a significant Eu anomaly in the main Irruptive border norite. That is, the original main Irruptive magma lacked a significant Eu anomaly and the border norite solidified as a relatively closed system. Hence, the RE fractionation pattern of the border norite should approximate that of the main Irruptive magma.

5-4-3. <u>Norite</u>

On both north and south ranges, norites have RE fractiona&-tion patterns parallel to those of the border norites but with lower ⲀREE, lower La/Yb ratios and higher Eu/Eu* ratios. These features are consistent with the petrographic evidence and with RE behaviour in layered basic intrusions.

Petrographic evidence indicates that hypersthene and plagioclase are cumulus minerals in the norite and that augite becomes a cumulus mineral in the upper part of the north range felsic norite (Naldrett and Kullerud, 1967; Naldrett et al., 1970). The rationale that noritic cumulates immediately overlying the border norite should have lower total RE content than the main Irruptive magma has already been discussed in section 5-3-2. The lack of a significant Eu anomaly in the border norite indicates that the magma has neither precipitated (lost) feldspar nor assimilated material possessing an Eu anomaly prior to the emplacement in its present site. The positive Eu anomaly in the norite has, therefore, been formed after the solidification of the border norite as a result of plagioclase accumulation in these rocks (see Fig. 5-8) and is not an inherited feature of the parent magma.

From the modal and cryptic layering correlations between the north and south range rocks (Fig. 2-2), Naldrett et al., (1970; 1972) considered that the north range felsic norite was more comparable with the upper section of the south range norite. Since the difference in modal

composition of north and south range norites is not large and if the
main Irruptive is a layered series in which the north range norite re-
presents cumulate from a higher stratigraphic level, then north range
norite should have higher total RE content and La/Yb ratio than the
lower portion of the south range norite (for reasons, see discussions in
section 5-3-2). Furthermore, according to Naldrett et al. (1970), the
north range felsic norites are orthocumulates and the south range norites
are mesocumulates. Hence, the north range felsic norite would likely
contain more intercumulus material than the south range norite. From
the discussion in section 5-3-2, it follows that the total RE content and
La/Yb ratio of the north range felsic norite should be higher than the
south range norite. The observed higher total RE content and La/Yb
ratio in the north range felsic norite (Fig. 5-9 and Table 5-3) appears
to support the above arguments.

5-4-4. Oxide-Rich Gabbro

The school favouring a multiple intrusion model for the
Nickel Irruptive considered the oxide-rich gabbro a hybrid zone be-
tween norite and micropegmatite, whereas the advocates of a single
intrusion consider the oxide-rich gabbro a transition rock in a continuous
differentiation series from norite to micropegmatite (see Chapter Two).

In summary, the RE data support the view that the oxide-rich gabbro is a product of fractional fractionation of the noritic magma.

5-4-5. Micropegmatite

Data on RE behaviour in granitic rocks are not as abundant as for mafic or ultramafic rocks. Towell et al.'s (1965) study on the Southern California Batholith (see Fig. 5-6) showed that the total RE content, the degree of light RE enrichment, and the extent of Eu depletion increased with increasing acidity of the rocks. Other individual granites generally show similar trends of strong enrichment in total RE content, strong fractionation with enrichment of light REE and a large negative Eu anomaly in their chondrite normalized RE patterns (Haskin et al., 1966a; Taylor et al., 1968; Nagasawa, 1970; Buma et al., 1971; Condie and Lo, 1971; Bowden and Whitley, 1974; Koljonen and Rosenberg, 1974).

Another type of RE fractionation pattern observed in granitic rocks is characterized by high La/Yb ratio (depletion in heavy REE) and a slight Eu anomaly. This pattern has been observed in granitic rocks from Precambrian greenstone-granite terrane (Haskin et al., 1966a; Arth and Hanson, 1972; Jahn et al., 1974) and in the Westerly granite from Rhode Island (Buma et al., 1971). The RE features are interpreted by these authors as the result of partial melting at deep crust or mantle depths leaving a residue containing garnet. The strong

depletion in heavy REE is attributed to garnet extraction (residue) during partial melting in that garnet strongly retains heavy REE relative to light REE.

The high total RE content, strong light RE enrichment and negative Eu anomaly of the Sudbury micropegmatite is similar to the RE properties of granitic rocks of the first category. The large negative Eu anomaly is a primary feature in many such granitic rocks and may be caused by three major processes:

1) complete melting of a pre-existing granitic rock with a strong negative Eu anomaly;

2) fractional crystallization at crustal depths with feldspar loss producing an Eu-depleted residual melt;

3) partial melting of feldspar-bearing source rock with retention of some feldspar in the residual phase producing an Eu-depleted melt.

For the Sudbury micropegmatite, these possibilities are further restricted by the surrounding country rocks, at least in regard to their likelihood as potential sources of melts produced perhaps during a meteorite impact. For example, Dence (1972) suggested that at least part of the micropegmatite represents an original impact melt from the target rocks.

As mentioned in section 5-3-2, trace element behaviour during partial melting can be described by equations similar to those applied to fractional crystallization models. The average trace element concentration $(\overline{C}^l)$ in an accumulated melt after some fraction F of the initial system (C^o) has melted is given by

$$\overline{C}^l = C^o (1 - (1-F)^{1/D}) / F \qquad \dots \quad 5\text{-}16$$

for the case in which a constant combined distribution coefficient D is assumed.

For partial melting of rocks, more often than not equation 5-16 is inadequate as the proportions of mineral phases in the source rock does not remain constant during the melting process. Shaw (1970) derived equations to describe trace element behaviour during more realistic (non-modal) melting processes of this nature in which the average trace element concentration in an accumulated melt is given as

$$\overline{C}^l = C^o (1 - (1-PF/D_o)^{1/P}) / F \qquad \dots \quad 5\text{-}17$$

where $\overline{C}^l$ = average concentration in the accumulated melt,

C^o = concentration in the initial system,

P = combined distribution coefficient for the solid phases that have melted

D_o = combined distribution coefficient for the initial system,

F = weight fraction of the initial system (rock) that has melted.

Using these equations, RE fractionation patterns in melts

derived directly from country rocks surrounding the Sudbury Nickel

Irruptive can be estimated. The main limitation on these considerations

is that it was only possible to analyse one of the many types of country

rock surrounding the Irruptive.

The RE fractionation pattern of the south range Huronian

metagreywacke-metavolcanic terrane may be approximately represented

by the average for Canadian Shield metagreywackes (Wildeman and

Haskin, 1973; Wildeman and Condie, 1973) shown in Fig. 5-11. It is

generally accepted that continental crust has an average RE pattern

similar to that in the composite North American Shale (Haskin et al.

1966b) which has a RE pattern similar to that of the Canadian Shield

metagraywackes. These rocks have absolute light RE abundances

similar to average micropegmatite but with absolute heavy RE abundances

which are two to three times higher than the micropegmatite. It is

obvious that complete melting of such rocks will not produce a micro-

pegmatite RE pattern.

The RE fractionation pattern of partial melts from these

rocks can be estimated by the following process. Assume that the

Huronian metasediments of the crust around the Nickel Irruptive have

an overall composition of greywacke with a modal composition of 20%

quartz, 15% K-feldspar, 50% plagioclase, 7.5% biotite, 7.5% hornblende.

Assume that 10% non-modal melting has occurred producing a granitic

melt with an average composition of 35% quartz, 30% K-feldspar and 35% plagioclase. Using RE distribution coefficients for minerals in acid rock systems (Appendix C) and equation 5-17, we can calculate the RE fractionation pattern of this melt. The result is shown as line A in Fig. 5-11. Smaller degrees of melting will produce even higher total RE contents than line A. It is apparent that these melts have too high total RE contents and too low Eu/Eu* and La/Yb ratios to be directly responsible for the micropegmatite.

The Superior gneiss is the main basement rock around the Nickel Irruptive. Its RE pattern and major element composition differ from that of the main Irruptive micropegmatite. Complete or near complete melting cannot be the direct source of the micropegmatite. Partial melting calculations similar to the previous paragraph can also be performed for this rock. Taking a composition of 35% quartz, 40% plagioclase, 5% K-feldspar, 10% clinopyroxene, 5% biotite, 5% hornblende (Naldrett and Kullerud, 1967) for Superior province gneiss and making the same assumption as in the previous case, the RE pattern of a 10% melt may be calculated. The calculated melt is shown as line B in Fig. 5-11. It appears that this melt has too high a La/Yb ratio and too low an Eu/Eu* ratio to be directly responsible for the micropegmatite.

Fig. 5-11. Calculated Rare Earth Fractionation Patterns of

Melts Resulting from Direct Non-Modal Melting

of Country Rocks.

G: Canadian Shield Metagreywacke,

M: Average Micropegmatite,

A: 10% melting of G,

S: Superior Province Gneiss,

B: 10% melting of S.
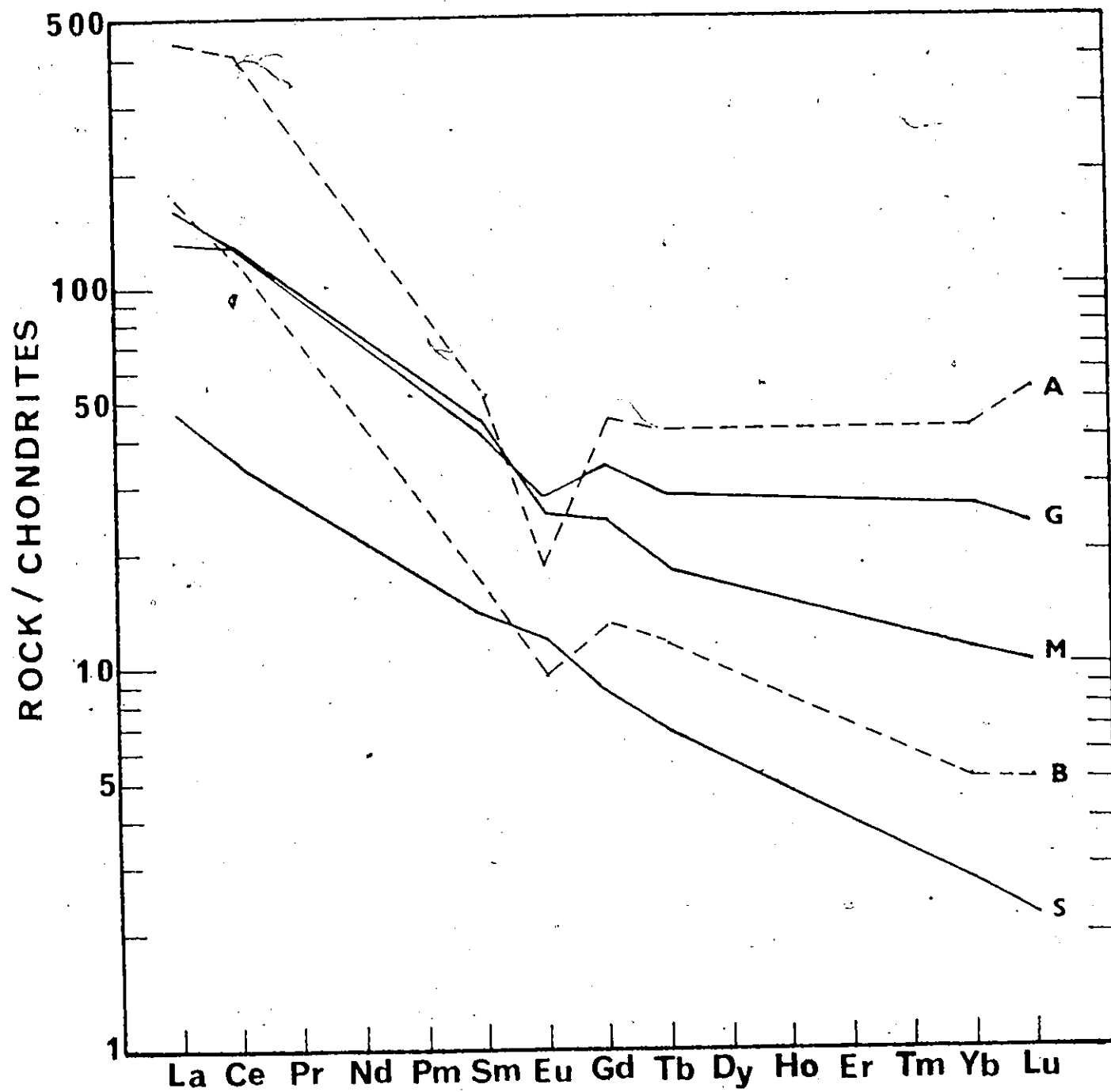
To summarize, these calculations indicate that direct

melting of Huronian metasediments or Superior gneiss does not

yield RE patterns similar to that of the micropegmatite. One

cannot rule out the possibility that mixing of suitable proportions

of these melts or some other melting mechanisms (see greywacke

melting model of Arth and Hanson, 1975) may produce a granitic

melt with RE characteristics compatible with those observed

in the micropegmatite. Further, adequate characterization

of the country rock is extremely difficult. Shallow depth fractional

crystallization of the main Irruptive magma, involving the precipitation of

significant amounts of plagioclase is a direct approach which would

produce a residual liquid with a micropegmatite RE pattern. Plagio-

clase removal would effect a negative Eu anomaly and mafic mineral

removal would produce the increasing light RE and total RE enrichment

in the residual liquid.

5-4-6. Petrogenetic Relationship between Norite and

Micropegmatite

The most commonly suggested hypotheses (see Chapter Two)

on the petrogenetic relationships between the main Irruptive norite and

micropegmatite are the following:

1)   a single intrusion of magma was followed by in situ gravitational

differentiation producing norite as an early cumulate and leaving

micropegmatite to crystallize from the residual liquid;

2)   multiple magma' intrusions occurred with norite and micropegmatite

viewed as melts or residual liquids from either common or dif-

ferent sources which were intruded separately into the present site.

The spatial relationships, the overall similarities in the

RE fractionation patterns, the increasing total RE contents and La/Yb

ratios from norite to micropegmatite, and the corresponding opposite

anomalous Eu behaviour between norite and micropegmatite strongly

suggest that they are genetically related by fractional crystallization

processes. As discussed in section 5-4-3, the positive Eu anomaly in

the main Irruptive norite is caused by the presence of cumulus plagioclase

in this rock. From RE mass balance considerations, the residual liquid

left after crystal settling of a feldspar-rich phase should possess a

negative Eu anomaly with respect to the original magma. The magnitude

of the Eu anomaly in this residual liquid will depend on the relative

amount of feldspar previously crystallized. The compensating positive

and negative Eu anomalies in norite and micropegmatite with respect

to the border norite are consistent with the interpretation that the main

Irruptive is a gravitationally differentiated intrusion. On the other hand, it

requires a high degree of coincidence to have a micropegmatite magma of

alien origin to possess the requisite RE properties.

To test the gravitational differentiation model it is pertinent

to ask if the amount of cumulus plagioclase which must be removed from

the magma to account for the micropegmatite Eu anomaly is petrologically

reasonable. This requires consideration of Eu partition between plagio-

clase and the magma. The maximum amount of plagioclase which can be

removed from a basaltic magma with normal Eu abundance ($Eu/Eu^* =$

1) to produce a specific negative Eu anomaly in the residual liquid can be

estimated from the following equation which is derived from equation 5-3

(Philpotts and Schnetzler, 1968):

$$(Eu/Eu^*)^{\mathcal{L}} = (1-X)^{D^{Eu} - D^{Eu^*}} \quad \ldots \ldots \quad 5\text{-}18$$

where X = weight fraction of the original liquid that has crystallized

as plagioclase, assuming plagioclase is the only cry-

stallizing solid phase,

D^{Eu} = Eu distribution coefficient for plagioclase,

D^{Eu^*} = Eu distribution coefficient for plagioclase if Eu behaved as an

adjacent REE,

$(Eu/Eu^*)^{\mathcal{L}}$ = Eu/Eu* ratio in the residual liquid.

Using D^{Eu} and D^{Eu^*} values from Fig. 5-1 and setting $(Eu/Eu^*)^{\mathcal{L}}$ = 0.76

(average value in micropegmatite) a value of 0.55 is obtained for X. Thus,

fractional crystallization of 55% of the original melt as plagioclase will

yield an Eu/Eu* ratio of 0.76 in the residual liquid. This amount of plagio-

clase appears to be reasonable when compared with the composition of the

main Irruptive border norites.

In sum, the RE patterns of the main Irruptive norite and micro-

pegmatite strongly suggest that they are genetically related by fractional

crystallization processes.

5-4-7. Shape of the Main Irruptive

Because of the large volume of micropegmatite as compared to

norite in surface outcrop (3:1 on the north range and 1:1 on the south range),

several structural models ranging from ring-dike to folded-sill to funnel-

shaped intrusion have been proposed for the Nickel Irruptive (see

Chapter Two). A test of these models can be attempted by considering

the behaviour of Eu in layered intrusions.

The distribution coefficient D in the Rayleigh fractionation

model represents the combined distribution coefficients of constituent

minerals applicable to an aggregate solid phase (rock). That is,

$$D = \sum_{i=1}^{n} D_i f_i \qquad \qquad \dots \dots \quad 5\text{-}19$$

where D_i = distribution coefficient for mineral i,

f_i = weight fraction of mineral i in the solid phase,

$$\sum_{i=1}^{n} f_i = 1.$$

Therefore, equation 5-18 can be written in a more general form as

$$(Eu/Eu^*)^{\ell} = (Eu/Eu^*)^{o}(1-X)^{\left(\sum_{i=1}^{n} D_i^{Eu} f_i - \sum_{i=1}^{n} D_i^{Eu} f_i\right)} \qquad \dots \dots \quad 5\text{-}20$$

and when plagioclase is one of the mineral phases, equation 5-20

can be written as

$$(Eu/Eu^*)^{\ell} = (Eu/Eu^*)^{o}(1-X)^{\left[(D_{Pl}^{Eu} f_{Pl} + \sum_{i=1}^{n-1} D_i^{Eu} f_i) - (D_{Pl}^{Eu^*} f_{Pl} + \sum_{i=1}^{n-1} D_i^{Eu^*} f_i)\right]}$$

$$\dots \dots \quad 5\text{-}21$$

where D_{Pl}^{Eu} = the Eu distribution coefficient for plagioclase,

D_{Pl}^{Eu*} = the Eu distribution coefficient for plagioclase if Eu behaved as an adjacent REE,

f_{Pl} = the weight fraction of plagioclase in the solid phases,

$\sum_{i=1}^{n-1} D_i^{Eu} f_i$ = the combined Eu distribution coefficient for minerals in the solid phases other than plagioclase,

$\sum_{i=1}^{n-1} D_i^{Eu*} f_i$ = the combined Eu distribution coefficient for minerals in the solid phases other than plagioclase if Eu behaved as an adjacent REE in all these minerals.

Because igneous rock minerals, except for feldspars, do not show Eu anomalies in their distribution coefficient patterns, $\sum_{i=1}^{n-1} D_i^{Eu} f_i$ will always be equal to $\sum_{i=1}^{n-1} D_i^{Eu*} f_i$ and equation 5-21 becomes

$$(Eu/Eu*)^L = (Eu/Eu*)^o (1-X)^{f_{Pl}(D_{Pl}^{Eu} - D_{Pl}^{Eu*})} \qquad \dots \qquad 5\text{-}22$$

In a layered intrusion the top granophyre is likely to have solidified from the final dregs of the magma. The RE fractionation pattern of such granophyre would therefore represent that of the final residual liquid. Although exchange of K, Rb, Sr and Sr^{87} between country rocks and intrusive magmas have been observed (Hamilton, 1963;

Gates, 1971), the REE do not appear to have participated in such exchange processes (Philpotts and Schnetzler, 1968; Gates, 1971). Therefore, an Eu anomaly in a granophyre from a layered intrusion is likely to be representative of the last residual liquid unless appreciable bulk assimilation of the roof rocks has occurred.

If we consider that a layered intrusion solidified as a closed system with respect to REE, the magnitude of the negative Eu anomaly in the final granophyre will be a direct function of the amount of cumulus feldspar that has crystallized prior to the magma reaching a composition of granophyre. The amount of feldspar in the chilled marginal facies can be taken as the upper limit of the relative amount of feldspar (f_{Pl}) that has crystallized before the magma reaches a granophyric composition. Thus, from the magnitude of the negative Eu anomaly in the final granophyre, a lower limit can be set on the fraction of magma that has solidified before reaching the final granophyre stage. Therefore, in equation 5-22

$(Eu/Eu^*)^L$ = Eu/Eu* ratio in the final granophyre,

$(Eu/Eu^*)^O$ = Eu/Eu* ratio in the original melt (chilled

marginal facies),

f_{Pl} = fraction of feldspar in the chilled marginal facies,

X = total fraction of the original melt that has solidified.

Such a calculation indicates that in the case of the Sudbury
Nickel Irruptive $((Eu/Eu^*)^l = 0.76, f_{Pl} = 0.60)$ at least 73% of the
main Irruptive magma has solidified before it reaches the micropegmatite
stage. The calculation is, of course, dependent upon the absolute values
of D^{Eu} and D^{Eu^*} for plagioclase, parameters which are subject to some
uncertainty at this time. Also, the calculation treats the main Irruptive
magma as a closed system. As discussed in section 5-4-8, the basal
Onaping Formation rocks have a weaker negative Eu anomaly than the
micropegmatite. Direct assimilation of those rocks by micropegmatite
will decrease the magnitude of the Eu anomaly in the micropegmatite.
Therefore, equation 5-22 is considered to provide a lower limit, implying
that at least 73% of the main Irruptive magma has crystallized before
reaching the micropegmatite stage.

As a further test of the estimated norite/micropegmatite ratio,
the RE content of a hypothetical mixture of three parts average norite
and one part average micropegmatite was calculated element by element.
The RE pattern of the mixture together with patterns for average norite
and average micropegmatite are presented in Fig. 5-12 in which nor-
malization is against border norite rather than chondrites. The calculated
RE fractionation pattern for the 3:1 mixture closely approximates that
of the border norite. Further, the complimentary effect of the RE frac-
tionation patterns of norite and micropegmatite with respect to border

Fig. 5-12. Rare Earth Fractionation Patterns of Average

Norite, Average Micropegmatite and a 3:1

Norite to Micropegmatite Mixture normalized

against Average Border/Norite.
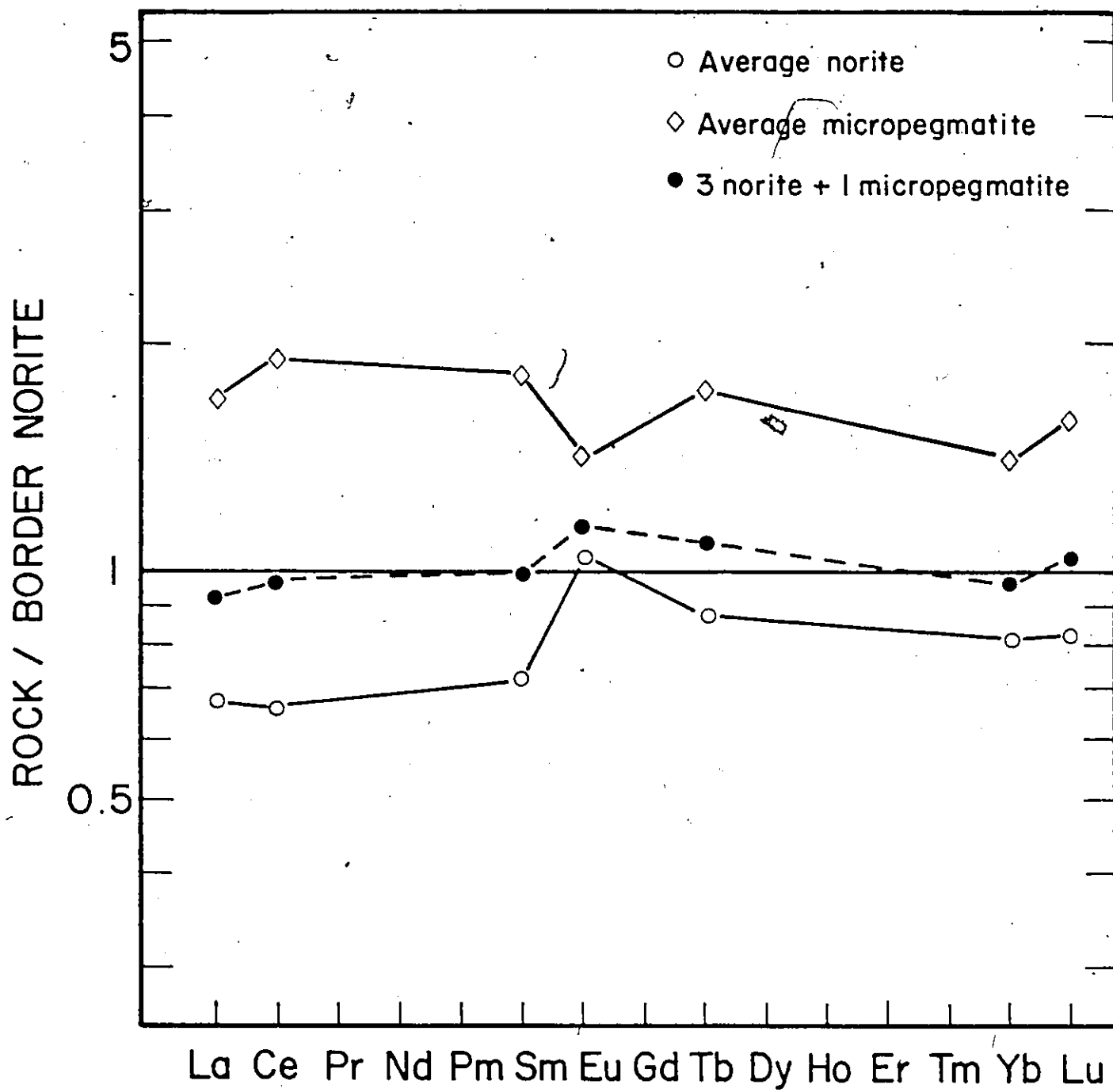
norite and the compensation of positive and negative Eu anomalies

is also apparent.

The estimated micropegmatite/norite proportions, therefore, suggest that micropegmatite should comprise, at most, one quarter of the volume of the main Irruptive magma. The actual surface outcrop areas of micropegmatite and norite as exposed by the present day erosional surface are 3:1 on the north and 1:1 on the south ranges. This observation taken in conjunction with the RE volume estimation above appears to favour Wilson's (1956) funnel-shaped model for the main Nickel Irruptive. For further discussion on the shape of the main Irruptive see section 5-9.

5-4-8. Assimilation in Micropegmatite

The high proportion of micropegmatite to norite in surface outcrop suggests to some authors that the large volume of micropegmatite is the result of assimilation of country rocks (Stevenson and Colgrove, 1968; Naldrett et al.', 1970; 1972). Others (Dence, 1972) regard the micropegmatite, in part at least, as the product of an impact melt. Peredery (1972) made a detailed study of the contact between the Onaping Formation and the micropegmatite. He observed a plagioclase-rich facies of micropegmatite on the stratigraphic top of the micropegmatite unit and suggested that the granophyre-rich micropegmatite which comprises the bulk of the unit was a latter surge of more differentiated

residual liquid from the main magma chamber. In was argued that this model explained the reversal in the trend of iron enrichment in micropegmatite pyroxenes observed by Naldrett et al. (1970).

Inspection of the RE data for north range micropegmatites in Table 3-5 suggests possible trends of increasing Eu/Eu* ratio and decreasing total RE content from stratigraphic bottom to top of the unit. Such variations are opposite to the usual RE differentiation trends. These observations tend to support in situ assimilation of lower Onaping Formation rocks by the micropegmatite. Because the lower Onaping Formation rocks have lower REE and weaker negative Eu anomalies than the micropegmatite, direct assimilation of these rocks into micro-pegmatite magma would increase the Eu/Eu* ratio and decrease the total RE content of the original micropegmatite. On the other hand, these trends might be explained by the higher plagioclase content of the upper micropegmatite rocks in that a higher content of plagioclase would increase the Eu/Eu* ratio and lower the total RE content of the final rock. Finally, the mechanism proposed by Peredery (1972) involving the intrusion of a late stage residual liquid (the granophyre-rich micro-pegmatite) underneath the plagioclase-rich micropegmatite would intro-duce a liquid having higher Eu/Eu* ratio and higher total RE content as discussed in section 5-3. This might also produce the observed trend.

In summary, one can only conclude that the available RE data do not exclude the possibility that some _in situ_ direct assimilation of the Onaping Formation rocks by the micropegmatite may have occurred during the differentiation of the main Irruptive magma.

5-4-9. Main Irruptive Magma

RE fractionation patterns in the Sudbury Irruptive border norite and in chilled marginal facies from other layered basic intrusions are compared in Fig. 5-13. As discussed in sections 5-2, 5-3 and 5-4-2, the RE fractionation patterns of the Bushveld and Stillwater (Frey et al., 1968) chilled gabbros may not represent the original magma. However, the RE patterns of the Sudbury, Skaergaard, and Stillwater (Kosiewicz, 1973) border facies very likely closely resemble the unfractionated initial magmas of these intrusions.

The RE fractionation pattern of the Sudbury border norite is relatively flat in the heavy RE region but highly fractionated in the light RE region with progressive enrichment from Sm to La. When compared with the chilled marginal facies from other layered basic intrusions the Sudbury border norite appears to have comparable absolute heavy RE abundances but higher absolute light RE abundances, especially La and Ce. That is, the Sudbury border norite has a more fractionated chondrite-normalized RE pattern (higher La/Yb ratio).

Fig. 5-13. Comparison of Rare Earth Fractionation Patterns

of Sudbury Irruptive Border Norite with Chilled

Border Facies of the Skaergaard, Stillwater and

Bushveld Intrusions.
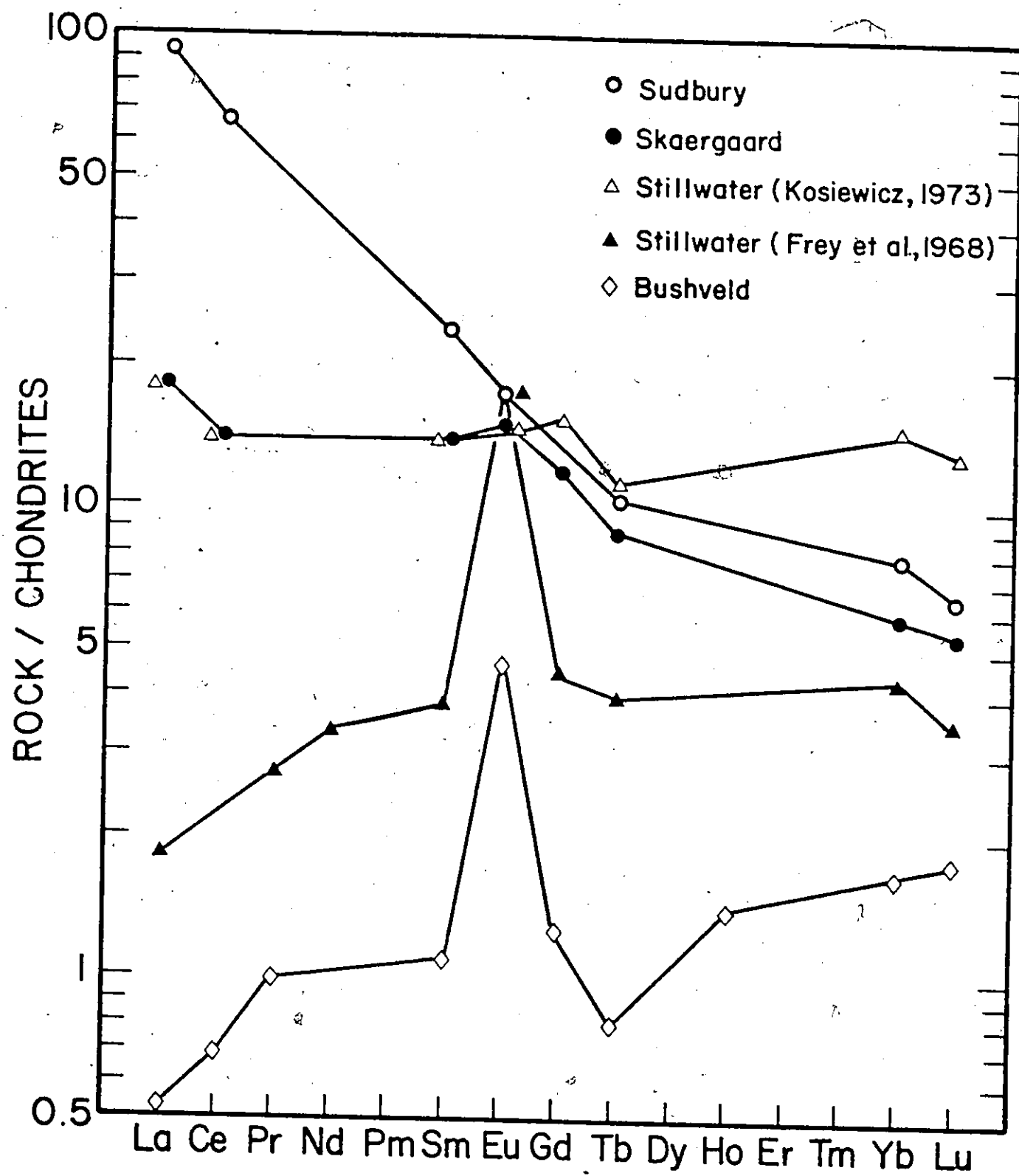
Mesozoic and Cenozoic continental tholeiitic diabases
from different continents have very uniform RE fractionation patterns
(Balashov and Nesterenko, 1966; Philpotts and Schnetzler, 1968;
Frey et al., 1968) which are similar to the average continental tholeiitic
basalt (Herrmann, 1970; Fig. 5-15). Gates (1971) determined RE contents
of Sudbury (1.66 b. y.), Matachewan (2.69 b.y.) and Mackenzie (1.66 b.y.)
diabase dikes from the Canadian Precambrian. His data are shown in
Fig. 5-14. The Matachewan and Mackenzie diabases are tholeiitic
in composition (Fahrig et al., 1965) and their RE fractionation patterns
are similar to average continental tholeiitic basalts shown in Fig. 5-15.
The Sudbury diabase is of alkali olivine basalt composition (Fahrig et al.,
1965). Its RE fractionation pattern is similar to other alkaline basalts
of younger ages which are characterized by high total RE contents and
highly fractionated RE patterns (Masuda, 1966; 1968; Frey et al., 1968;
Herrmann, 1968; Kay and Gast, 1973). The characteristic RE dis-
tribution patterns of alkaline basalts are believed to be the result of
very limited melting of peridotite at mantle depths where garnet is
involved in the residual phases (Kay and Gast, 1973). The Nipissing
diabase (2.2 b.y.) near Sudbury is tholeiitic in composition. No de-
tailed RE patterns are available, but Fairbairn et al. (1953) reported an
average value of 14 ppm La in the Nipissing diabase. This value is
the same as that reported by Gates (1971) for the Mackenzie and Mata-

Fig. 5-14.   Rare Earth Fractionation Patterns of Precambrian

Canadian Shield Diabases (after Gates, 1971).
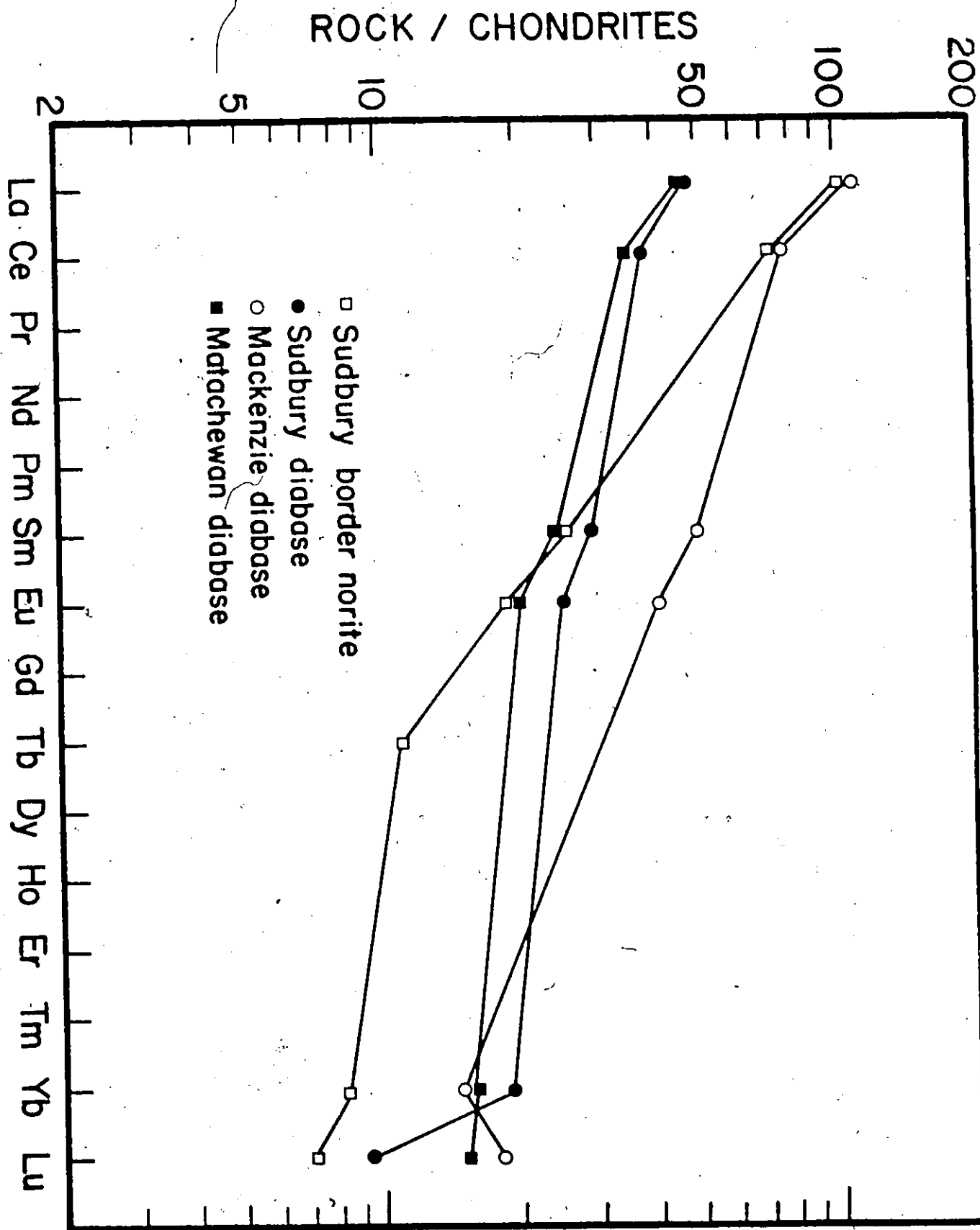
Fig. 5-15. Comparison of Rare Earth Fractionation Patterns

of the Sudbury Border Norite with Country Rocks,

Continental Tholeiitic Basalts (Herrmann, 1969) and

Ocean-Ridge Tholeiitic Basalts (Frey et al., 1971).

ROCK / CHONDRITES

⊙ Border norite
□ Superior Province granite
◇ Metagreywacke
△ Continental tholeiitic basalts
▽ Ocean-ridge tholeiitic basalts
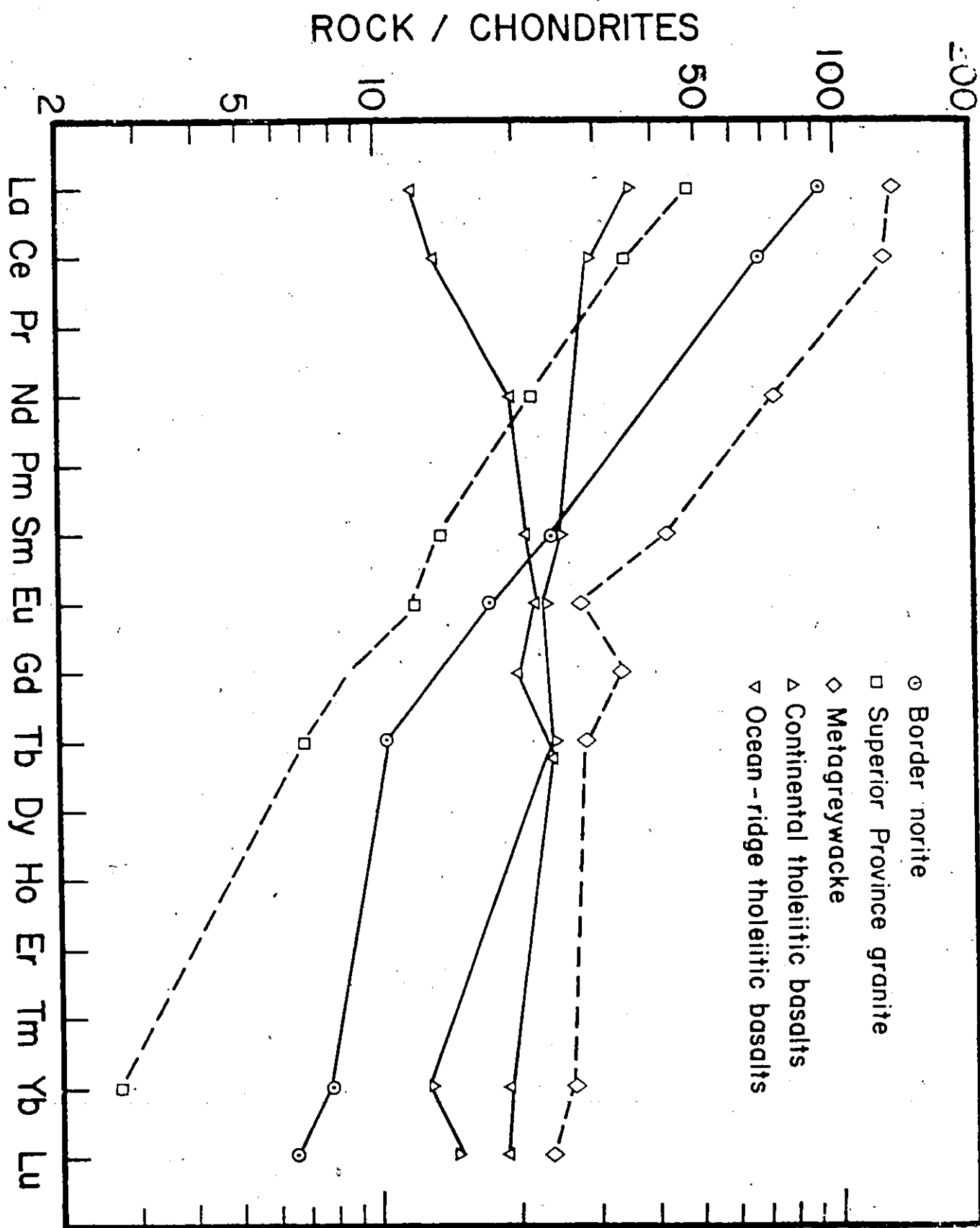
chewan diabases. Therefore, one suspects that the Nipissing diabase

also has a normal continental tholeiitic RE pattern similar to the

Mackenzie and Matachewan diabases. Thus, it appears that the RE

fractionation pattern of the upper mantle and the mechanisms of

continental basalt generation in this region of the Canadian Shield 1.7

to 2.2 b.y. ago were not much different than during younger geological,

eras.

When compared with the Precambrian Canadian Shield

diabases and average continental and ocean-ridge tholeiitic basalts,

the more fractionated RE pattern of the main Irruptive magma is

again apparent. The high total RE content and relatively fractionated

pattern of the main Irruptive magma are rather similar to the continental

plateau basalts (Frey et al. , 1968) and an "intermediate tholeiitic basalt"

reported by Herrmann (1968). These comparisons are in keeping with

the usually siliceous nature of the main Irruptive magma (Naldrett

et al. (1972)) as compared to other layered basic intrusions.

Many have suggested that the siliceous nature of the Sudbury

rocks results from assimilation of siliceous country rocks by the Ir-

ruptive magma. From Figs. 5-11 and 5-15, it is clear that bulk

assimilation of south range metagreywackes or impact melts from the

local country rocks into the main Irruptive magma would impose a

negative Eu anomaly on the resultant mixture. The total RE content

of the Superior gneiss is too low to account for the high total RE content

of the border norite. Thus, the highly fractionated nature and lack of

a significant Eu anomaly in the main Irruptive magma may suggest that

sialic rocks of deep-crustal origin participated in the generation of the

main Irruptive magma, or that a normal basalt has assimilated a melt

characterized by high total RE content, high La/Yb ratio and no Eu

anomaly. The type of RE fractionation pattern shown by the Superior

gneiss is presumed to have been derived by partial melting of eclogites

or amphibolites that contain garnet at mantle depths (Arth and Hanson,

1972). A smaller degree of partial melting of these source rocks (see

the RE fractionation pattern of the northern light gneiss in Arth and

Hanson (1972)) or other deep crustal rocks (see the RE pattern of the

Rhode Island granite in Buma et al. (1971)) would provide a melt with

the required RE properties to constitute a potential contaminant. The

high initial $(^{87}Sr/^{86}Sr)_o$ ratio in the norite (0.7065; Gibbins, 1973) also

suggests that the main Irruptive magma is not a simple mantle derivative.

In summary, the highly fractionated RE pattern of the main

Irruptive magma is in keeping with the siliceous nature of the Nickel

Irruptive. If these properties are the result of assimilation, the RE

data would suggest that a light REE enriched continental tholeiitic melt

has assimilated a silica-rich partial melt derived from deep-crustal

basement rocks to produce the main Irruptive magma.

5-5. Significance of Europium Anomalies in Layered Intrusions

5-5-1. Europium Anomalies in Residual Liquids

The significance of Eu anomalies in residual liquids of layered intrusions has been illustrated by calculations in sections 5-4-6 and 5-4-7. In brief, the magnitude of an Eu anomaly in the granophyre phase of a layered intrusion is directly related to the relative amount of feldspar that has settled out of the magma and, therefore, may be useful in estimating the total fraction of the magma that has solidified prior to reaching the final granophyre stage.

5-5-2. Europium Anomalies in Cumulates

Because of the preferential incorporation of Eu into feldspars, the Eu/Eu* ratio of cumulates from layered intrusions will be affected by the incorporation of feldspars into these rocks. The factors that govern the Eu/Eu* ratios in the cumulates can also be obtained from the Rayleigh fractionation law. In a manner similar to the approach used in equation 5-11, we can derive the following relationships from equations 5-1, 5-5 and 5-8, respectively:

$$(Eu/Eu^*)^s = (Eu/Eu^*)^{\ell} (D^{Eu}/D^{Eu^*}) \qquad \text{....} \qquad 5\text{-}23$$

$$(Eu/Eu^*)^S = (Eu/Eu^*)^L \left(\frac{1 + F\,(D^{Eu} - 1)}{1 + F\,(D^{Eu^*} - 1)} \right) \qquad \ldots \quad 5\text{-}24$$

$$(Eu/Eu^*)^S = (Eu/Eu^*)^L \left(\frac{F\,D^{Eu} + (1-F)(1-(1-X_t)^{D_t^{Eu}})/X_t}{F\,D^{Eu^*} + (1-F)(1-(1-X_t)^{D_t^{Eu^*}})/X_t} \right) \qquad \ldots \quad 5\text{-}25$$

where $(Eu/Eu^*)^S$ = Eu/Eu* ratio in the rock,

$(Eu/Eu^*)^L$ = Eu/Eu* ratio in the liquid phase (intercumulus

liquid) which is in equilibrium with the cumulus phases,

F = weight fraction of cumulus phases in the rock,

1-F = weight fraction of intercumulus material in the rock,

D^{Eu} = combined Eu distribution coefficient for the cumulus

phasës,

D^{Eu^*} = combined Eu distribution coefficient for the cumulus

phases if Eu behaved as an adjacent REE,

X_t = weight fraction of the intercumulus liquid that has

solidified fractionally,

D_t^{Eu} = combined Eu distribution coefficient for mineral phases
that crystallize from the intercumulus liquid,

$D_t^{Eu^*}$ = combined Eu distribution coefficient for mineral

phases that crystallize from the intercumulus

liquid if Eu behaved as an adjacent REE.

From these equations and equation 5-19 $(D = \sum_{i=1}^{n} D_i f_i)$
it is apparent that for given values of D_i^{Eu} and D_i^{Eu*}, the
magnitude of the Eu anomaly of a cumulate depends upon the components
of the cumulus minerals (f_i), the amount $(1-F)$ and Eu/Eu* ratio of the
intercumulus liquid, the fraction of intercumulus liquid that has cry-
stallized (X_t) and the mineral components (f_t) that have crystallized
from the intercumulus liquid.

Actual cases in nature may be more complex than described
by equation 5-25, and the parameters in the above equations cannot
always be estimated. Therefore, these equations cannot always be easily
adopted to accurately determine the magnitude of an Eu anomaly in
cumulates, or to estimate the proportion of magma crystallized at
certain stages of differentiation as was done in the case of a residual
granophyric liquid in sections 5-4-6 and 5-4-7. However, the general
relationships specified by these equations are clearly demonstrated
in calculations shown in Fig. 5-8 (section 5-3).

5-5-3. Europium Anomaly Compensation Effects

The discussion in the last section demonstrated that the
Eu/Eu* ratio in cumulates can be evaluated by equations 5-23, 5-24
and 5-25. From equation 5-3 it can be shown that

$$C_1^{\ell} = C^{O}\,(1-X_1)^{D_1-1} \qquad \dots \quad 5\text{-}26$$

where C_1^{ℓ} = concentration of the residual liquid L_1,

C^{O} = concentration of the original melt,

X_1 = weight fraction of the original melt that has crystallized,

D_1 = combined distribution coefficient for the solid phases.

If we consider that the residual liquid L_1 continues to crystallize until it reaches a composition of C_2^{ℓ}, then the following relationship holds:

$$C_2^{\ell} = C_1^{\ell}\,(1-X_2)^{D_2-1} \qquad \dots \quad 5\text{-}27$$

where X_2 = weight fraction of the residual liquid L_1 that has

crystallized,

D_2 = combined distribution coefficient for solid phases that

have crystallized from L_1 to L_2.

Substituting equation 5-26 in 5-27, then

$$C_2^{\ell} = C^{O}\,(1-X_1)^{D_1-1}\,(1-X_2)^{D_2-1} \qquad \dots \quad 5\text{-}28$$

In the same manner that equation 5-23 was derived, the following equation may be obtained from equation 5-28:

$$(Eu/Eu^*)_2^s = (Eu/Eu^*)^o (1-X_1)^{f_{Pl}^1(D_{Pl}^{Eu}-D_{Pl}^{Eu^*})} (1-X_2)^{f_{Pl}^2(D_{Pl}^{Eu}-D_{Pl}^{Eu^*})} (D^{Eu}/D^{Eu^*})$$

.... 5-29

In some basic intrusions, little if any cumulus plagioclase crystallizes in the ultramafic zone (Irvine, 1970; Jackson, 1967; Wager, 1968). If we assume that feldspar starts to crystallize only after the residual liquid reaches the composition C_1^{ℓ}, that is, $f_{Pl}^1 = 0$, then equation 5-29 becomes

$$(Eu/Eu^*)_2^s/(Eu/Eu^*)^o = (1-X_2)^{f_{Pl}^2(D_{Pl}^{Eu}-D_{Pl}^{Eu^*})} (D^{Eu}/D^{Eu^*})$$

.... 5-30

Since the value of D^{Eu} is greater than D^{Eu^*} and because the value of X_2 is very small at the onset of feldspar crystallization, the product of the terms on the right hand side of equation 5-30 will likely exceed unity. Thus an early stage cumulate containing feldspar will likely have a positive Eu anomaly with respect to the original magma. This explains the positive Eu anomalies in most gabbroic rocks noted in observation (4) in section 5-3-1.

As the value of X_2 in equation 5-30 becomes progressively larger, that is, as crystallization continues, the product of terms on the right hand side of the equation eventually equals unity. At this stage

the negative Eu anomaly in the liquid phase will be compensated by the positive Eu anomaly of the cumulus feldspar and rocks formed at this time will show no Eu anomaly with respect to the original magma. The stage of fractional crystallization at which this "Eu anomaly compensation effect" occurs will depend upon the balance between the values of X_2, f_{Pl}^2, D^{Eu} and D^{Eu^*} in equation 5-30. In terms of RE mass balance this stage will likely be reached as the value of $(1-X_2)^{f_{Pl}}$ be- comes smaller and smaller; that is, after the crystallization of large amounts of feldspar. Therefore, in layered basic intrusions this effect is likely to occur towards the latter stages of differentiation. The effect is observed in rocks from upper sections of the gabbroic cumu- lates in the Skaergaard (Fig. 5-2), Muskox (Fig. 5-5), Southern California (Fig. 5-6) and Sudbury (Figs. 5-9 and 5-10) intrusions. This effect will likely be observed in other intrusions when more RE analyses are available.

After the Eu anomaly compensation stage the value of $(Eu/Eu^*)_2^S$ will likely become less than that of $(Eu/Eu^*)_b$ as the values for X_2 and f_{Pl} become large and the magma approaches granophyre in composition. Rocks formed after this stage will likely show a negative Eu anomaly with respect to the original magma. Similar arguments may be developed for cumulates whose Eu/Eu* ratio is described by equations

5-24 and 5-25.   One may conclude that for fractional crystallization

involving feldspar, the Eu anomaly compensation effect will likely occur.

Analogous effects on the La/Yb ratio in rocks from layered

basic intrusions are to be expected.   That is, as fractionation progresses

the La/Yb ratio of the residual liquid will be increased by previous

separation of mafic minerals which have low La/Yb ratios.   At a certain

stage of fractionation, the low La/Yb ratio in the cumulus phase caused

by preferential incorporation of heavy REE into mafic minerals will be

compensated by the high La/Yb ratio in the coexisting liquid phase.

The effect will also be promoted by the coprecipitation of feldspars.

As a result, late stage differentiates may have a La/Yb ratio the same

as the chilled gabbro.   However, in this case, all cumulus phases are

involved and a more complex situation prevails.   Therefore, the effect

will not be as obvious as in the case of the Eu anomaly compensation

effect, but it is clearly demonstrated in Fig. 5-8.

The Eu anomaly behaviour discussed in this section may be

useful in recognizing genetic relationships in a plutonic feldspar-bearing

rock which has a chilled border facies with a more acid facies separated

by "transition zone rock".

5-6. Petrogenesis of the Sub-Layer Rocks as Inferred from Rare Earth Data

5-6-1. Mafic Sub-Layer Rocks

Only limited information is available on the sub-layer rocks. Souch et al. (1969) reported that the south range mafic sub-layer has a noritic silicate matrix with varying ratios of orthopyroxene/clinopyroxene. Hewins (1971) made a detailed study of the north range mafic sub-layer rocks which he found to be rather heterogeneous with variable orthopyroxene/clinopyroxene ratios. Based on petrographic and mineral composition studies, he concluded that the north range mafic sub-layer rocks are not cumulates and that they have crystallized in situ. He further argued that more calcic plagioclase, lower quartz content and higher sulfide content suggest that the mafic sub-layer rocks are more primitive than the main Irruptive rocks with respect to fractional crystallization of basaltic magma.

The RE properties of the mafic sub-layer generally support these arguments. They are similar to the main Irruptive norites but lack the positive Eu anomalies. When compared with average border norite, the mafic sub-layer rocks, with the exception of the Sultana sub-layer, are characterized by less fractionated RE patterns; that is, lower Σ REE and La/Yb ratios. The lack of significant Eu anomalies in most

mafic sub-layer rocks indicates that they are not cumulates and that they

have not crystallized from residual liquids from which significant amounts

of plagioclase have precipitated. Therefore, the difference in RE frac-

tionation patterns of mafic sub-layer rocks from different localities

suggests that these rocks have solidified from several batches of magma.

The general similarity in petrography and RE fractionation patterns of

these rocks and the main Irruptive magma suggests a similar origin

for both.

5-6-2. Offset Rocks

When compared with average border norite, the offset

rocks are characterized by higher total RE contents and variable

negative Eu anomalies which are weak in the Frood and Foy offsets

but strong in the Copper Cliff offset. These RE properties suggest

the offsets are more differentiated than the main Irruptive magma.

The more siliceous nature of the offset rocks has been

attributed to reaction with the country rocks (Hawley, 1962). On

the south range, both the Copper Cliff and Frood offsets cut the south

range Huronian rocks. Yet the Copper Cliff offset has a strong negative

Eu anomaly while the Frood offset has only a weak negative Eu anomaly

suggesting no consistent influence of country rock with respect to the

Eu anomaly characteristics of the offsets. On the north range, the Foy

offset has Σ REE about three times that of the Superior gneiss. There-fore, bulk assimilation of surrounding country rock by the offset magma alone does not explain the high RE content of the Foy offset. Rather, the sub-layer magmas probably acquired their RE fractionation patterns before emplacement.

The Copper Cliff offset has the highest total RE content of any analysed sub-layer rocks and a strong negative Eu anomaly (Eu/Eu* = 0. 74). These features suggest prior equilibration with a feldspar phase. Since the major element content of the Copper Cliff sample, especially the alumina content, is similar to that of the other offset rocks (Appendix A), its composition is therefore not simply related to other sub-layer rocks by fractionation processes involving feldspar. Rather, it is likely that mixing with an Eu depleted melt may have played a role in establishing the compositional properties of this rock.

Thus, the general similarity in RE fractionation patterns among the sub-layer rocks and their general similarity with the main Irruptive magma suggests a similar origin. The differences in their RE fractionation patterns are in general comparable with the observed RE pattern variations in magmas representing slightly different degrees of fractional crystallization of basaltic magma or batches of magma pro-duced by different degrees of partial melting of source rocks (Schilling

and Winchester, 1969; Zielinski and Frey, 1970; Helmke and Haskin, 1973). However, it is not possible to differentiate between these two mechanisms.

5-7. Origin of the Sub-Layer Inclusions as Inferred from Rare Earth Evidence

5-7-1. Rare Earth Patterns in Ultramafic Rocks

A number of RE studies on ultramafic rocks of different origin have been reported (Balashov and Turanskaya, 1962; Frey, 1969, 1971; Flower, 1971; Frey et al., 1971: Potts and Condie, 1971; Reid and Frey, 1971; Frey and Green, 1974; Paul et al., 1975). RE fractionation patterns in some pertinent ultramafic rock types are discussed below:

1) Alpine-type ultramafic rocks: the REE in alpine ultramafics show a variety of fractionation patterns including light REE enrichment, chondritic, light REE depleted and V-shaped. Some representative RE fractionation patterns are shown in Fig. 5-16. They all have low total RE contents.

High-temperature alpine peridotites (Lizard intrusion, Cornwall; Mt. Albert, Quebec and Tinaquillo, Venezuela) have RE fractionation patterns characterized by extreme depletion in light REE

Fig. 5-16. Rare Earth Fractionation Patterns of Some

Alpine Ultramafic Rocks (after Frey, 1969 and Frey

et al., 1971).
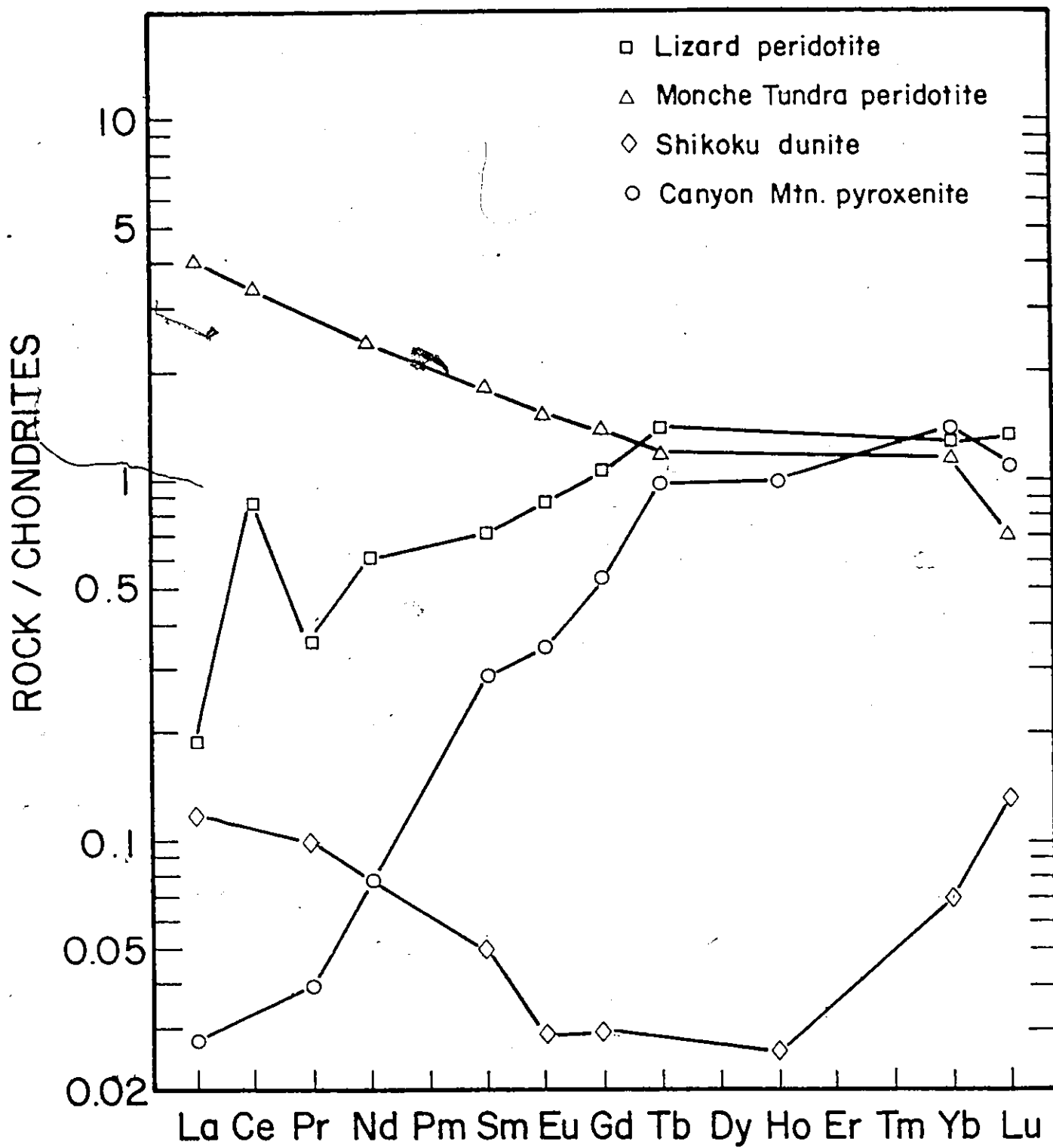
(Haskin and Frey, 1966; Frey, 1969; Frey et al., 1971). This pattern is

believed to result from partial melting in the mantle with the perido-

tites representing residual material left after the extraction of basaltic

melts.

It is generally assumed that average terrestrial material

overall has the same chemical composition as chondrites. If this assump-

tion is valid, then undifferentiated mantle materials would have RE

fractionation patterns similar to chondrites. Furthermore, the consist-

ent light RE enrichment observed in continental and oceanic island

basalts implies that this enrichment may be characteristic of the

processes responsible for formation of basaltic material in the mantle.

Residual ultramafic material left after basalt generation would therefore

be expected to be depleted in the light REE (Frey et al., 1971).

2) Precambrian ultramafic lavas and associated intrusions: recent

studies on Precambrian ultramafic lavas and associated intrusions in

South Africa (Viljoen and Viljoen, 1969), Western Australia (Nesbitt,

1971; McCall and Leishman, 1971), and Canada (Naldrett and Mason, 1968;

Pyke et al., 1973) indicate that a very high degree of partial melting

(60 to 80 percent) of mantle material is necessary to produce such

magma (Green, 1972, 1975; Green et al., 1975). Pillowed ultramafic

komatiite from South Africa have primitive chondritic RE fractionation

patterns (Shih and Jahn, 1973; Herrmann et al., 1974). This may

suggest that undifferentiated Precambrian mantle also has a RE

fractionation pattern similar to chondrites.

3) Ultramafic nodules in basalts and kimberlites: Kimberlites

are characterized by strong enrichment in total REE and a linear RE

fractionation pattern with steep negative slope with a steady increase

from Lu to La (Haskin et al., 1966; Frey et al., 1971; Paul et al., 1975).

These authors considered that fractionation patterns of this type may

reflect prior equilibration of the magma with a garnet phase as garnet

is known to be strongly enriched in heavy REE.

Both kimberlites and basaltic lavas often contain inclusions

of ultramafic rocks. These inclusions may be cognate with the host rock

or accidental xenoliths. RE fractionation patterns ranging from light

REE enrichment, chondritic, light REE depleted, and V-shaped have

been reported in these nodules. Their RE fractionation patterns in some

cases may be helpful in understanding their origin (Philpotts et al., 1972;

Nagasawa et al., 1969).

4) Ultramafic rocks in layered intrusions: RE fractionation patterns

of ultramafic rocks from the Stillwater, Bushveld, and Muskox intrusions

were shown in Figs. 5-3, 5-4 and 5-5 respectively. These ultramafic

cumulates have low absolute total RE contents and their RE fractionation

patterns range from enrichment in light REE, to relatively flat

patterns, to slight depletion in light REE.

As shown in section 5-3-2, the RE fractionation pattern of

a cumulate depends upon the RE fractionation pattern of the equilibrium

liquid phase, the mineralogical components of the rock, and the amount

of intercumulus material. In general, ultramafic cumulates form at an

early stage of differentiation when the magma has an RE pattern similar

to that of the original magma. Therefore, an ultramafic orthocumulate

will have an RE fractionation pattern similar to that of the original

magma whereas an extreme ultramafic adcumulate will have an RE pat-

tern reflecting the combined patterns of its constituent minerals, and

thus deviate somewhat from that of the original magma (see discussions

in section 5-3).

In summary, various RE fractionation patterns are found

in ultramafic rocks of different origin. One would only expect undif-

ferentiated mantle material to have a flat chondritic RE pattern. A

simple residue left after extraction of basaltic melt would have a

nearly chondritic to light REE depleted pattern with low absolute total RE

content. However, the reverse relationships may not always hold.

5-7-2. Origin of the Sub-Layer Inclusions

None of the Sudbury sub-layer ultramafic inclusions have a chondritic (except possibly No. L-71-2) or a light REE depleted pattern as would be expected in undifferentiated or simple residual upper mantle materials. The high total RE contents and light REE enrichment patterns in these inclusions therefore, limit their origin to:

1) rocks from a single source or different sources contaminated by host sub-layer norites and hence masked by its light REE enriched pattern;

2) rocks formed by _in situ_ solidification of ultramafic magma with a light REE enriched pattern;

3) cumulates from basic magma with a light REE enriched pattern.

If the original total RE contents of the sub-layer inclusions were very low, contamination by sub-layer norite would alter the original RE fractionation patterns of the inclusions. Some Fe-Mg exchange between the sub-layer silicate matrix and the inclusions has been observed, but the extent of the exchange is small (Hewins, 1971). The majority of the inclusions were collected from Strathcona sub-layer where massive sulfides are the major matrix of the sub-layer. Wherever possible, samples were collected from the center portions

of large inclusions taken from the wall of an operating mine stope

to avoid possible contamination. An argument against contamination

is that although sub-layer rocks from different localities show a

significant range of RE patterns, the RE patterns of inclusions do not

correspond with their sub-layer host rocks. Some inclusions (S-23-32D,

W-9) have higher REE and La/Yb ratios than their host sub-layer

rocks, which would not be expected in the case of contamination. Thus,

direct contamination of ultramafic inclusions by sub-layer norite should

produce a pattern with REE and La/Yb ratio lower than the sub-layer

rocks. Also, the positive Eu anomalies in two gabbroic inclusions

(W-23, S-20-40-A) are preserved. Since the sub-layer rocks have no

Eu anomalies or have negative Eu anomalies, serious contamination

would tend to decrease or eliminate the positive Eu anomalies in these

inclusions. Therefore, a significant masking effect by the sub-layer

host rocks is considered unlikely and the general similarity between

the RE fractionation patterns of the sub-layer inclusions is not the result

of contamination by sub-layer magma.

As a second process (No. 2 above) which might produce

light REE enriched mafic to ultramafic rocks, a primitive, unfractionated

upper mantle melt was considered from which some olivine, pyroxene or

garnet crystallizes. As the RE distribution coefficients for these

minerals favour preferential incorporation of heavy REE in the crystals,

a liquid from which these phases have been removed will be characteri-

zed by light REE enrichment relative to the original melt. By a cal-

culation similar to that used in section 5-4-7, the amount of these minerals

which must crystallize from a magma to produce a residual liquid with

the observed light REE enriched pattern can be estimated.

From equation 5-3, the following relationship can be derived:

$$(La/Yb)^{\ell} = (La/Yb)^{o} (1-X)^{D^{La} - D^{Yb}} \quad \dots \quad 5\text{-}31$$

or

$$\frac{(La/Yb)^{\ell}}{(La/Yb)^{o}} = (1-X)^{D^{La} - D^{Yb}} \quad \dots \quad 5\text{-}32$$

where X = weight fraction of the original liquid that crystallized

   as mafic minerals,

D^{La} = combined La distribution coefficient for the mafic minerals,

D^{Yb} = combined Yb distribution coefficient for the mafic minerals,

$(La/Yb)^{\ell}$ = La/Yb ratio in the liquid phase,

$(La/Yb)^{o}$ = La/Yb ratio in the original liquid.

Assuming the initial system has a flat chondrite normalized RE pattern,

the equation becomes

$$(La/Yb)_N^{\ell} = (1-X)^{D^{La}-D^{Yb}} \qquad \dots \qquad 5\text{-}33$$

here $(La/Yb)_N^{\ell}$ = chondrite normalized La/Yb ratio in the liquid phase.

The sub-layer inclusions have an average chondrite nor-malized La/Yb ratio of 5.10. Setting $(La/Yb)_N^{\ell}$ = 5.10 and sub-stituting D^{La} and D^{Yb} from Fig. 5-1 into the above equation, one can calculate that more than 99 percent of an initial melt characterized by a flat RE fractionation pattern would have to crystallize as clino-pyroxene, or orthopyroxene or olivine or any combination of these minerals to produce a residual liquid with a La/Yb ratio of 5.10. The viability of such a process is extremely questionable both with respect to the likelihood of producing sufficient melt and the capability of such a melt of crystallizing ultramafic rocks.

Similar calculations show that crystallization of 4.2 percent of an initial melt as garnet would leave a residual liquid with a chondrite normalized La/Yb ratio of 5.10. However, other aspects of the RE pattern of a primordial melt from which garnet has been removed are less favourable. For example, crystallization of garnet would also produce a RE pattern characterized by a steady increase of enrichment from Lu and La in the residual liquid. Thus, the liquid will have a linear RE fractionation pattern with a steep negative slope unlike the fractionation patterns of the sub-layer inclusions. Also

calculations using an equation analogous to 5-33 show that crystal-
lization of 4.2 percent of garnet from a melt with flat RE fractionation
pattern will produce a residual liquid with a minimum chondrite normalized
Tb/Yb ratio of 3.05. Most of the sub-layer inclusions, however, show
RE fractionation patterns with progressive enrichment from Tb to La
and a relatively flat trend from Lu to Tb. The inclusions have an
average chondrite normalized Tb/Yb ratio of 1.17 with all the samples
having ratios less than 3.05. On the other hand, high degrees of melting
of ultramafic rocks will produce melts with RE patterns similar to
the source rocks (as for example, in the case of the Precambrian
peridotite-komatiites) and therefore would not be able to produce a light
REE enriched ultramafic melt as required by many of the sub-layer
inclusions.

These calculations, the absence of any traces of garnet in
the sub-layer inclusions and the presence of cumulus texture in the
inclusions indicate that in situ crystallization of light REE enriched
ultramafic magma is an unlikely explanation for the sub-layer inclusions.

Thus, the sub-layer inclusions are most likely cumulates
which have crystallized from basic magma characterized by light REE
enrichment. In true cumulates or extreme adcumulates, the RE
fractionation pattern of the rock would reflect the combination of the
relative RE patterns of its constituent minerals.

Equation 5-34 ,

$$C_j^s = \sum_{i=1}^{n} C_j^{\ell} M^i D_j^i \quad ,$$

.... 5-34

where C_j^s = concentration of element j in the cumulate,

C_j^{ℓ} = concentration of element j in the liquid phase which is in

equilibrium with the cumulus phases,

M^i = weight fraction of mineral i,

D_j^i = distribution coefficient of element j for mineral i,

allows one to calculate the approximate RE pattern of the liquid from

which the cumulus minerals crystallized. Using distribution coefficients

from Fig. 5-1, the measured RE concentrations (Table 5-7) and the major

mineral composition (87% clinopyroxene, 11% orthopyroxene, 2% plagio-

clase) of Strathcona sub-layer pyroxenite inclusion S-29-139-1804, the

RE pattern of the liquid in equilibrium with this inclusion was calculated.

It is shown as line A in Fig. 5-17. Similar calculations on other inclu-

sions gave similar fractionation patterns for the coexisting liquids, but

varying absolute abundances.

The RE fractionation pattern of these coexisting liquids

are in general similar to that of the Irruptive border norite but are much

higher in absolute RE abundances, especially in the light REE; that is,

Fig. 5-17. Comparison of Rare Earth Fractionation

Patterns of Strathcona Sub-Layer Pyroxenite with

Calculated Patterns of Cumulates from the Main Irruptive

Border Norite Containing Varying Amounts of Inter-

cumulus Material.

ROCK / CHONDRITES

200
100
50
10
5
2

La Ce Pr Nd Pm Sm Eu Gd Tb Dy Ho Er Tm Yb Lu

10%
20%
30%
50%
70%

▼ Strathcona sub-layer pyroxenite
    S-29-139-1804
⊙ Border norite (B.N.)
● Calculated value (C.)
○ C + 10% B.N.
△ C + 20% B.N.
◇ C + 30% B.N.
▽ C + 50% B.N.
◆ C + 70% B.N.

A
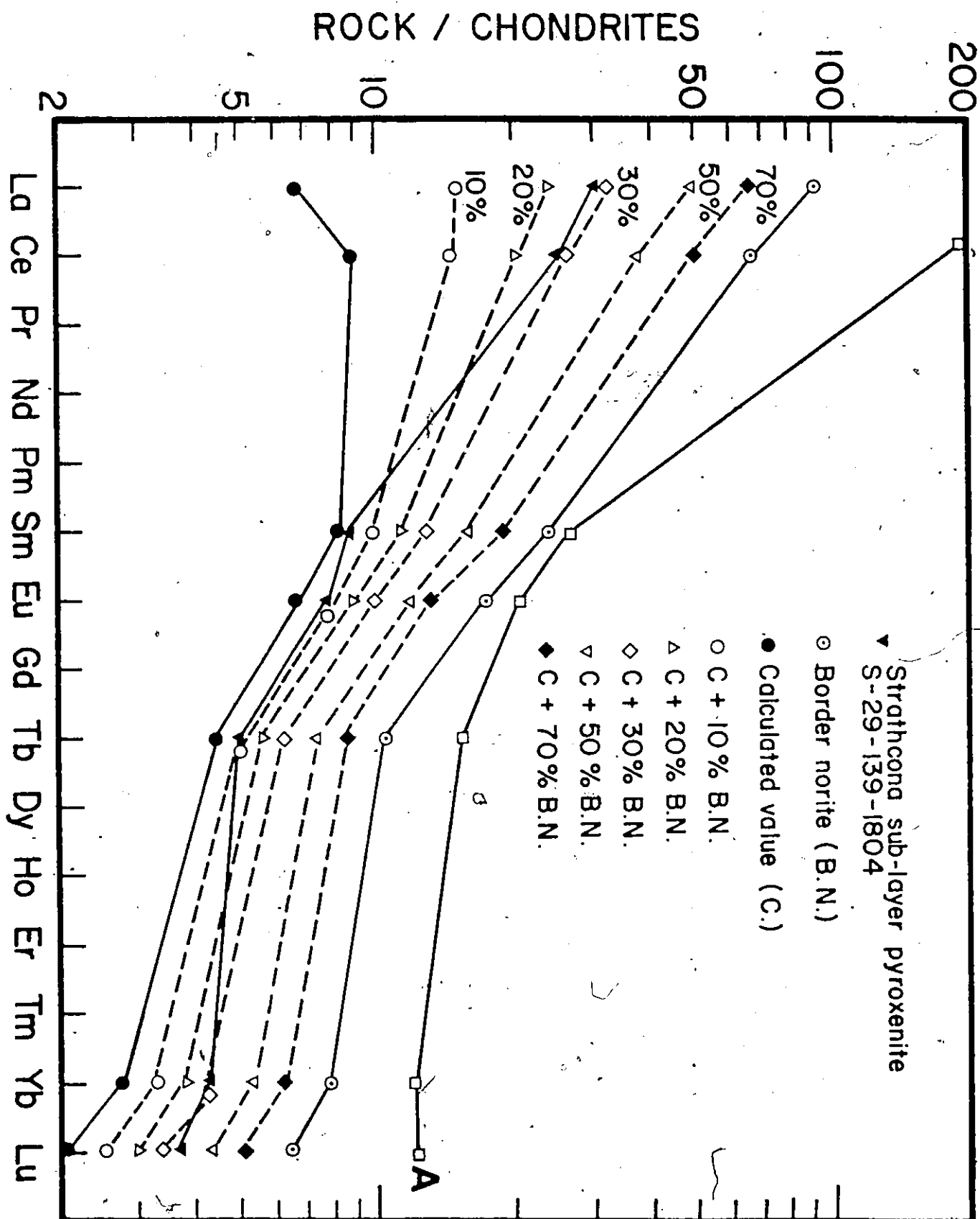
they have very high La/Yb ratios. For example, line A in Fig. 5-17 has a La/Yb ratio of 34.7 as compared to 11.8 of average border norite. Such high La/Yb ratios are observed only in some alkaline rocks (Frey et al., 1968; Schilling and Winchester, 1966; Zielinski and Frey, 1970; Flower, 1971; Nagasawa, 1973; Kay and Gast, 1973). Yet the RE fractionation patterns of these calculated coexisting liquids lack the characteristic linear pattern of these alkaline rocks.

From equation 5-34, one can also calculate the RE pattern of cumulates that crystallize from a liquid with known RE pattern. Thus, for a mineral composition similar to that of S-29-139-1804 (as an example), the RE pattern of a cumulate produced by fractional crystallization from a liquid with an RE pattern similar to the Sudbury border norite and other basalts or Precambrian diabases of the region can be calculated. Such calculations indicate that these liquids yield cumulates with RE patterns that are higher in heavy REE and lower in light REE (that is, lower La/Yb ratio) than S-29-139-1804. The Sudbury border norite yields a pattern most similar to the inclusion but still with too low a light REE compliment. The calculated rock pattern representing fractional crystallization from border norite is shown in Fig. 5-17 (solid circles) together with the patterns for the border norite and S-29-139-1804. Although the border norite has a high La/Yb ratio,

the calculated La/Yb ratio is three times less than that actually ob-
served in the rock.

The discrepancies in these calculations are caused by the
fact that contributions from intercumulus material have not been con-
sidered. As discussed in section 5-3, intercumulus material contri-
butes significantly to both the total RE contents and the RE fractionation
patterns of the cumulates. Calculations are therefore performed using
equation 5-4 which takes into account the intercumulus liquid. Patterns
of calculated RE concentrations for S-29-139-1804 together with varying
amounts of intercumulus material of border norite RE composition are
shown in Fig. 5-17. The calculations demonstrate that addition of 20
to 30 percent intercumulus material yields an RE pattern similar to
that observed in the inclusion. Therefore, varying amounts of trapped
intercumulus liquid are likely the major controlling factor on the ob-
served RE patterns in the sub-layer inclusions.

In conclusion, from these considerations and the nature of
RE behaviour in layered intrusions (section 5-3), it appears that the
range of variation and overall similarity of RE patterns of the sub-
layer inclusions indicate that they represent samples from a series of
cumulates containing varying amounts of intercumulus material.
Their similarity to the RE pattern of the Sudbury border norite and
the calculations represented in Fig. 5-17 suggest that these inclusions

are likely cumulates that have crystallized from a liquid phase with
an RE pattern similar to that of the Sudbury border norite.

5-8. Origin of the Onaping Formation Rocks as Inferred from Rare Earth Evidence

5-8-1. Volcanic Origin of the Onaping Formation

The advocates of a volcanic origin of the Onaping Formation
suggest that these rocks are mainly fissure type ash flows representing
final differentiation products of a magma probably related to the Nickel
Irruptive (Chapter Two). High concentrations of volatiles provide the
necessary mechanism for explosive pyroclastic eruptions. Hamilton
(1960) showed chemical similarities between the micropegmatite and
the overlying Onaping Formation rocks and suggested that both were
early silicic differentiates of the main Irruptive. Dietz (1972), in a
recent version of the meteorite impact model, suggested that the
Onaping Formation developed as a cap of welded tuffs overlying the
"extrusive Irruptive lopolith" which was emplaced immediately after
impact.

Recent RE studies in cogenetic ash-flows (Rankin et al.,
1974) and acid lavas (Ewart et al., 1968, 1973; Condie and Swenson
1973; Price and Taylor, 1973; Koljonen and Rosenberg, 1974) suggest a
close similarity of RE patterns in cogenetic volcanic rocks with lower

Eu/Eu* ratios and possibly higher heavy REE in the more differentiated

units. In the Bushveld intrusion, the relationships of the top granites,

granophyres, and felsites to the Bushveld layered rocks have also been

a point of debate (Wager and Brown, 1967). Daly (1928) considered the

Bushveld felsites as the crust of a roofless lopolith. Recently, Rhodes

and Elston (1974) have proposed a meteorite impact model for the

Bushveld structure and suggested that the lower unit of the felsite is an

impactite. Most studies, however, suggest that at least the granite and

felsite are cogenetic (Hunter, 1974). Weight (1961) considered that the

granites, granophyres, and felsites represented a single event during

which the plutonic rocks intruded their own effusive roof, a view that

is similar to the ash-flow model for the Onaping Formation proposed

by Hamilton (1960). The almost identical RE patterns of the Bushveld

granites and felsites (Fig. 5-4) do suggest a comagmatic link between

these two rocks.

According to the volcanic model, the matrix of the grey

Onaping (pumice) and the melt rock (volcanic glass) should have similar

chemical compositions being derived from the same volcanic source.

They should, therefore, have similar RE fractionation patterns showing

characteristics of acidic lavas. Furthermore, if they are derivatives of

the Nickel Irruptive magma, their RE fractionation patterns should be

systematically related to the Nickel Irruptive rocks. The melt rock

sample, O-2F, does have an RE fractionation pattern similar to the

rhyolite composite of Haskin et al. (1966) and the main Irruptive micro-

pegmatite, but its total RE content is much lower. The grey Onaping

and the matrix of the basal breccia have RE fractionation patterns

similar to the melt rock but have lower total RE contents and lack the

strong negative Eu anomaly. In order to generate the large negative

Eu anomaly of the melt rock from the grey Onaping, precipitation of

large amounts of feldspar is required. However, the melt rocks have

higher Al_2O_3 content than the grey Onaping and the basal breccia

matrix (Appendix A). Also the Sr content of the melt rock (average

149 ppm) is much higher than the grey Onaping (average 56.2 ppm)

(Fullagar et al., 1971). Therefore, the removal of large amounts of

feldspar from grey Onaping is not a plausible mechanism to explain

the Eu anomaly in the melt rock. When compared to the micropegmatite,

the REE in the Onaping Formation rocks are lower by a factor of more

than two. Hence, these observations suggest that the RE properties of

the Onaping Formation rocks are not simply related to those of the

Nickel Irruptive magma and it is regarded as unlikely that the Onaping

Formation, at least the grey Onaping and basal breccia matrix, and

the micropegmatite are derived from a common volcanic source.

Stevenson (1961, 1963) described the basal breccia immediately overlying the micropegmatite as a tectonically brecciated quartzite that had been altered metasomatically by intrusion of the micropegmatite. As shown in Fig. 4-5, the matrix of the basal breccia has an RE pattern similar to that of the grey Onaping. Neither RE pattern shows evidence of being affected by the intrusion of the micropegmatite. The strong negative Eu anomaly and high total RE content of the micropegmatite should have imposed similar characteristics on the basal breccia and grey Onaping if extensive metasomatism of these rocks occurred in response to intrusion of the micropegmatite.

5-8-2. Rare Earth Patterns in Rocks from Meteorite Impact Sites

The conclusion from meteorite impact glass (impactites) studies is that the composition of the impact glass is similar to that of the target rocks within a few percent for most elements. Only the most volatile components (H_2O, CO_2, halogens and possibly other elements more volatile than cesium) may be selectively lost during fusion of the target rock (Taylor, 1973). However, identification of the precise stratum in which melting has occurred during impact may be difficult in complex geological terranes.

Impact glass, fallback breccia and possible target rock at several known terrestrial impact sites have been studied with respect to RE compositions. At the Ries crater, Germany, the rim of the impact crater is built of suevite breccia which consists of the melted crystalline rocks, glass bombs, and chilled fragments of the crystalline rocks including granite, amphibolites, diorite, gneiss, etc. (Shoemaker and Chao, 1961). Despite the diverse rock types rimming the crater, the RE patterns of the impact glass and the suevite breccia (fallback breccia) are very similar to each other and fall in the range observed in the country rocks (granite and amphibole fragments within the suevite breccia and claystone and sandstone surrounding the crater; Bouska et al., 1973; see Fig. 5-18). Bouska et al. (1973) concluded that the impact glass was derived from the remelting of crystalline rocks from the basement of the impact crater.

At the Henbury impact site, Australia, Taylor (1966) found similar compositions in impact glass and subgreywacke country rock for a comparison of 51 elements. He also observed similar RE fractionation patterns in the impact glass and the sediments (Fig. 5-19).

Schnetzler et al. (1967) analyzed REE in impact glass and sedimentary country rocks from the vicinity of the impact crater at Bosumtwi, Ghana. The RE pattern of the two analyzed impact glass samples are very similar and resemble that of the country rocks. Their

Fig. 5-18. Rare Earth Fractionation Patterns in Impact Glass,

Suevite Breccia and Country Rocks from the Ries Crater,
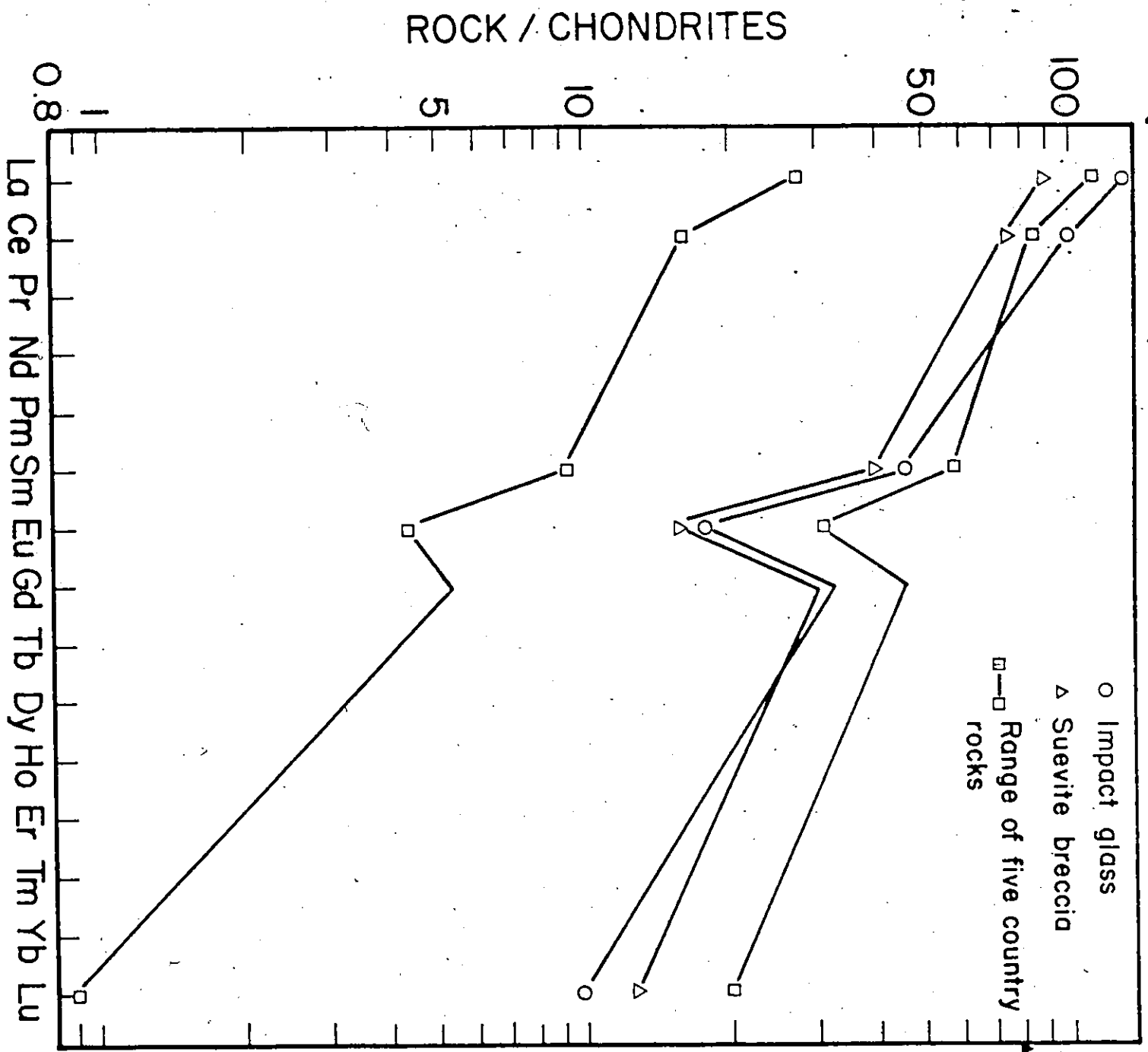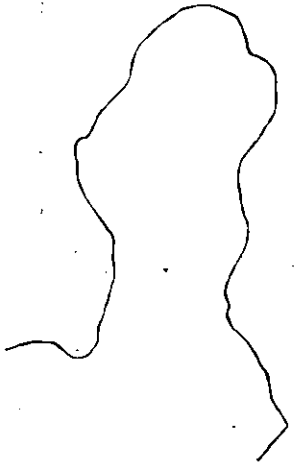
Germany (from Bouska et al., 1973).

Fig. 5-19. Relative Rare Earth Fractionation Patterns of Impact

Glass and Country Rocks from the Henbury Crater,

Australia (from Taylor, 1966).

ROCK / CHONDRITES

La Ce Pr Nd Pm Sm Eu Gd Tb Dy Ho Er Tm Yb Lu

○ Impact glass
□ Subgreywacke A
◇ Subgreywacke B
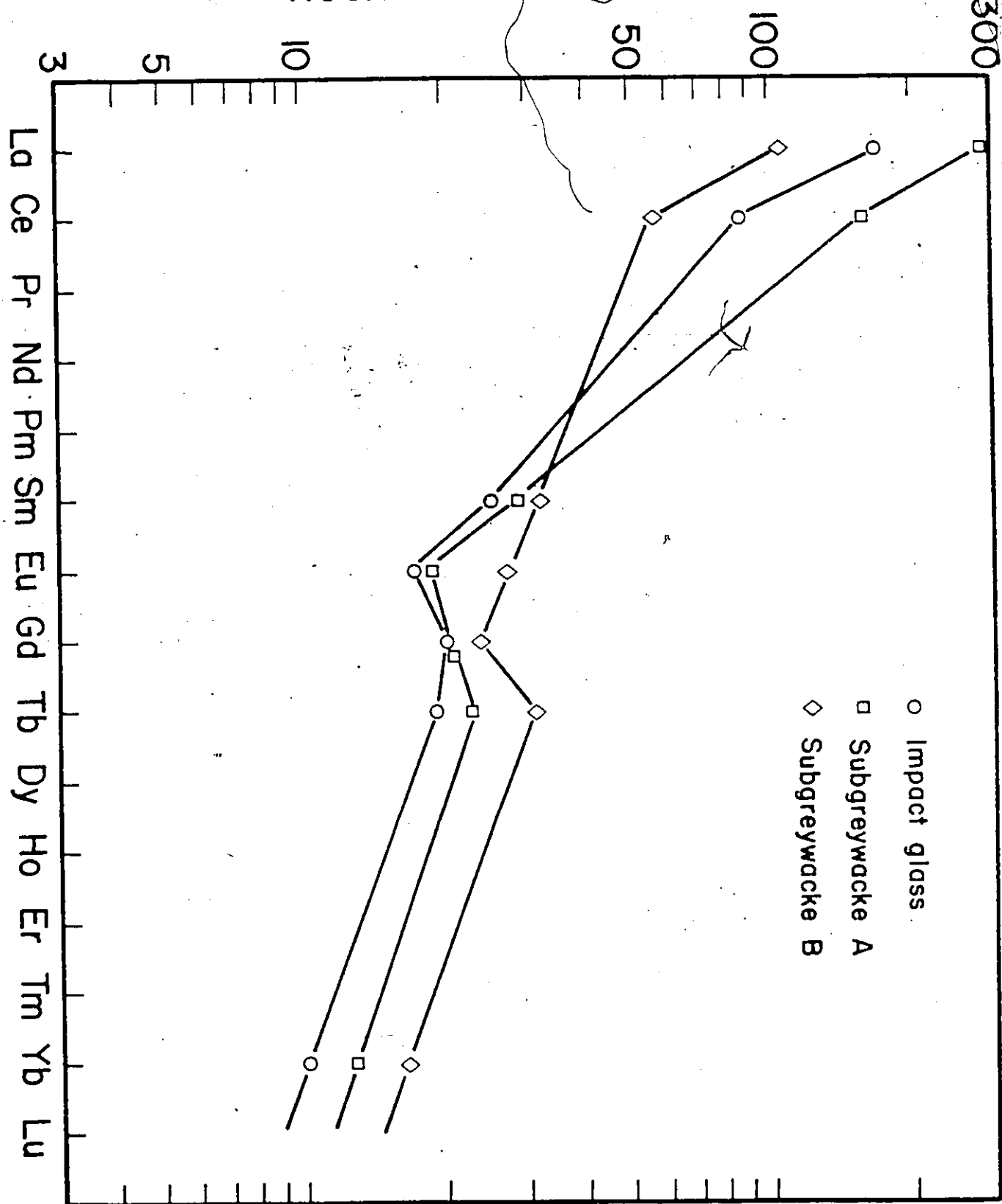
patterns fall within the narrow range observed in the country rocks

(Fig. 5-20). Schnetzler et al. (1967) suggested that the impact glass

represents material from a large area which has been homogenized by

the meteorite impact.

These studies suggest that impact glass and fallback breccia

formed during meteorite impact should have RE patterns similar to

the country rock or reflect a mixture of country rocks when diverse

rock types are present in the target area.

5-8-3. Rare Earth Evidence for an Impact Origin of the Onaping Formation

According to the meteorite impact model, the basal

breccia comprises the earliest fallback rock together with in situ

shattered country rocks while the grey Onaping represents a later

stage of fallback. Therefore, they are both mechanical mixtures of

brecciated country rocks and should have similar RE patterns which

reflect a mixture of the country rocks.

The RE pattern of the north range Superior gneiss is

shown in Fig. 4-5. No sample of south range country rocks was

analyzed for REE. It is also difficult to estimate the proportion of

north and south range country rocks which were mixed and/or melted

during the meteorite impact. The two fallback samples (basal breccia

and grey Onaping) have very similar RE patterns. When compared to

the north range country rocks, the fallback samples are slightly higher

Fig. 5-20. Relative Rare Earth Fractionation Patterns of

Impact Glass and Country Rocks from Bosumtwi Crater,

Ghana (from Schnetzler et al. 1967).

ROCK / CHONDRITES

○ Impact glass
▲ Range of three sediments

La Ce Pr Nd Pm Sm Eu Gd Tb Dy Ho Er Tm Yb Lu
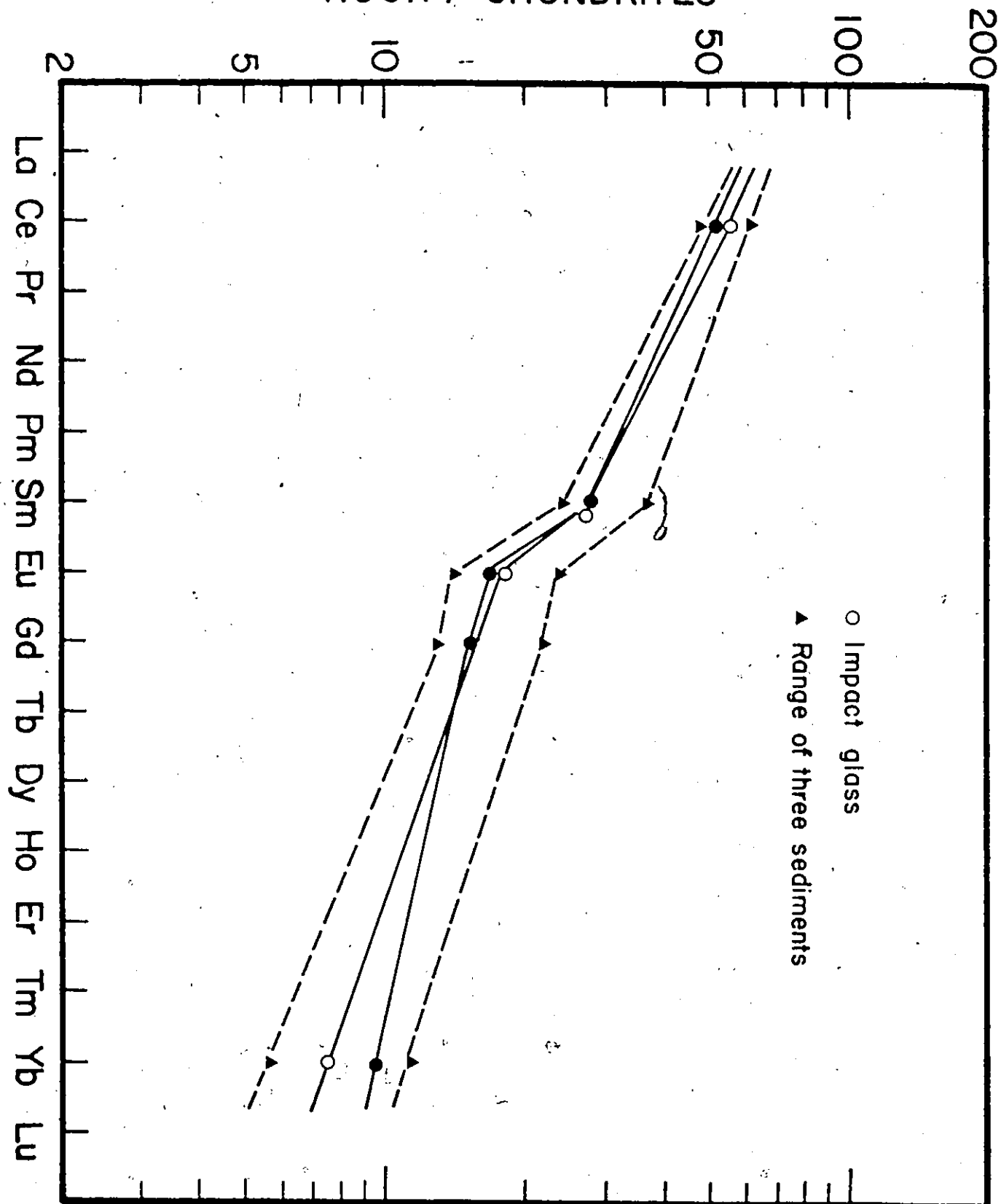
in the light REE and much higher in the heavy REE. Therefore, if the fallback rocks are mechanical mixtures of country rocks, another component with higher absolute RE abundances, especially the heavy REE, must be present in the target area.

The previous suggestion (section 5-4-5) that the average RE pattern of the Canadian Shield metagreywackes (Fig. 4-5) may represent the RE pattern of the south range Huronian rocks appears to be a reasonable one. This average metagreywacke has higher total RE contents, particularly with respect to the heavy REE, than the Onaping Formation rocks and the north range country rocks. The pattern represents the component needed to satisfy the mechanical mixing model proposed above.

Further support for the impact model is found in the RE pattern of the Onwatin slate (Wildeman and Haskin, 1973; see Fig. 4-5) which is intermediate between Onaping Formation rocks and the metagreywackes. In a meteorite impact model, it is suggested that the Onwatin Formation consists of reworked material from the Onaping Formation with an increasing admixture of normal detrital materials from the surrounding terrane (French, 1970; Dietz, 1972). From Fig. 4-5, it is evident that addition of more greywacke to Onaping Formation rocks will produce a RE pattern similar to that observed in the Onwatin slate; that is, a rock with higher total RE contents and with a

greater heavy RE component than Onaping Formation rocks. The Eu/Eu* ratio of the Onwatin Formation which is intermediate between lower Onaping Formation rocks and the metagreywackes also appear to support this mixing model.

Melt rocks in the Onaping Formation are chemically inhomogeneous and highly variable in chemical composition (Peredery, 1972). The analyzed melt rock sample has a strong negative Eu anomaly which is lacking in the north range country rocks. In an impact model, melt rocks represent fusion of country rocks during the impact. The large negative Eu anomaly is not obviously explained on a basis of available evidence, but may indicate the presence of some south range country rock with a large negative Eu anomaly.

In conclusion, the RE data indicate that the Onaping Formation rocks are not genetically related to, or strongly affected by the Nickel Irruptive. A meteorite impact fallback origin of the Onaping Formation rocks explains some features of the RE patterns of these rocks.

5-9. Rare Earth Constraints on the Genesis of the Sudbury Nickel Irruptive

RE patterns in the Sudbury rocks provide additional limits on the interpretation of geological history at Sudbury.

RE data on Onaping Formation rocks are better explained as mechanical mixtures of country rocks than as patterns representative of felsic volcanic differentiates of the main Irruptive magma. The meteorite impact model is therefore favoured. The original impact crater at Sudbury is estimated to have had a diameter of 40 (Dietz, 1972) to 100 km (French, 1970; Bray, 1972; Dence, 1972), and a depth between 4 (Dietz, 1972) to 30 km (Dence, 1972). Numerous inclusions of basement rocks have been recognized in the Onaping Formation (French, 1972; Peredery, 1972). The RE patterns of the lower Onaping Formation rocks which would seem to require input from both north and south range country rocks suggest that the impact crater was deep enough to break through the surface Huronian rocks and shatter and pulverize the underlying gneissic basement.

The overall properties of the REE in the Sudbury Irruptive rocks are consistent with the general features of RE behaviour observed in layered basic intrusions as discussed in section 5-3. Some of the more important properties include the following: the RE characteristics of the border norite; the lower total RE content and La/Yb ratio in norite and higher total RE content and La/Yb ratio in micropegmatite as compared with the border norite; the positive Eu anomaly in norite,

weak Eu anomaly in the oxide-rich gabbro, and mirror image

negative Eu anomaly in micropegmatite; and, the lack of large varia-

tions of RE patterns between these rocks. It is concluded that the

observed RE data indicate that the main Irruptive rocks are related

to each other by fractional crystallization processes.

The lack of a significant Eu anomaly in the border norite

indicates that no significant amount of plagioclase had settled out of

the main Irruptive magma prior to its intrusion into the present site.

This observation and the positive Eu anomaly in the norite, therefore,

further indicate that the norite, oxide-rich norite, and at least part

of the micropegmatite are in situ fractional crystallization products of

a single magma.

Whether the apparently large volume of micropegmatite is

the result of in situ assimilation of Onaping Formation rocks or the

result of latter surges of micropegmatite magma from the main magma

chamber of the Irruptive cannot be distinguished by the present RE

information. The shape of the main Irruptive in turn depends upon

these speculations. The size of the negative Eu anomaly in the

micropegmatite suggests a micropegmatite/norite ratio of 1/3 for the

main Irruptive. Since the lower Onaping Formation rocks have

higher Eu/Eu^* ratios than the micropegmatite, assimilation of Onaping

Formation rocks would require that the original micropegmatite should have a lower Eu/Eu* ratio than presently observed. This in turn would suggest a norite/micropegmatite ratio greater than 3 and infer a steep, funnel-shaped form for the main Irruptive. If a later surge of micro-pegmatite magma as proposed by Peredery (1972) has occurred, then the main Irruptive would probably require a shallow, funnel-shaped or bowl-shaped form. The present day configuration of norite and micropegmatite may represent the ring portion of this bowl-shaped lopolith with essentially no micropegmatite remaining at the center of the lopolith.

The strong light RE enrichment pattern and siliceous nature of the main Irruptive magma suggest involvement of lower crust in producing the magma. The RE properties of the sub-layer rocks suggest their formation from several batches of genetically-related magma. Their common features, particularly their inclusion- and sulfide-rich nature, suggests that they were formed in a similar environment or by similar processes. The general similarity of their RE patterns to that of the main Irruptive points to a probable genetic link.

None of the analysed sub-layer ultramafic inclusions represent undifferentiated or residual mantle material. The RE data suggests that they are fragments from a series of cumulates that contain

varying amounts of intercumulus material. These cumulates probably formed above the source zone of sub-layer melts and were disrupted by the ascending sub-layer magmas. The time interval between the intrusion of the main Irruptive and the sub-layer was probably very short (Naldrett et al., 1972; Gibbins, 1973). The volume of main Irruptive magma is large compared with that of the sub-layer magmas and the main Irruptive rocks are free of ultramafic inclusions and are not rich in sulfide. No other younger mafic intrusions in the Sudbury area rich in both ultramafic inclusions and sulfides has been reported. The ultramafic cumulates, therefore, must have formed during or after the formation of the main Irruptive magma but before the intrusion of the sub-layer melts. Logic leads one to suggest that these ultramafic cumulates formed at the bottom of a funnel-shaped Nickel Irruptive (Wilson, 1956; Naldrett and Kullerud, 1967). The RE data lend support to these considerations by indicating that the sub-layer inclusions have been in equilibrium with a liquid that has an RE pattern similar to that of the main Irruptive magma.

Naldrett et al. (1970), however, pointed out that if the marginal zones are characteristic of the Nickel Irruptive magma at the time of its final intrusion, the Irruptive magma would have been too siliceous to precipitate olivine. Therefore, they suggested that the ultramafic inclusions were probably derived from a deep-seated source

chamber where an initial parent magma underwent fractionation before its siliceous residual liquid was intruded into the present site of the Irruptive. The RE characteristics of the ultramafic sub-layer inclusions suggest the presence of varying amounts of intercumulus material with RE properties similar to the main Irruptive magma. Furthermore, the pronounced light REE enrichment of the Irruptive magma suggests mixing of a basic melt with a siliceous partial melt from the gneissic basement. It is tentatively proposed that the crystallization of the ultramafic and mafic cumulates and the incorporation of siliceous melt into the initial (basic) Irruptive magma were more or less contemporaneous. Thus, the RE properties of settled ferromagnesian cumulates may have been affected by an intercumulus liquid which became progressively more silic as mixing with crustal melt continued.

A meteorite impact model probably provides the best mechanism for producing both crustal and deeper mantle melting. Shock heating of rocks and pressure reduction by excavation of the crater, would both tend to promote partial melting at depth. Partial melting in both the upper mantle and lower crust probably occurred. Tectonic instability and re-adjustment following the meteorite impact may provide the mechanism needed for the formation and emplacement of several batches of sub-layer magma at short intervals.

CHAPTER SIX

CONCLUSIONS

A review of RE patterns in layered basic intrusions revealed several common features of RE behaviour in these intrusions. The anomalous behaviour of europium in layered intrusions appears to be particularly significant. The major conclusions derived from the RE study on the Sudbury Nickel Irruptive rocks are the following:

1. Border norites on both north and south ranges solidified as relatively closed systems, and their RE fractionation pattern should resemble that of the main Irruptive magma upon intrusion.

2. RE fractionation patterns of Irruptive norite, oxide-rich gabbro and micropegmatite indicate that these rocks are comagmatic and that they are related by gravitational fractionation crystallization process. Norites are cumulates from this magma and micropegmatite formed from the residual liquid.

3. A minimum norite to micropegmatite ratio of three is suggested by RE mass balance considerations, and lends support to a funnel-shaped model for the main Irruptive.

4. The strong light RE enrichment pattern of the main Irruptive magma as compared with chilled gabbros of other layered basic intrusions, is in keeping with the unusually siliceous nature of the main Irruptive.

5. Mafic sub-layer and offset rocks solidified from several batches of magma with RE patterns similar to that of the main Irruptive magma. The source of sub-layer and main Irruptive magma is probably similar.

6. None of the sub-layer inclusions represents either a simple residuum or undifferentiated primordial mantle material. They were probably derived from pre-existing mafic-ultramafic cumulates that were genetically related to the parental main Irruptive magma.

7. RE patterns of the Onaping Formation rocks are not compatible with a volcanic ash-flow origin in which the volcanics are differentiates of the main Irruptive magma. They are better explained as country rock fallback breccias such as might be produced by a meteorite impact.

8. The possibility of in situ assimilation of lower Onaping Formation rocks into micropegmatite cannot be ruled out by RE considerations.

In the author's opinion the model of Naldrett et al. (1972), on a whole, appears to provide the best explanation for the observations reported in recent years on the Nickel Irruptive. Based on his model, a history of the Sudbury Nickel Irruptive, modified by conclusions derived from the present study, is presented:

A meteorite impact formed the Sudbury structure. It shattered, mixed and partially melted a succession of Huronian rocks and the underlying gneissic basement. In addition, it triggered the formation of the parental Irruptive magma in the upper mantle and probably significant amounts of partial melting in the overlying crystal basement. The settling of fallback breccias in the center of the impact crater formed the Onaping Formation. A basic parental Irruptive magma intruded part way into the crust, carrying olivine and pyroxene pheno-crysts and droplets of immiscible sulfide. It then pooled, settling of phenocrysts and sulfides cocurred to form a zone of ultramafic cumulates and the basic magma was contaminated with a more silicic melt or with more silicic rocks. Continued re-adjustment in the crust after the shock of the impact caused continued intrusion of the magma, now deficient in phenocrysts and sulfide and higher in silica content, into its present site. There it differentiated under the influence of gravity to form norite and micropegmatite in a funnel-shaped configuration. Assimilation of lower Onaping Formation rocks into the micropegmatite may have occurred at this time. Finally, several batches of sub-layer magma originating at the original zone of melting in the mantle were in-jecting up the same conduit. These magmas disrupted the cumulates,

picked up sulfides and ultramafic xenoliths, mixed with the remaining magma in the original magma chamber and/or melts from country rocks, and were emplaced at the margins of the main Irruptive forming the ore bodies.

REFERENCES

Arth, J.G. and Hanson, G.N. (1972) Quartz diorites derived by partial melting of eclogite or amphibolite at mantle depths, Contrib. Mineral. Petrol., v. 37, pp. 161-174.

_____ and _____ (1975) Geochemistry and origin of the early Precambrian crust of northeastern Minnesota, Geochim. Cosmochim. Acta, v. 39, pp. 325-362.

Balashov, Yu. A. and Nesterenko, G.N. (1966) Distribution of the rare earths in the trapes of the Siberian platform, Geochemistry Internat., v. 3, pp. 672-679.

_____ and Turanskaya, N.V. (1962) Rare earth elements in the peridotite of the polar Urals, Geochemistry, No. 4, pp. 433-435.

Bouska, V., Benada, J., Randa, Z. and Kuncir, J. (1973) Geochemical evidence for the origin of moldavites, Geochim. Cosmochim. Acta, v. 37, pp. 121-131.

Bowden, P. and Whitley, J.E. (1974) Rare earth patterns in peralkaline and associated granites, Lithos, v. 7, pp. 15-21.

Bray, J.V.G. (1972) in New Developments in Sudbury Geology (editor J.V. Guy-Bray), Geol. Assoc. Canada Spec. Paper No. 10, pp. 1-5.

Bray, J.V.G. and Geological Staff (1966) Shatter cones at Sudbury,

    J. Geol., v. 74, pp. 243-245.

Brocoum, S.J. and Dalziel, I.W.D. (1974) The Sudbury basin, the South-

    ern Province, the Grenville Front, and the Penokean Orogeny,

    Geol. Soc. Amer. Bull., v. 85, pp. 1571-1580.

Buma, G., Frey, F.A. and Wones, D.R. (1971) New England granites:

    trace element evidence regarding their origin and differentia-

    tion, Contrib. Mineral. Petrol., v. 31, pp. 300-320.

Burrows, A.G. and Rickaby, H.C. (1929) Sudbury basin area, Ont.

    Dept. Mines, v. 38, part 3, pp. 1-55.

Card, K.D. and Hutchinson, R.W. (1972) The Sudbury structure: its

    regional geological setting, in New Developments in Sudbury

    Geology (editor, J.V. Guy-Bray), Geol. Assoc. Canada Spec.

    Paper No. 10, pp. 67-78.

Chase, J.W., Winchester, J.W. and Coryell, C.D. (1963) Lanthanum,

    europium, and dysprosium distributions in igneous rocks and

    minerals, J. Geophys. Res., v. 68, pp. 567-575.

Cheng, K.L. (1958) EDTA titration of microquantities of rare earths,

    Chemist-Analyst, v. 47, pp. 93-94.

Chyi, L.L. (1972) Distribution of some noble metals in sulfide and oxide

    minerals in Strathcona mine, Sudbury, Ph.D. Thesis,

    McMaster University.

Coleman, A.P. (1905) The Sudbury Nickel region, Ont. Dept. Mines, v.14, part 3.

_____ (1913) The nickel industry, Mines Branch, Dept. Mines, Canada.

Collins, W.H. (1934) Life-history of the Sudbury Nickel Irruptive; part I, Trans. Roy. Soc. Canada, 3rd Ser., No. 28, pp. 123-177.

_____ (1935) Idem., part II, No. 29, pp. 27-47.

_____ (1936) Idem., part III, No. 30, pp. 29-35.

_____ (1937) Idem., part IV, No. 31, pp. 15-43.

Condie, K.C. and Baragar, W.R.A. (1974) Rare-earth element distributions in volcanic rocks from Archean greenstone belts, Contrib. Mineral. Petrol., v. 45, pp. 237-246.

_____ and Lo, H.H. (1971) Trace element geochemistry of the Louis lake batholith of early Precambrian age, Wyoming, Geochim. Cosmochim. Acta, v. 35, pp. 1099-1119.

_____ and Swenson, D.H. (1973) Compositional variation in three Cascade stratovolcanoes: Jefferson, Rainier, and Shasta, Bull. Volcanol., v. 37, pp. 205-230.

Coryell, C.D., Chase, J.W. and Winchester, J.W. (1963) A procedure for geochemical interpretation of terrestrial rare earth abundance patterns, J. Geophys. Res., v. 68, pp. 559-566.

Cowan, J.C. (1968) The geology of the Strathcona ore deposit, Can. Mining Met. Bull., v. 60, pp. 3854.

Cullers, R. L., Medaris, G. L. and Haskin, L.A. (1973) Experimental studies of the distribution of rare earths as trace elements among silicate minerals and liquids and water, Geochim. Cosmochim. Acta, v. 37, pp. 1499-1512.

_____, Yeh, L. T., Chaudhuri, S. and Guidotti, C. F. (1974) Rare earth elements in Silurian pelitic schists from N. W. Maine, Geochim. Cosmochim. Acta, v. 38, pp. 389-400.

Daly, R.A. (1928) Bushveld igneous complex of the Transvaal, Geol. Soc. Amer. Bull., v. 39, pp. 703-768.

Dence, M. R. (1972) Meteorite impact craters and the structure of the Sudbury basin, in New Developments in Sudbury Geology (editor, J.V. Guy-Bray), Geol. Assoc. Canada Spec. Paper No. 10, pp. 7-18.

Denechaud, E. B., Helmke, P.A. and Haskin, L.A. (1970) Analysis for the rare-earth elements by neutron activation and Ge(Li) spectrometry, J. Radioanal. Chem., v. 6, pp. 97-113.

Dietz, R. S. (1964) Sudbury structure as an astrobleme, J. Geol., v. 72, pp. 412-434.

_____ (1972) Sudbury astrobleme, splash emplaced sub-layer and possible cosmogenic ores, in New Developments in Sudbury Geology (editor, J.V. Guy-Bray), Geol. Assoc. Canada Spec. Paper No. 10, pp. 29-40.

Dietz, R.S. and Butler, L.W. (1964) Shatter-cone orientation at Sudbury, Canada, Nature, v. 204, pp. 280-281.

Dostal, J. (1973) Geochemistry and petrology of the Loon Lake pluton, Ontario, Ph.D. Thesis, McMaster University.

Drake, M.J. (1975) The oxidation state of europium as an indicator of oxygen fugacity, Geochim. Cosmochim. Acta, v. 39, pp. 55-64.

Dudas, M.J., Schmitt, R.A. and Harward, M.E. (1971) Trace element partitioning between volcanic plagioclase and dacitic pyroclastic matrix, Earth Planet. Sci. Lett., v. 11, pp. 440-446.

Ewart, A., Bryan, W.B. and Gill, J.B. (1973) Mineralogy and geochemistry of the younger volcanic islands of Tonga, S.W. Pacific, J. Petrol., v. 14, pp. 429-465.

_____, Taylor, S.R. and Capp, A.C. (1968) Trace and minor element geochemistry of the rhyolitic volcanic rocks, central north island, New Zealand, Contrib. Mineral. Petrol., v. 18, pp. 76-104.

Fahrig, W.F., Gaucher, E.H. and Larocelle, A. (1965) Paleomagnetism of diabase dikes of the Canadian shield, Can. J. Earth Sci., v. 2, pp. 278-298.

Fairbairn, H.W., Ahrens, L.H. and Gorfinkle, L.G. (1953) Minor element content of Ontario diabase, Geochim. Cosmochim. Acta, v. 3, pp. 34-46.

Fairbairn, H.W., Hurley, P.M. and Pinson, W.H. (1960) Mineral and
rock ages at Sudbury-Blind River, Ontario, Proc. Geol. Assoc.
Canada, v. 12, pp. 41-66.

_____, _____ and _____ (1965) Re-examination of Rb-Sr whole-
rock ages at Sudbury, Ontario, Proc. Geol. Assoc. Canada,
v. 16, pp. 95-101.

_____, _____ and _____ (1968) Rb-Sr whole-rock age of the
Sudbury lopolith and basin sediments, Can. J. Earth Sci.,
v. 5, pp. 707-714.

Faure, G., Fairbairn, H.W., Hurley, P.M. and Pinson, W.H. (1964)
Whole-rock Rb-Sr age of norite and micropegmatite at Sudbury,
Ontario, J. Geol., v. 72, pp. 848-854.

Flanagan, F.J. (1973) 1972 values for international geochemical
reference samples, Geochim. Cosmochim. Acta, v. 37, pp.
1189-1200.

Flower, M.F.J. (1971) Rare earth element distribution in lavas and ultra-
mafic xenoliths from the Comores Archipelago, western Indian
Ocean, Contrib. Mineral. Petrol., v. 31, pp. 335-346.

French, B.M. (1967) Sudbury structure, Ontario: some petrographic
evidence for origin by meteorite impact, Science, v. 156,
pp. 1094-1098.

French, B.M. (1968) Sudbury structure, Ontario: some petrographic evidence for an origin by meteorite impact, in Shock Metamorphism of Natural Materials (editor, French and Short), pp. 383-412, Mono Book Corp.

_____ (1970) Possible relation between meteorite impact and igneous petrogenesis, as indicated by the Sudbury structure, Ontario, Canada, Bull. Volcanol., v. 34, pp. 466-517.
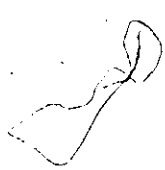
Frey, F.A. (1969) Rare earth abundances in a high-temperature peridotite intrusion, Geochim. Cosmochim. Acta, v. 33, pp. 1429-1447.

_____ (1970) Rare earth and potassium abundances in St. Paul's rocks, Earth Planet. Sci. Lett., v. 7, pp. 351-360.

_____ and Green, D.H. (1974) The mineralogy, geochemistry and origin of lherzolite inclusions in Victorian basanites, Geochim. Cosmochim. Acta, v. 38, pp. 1023-1059.

_____, Haskin, L.A. and Haskin, M.A. (1971) Rare-earth abundances in some ultramafic rocks, J. Geophys. Res., v. 76, pp. 2057-2070.

_____, Haskin, M.A., Poetz, J.A. and Haskin, L.A. (1968) Rare earth abundances in some basic rocks, J. Geophys. Res., v. 73, pp. 6085-6098.

Fullagar, P.D., Bottino, M.L. and French, B.M. (1971) Rb-Sr study of shock metamorphosed inclusions from the Onaping formation, Sudbury, Ontario, Can. J. Earth Sci., v. 8, pp. 435-443.

Gasparrini, E. and Naldrett, A.J. (1972) Magnetite and ilmenite in the Sudbury Nickel Irruptive, Econ. Geol., v. 67, pp. 605-621.

Gast, P.W. (1968) Trace element fractionation and the origin of tholeii-tic and alkaline magma types, Geochim. Cosmochim. Acta, v. 32, pp. 1057-1086.

_____, Hubbard, N.J. and Wiesman, H. (1970) Chemical composition and petrogenesis of basalts from Tranquillity base, Proc. Apollo 11 Lunar Sci. Conf., Geochim. Cosmochim. Acta Suppl. 1, v, 2, pp. 1143-1163, Pergamon.

Gates, T.M. (1971) K, Rb, Sr, and Sr isotopic evidence for near surface crustal contamination of diabase dikes, Ph.D. Thesis, Section III, M.I.T.

Gibbins, W. (1973) Rubidium-strontium mineral and rock ages at Sudbury, Ontario, Ph.D. Thesis, McMaster University.

Goldschmidt, V.M. (1954) "Geochemistry", Clarendon Press, Oxford.

Gordon, G.C., Randle, K., Goles, G.G., Corliss, J.B., Beeson, M.H.H. and Oxley, S.S. (1968) Instrumental activation analysis of standard rocks with high-resolution gamma-ray detectors, Geochim. Cosmochim. Acta, v. 32, pp. 369-396.

Graber, F. M., Lukens, H. R. and Mackenzie, J. K. (1970) Neutron activation analysis determination of all 14 stable rare earth elements with group separation and Ge(Li) spectrometry, J. Radioanal. Chem., v. 4, pp. 229-239.

Green, D. H. (1972) Archean greenstone belts may include terrestrial equivalents of lunar maria, Earth Planet. Sci. Lett., v. 15, pp. 263-270.

_____ (1975) Genesis of Archean peridotite magmas and constraints on Archean geothermal gradients and tectonics, Geology, v. 3, pp. 15-18.

_____, Nicholls, I. A., Viljoen, M. and Viljoen, R. (1975) Experimental demonstration of the existence of peridotitic liquids in earliest Archean magmatism, Geology, v. 3, pp. 11-14.

Green, T. H., Brunfelt, A. O. and Heier, K. S. (1972) Rare-earth element distribution and K/Rb ratios in granulites, mangerites and anorthosites, Lofoten-Vesteraalen, Norway, Geochim. Cosmochim. Acta, v. 36, pp. 241-257.

Greenland, L. P. (1970) An equation for trace element distribution during magmatic crystallization, Amer. Mineral., v. 55, pp. 455-465.

Greenman, L. (1970) Petrology of the footwall breccias in the vicinity
of the Strathcona mine, Levack, Ontario, Ph.D. Thesis,
University of Toronto.

Hamilton, W. (1960) Form of the Sudbury lopolith, Can. Mineral.,
v. 6, pp. 437-447.

Hamilton, E.I. (1963) The isotopic composition of strontium in the
Skaergaard intrusion, east Greenland, J. Petrol., v. 4,
pp. 383-391.

Haskin, L.A. and Frey, F.A. (1966) Dispersed and not-so-rare earths,
Science, v. 152, pp. 299-314.

_____ and Gehl, M.A. (1962) The rare-earth distribution in sediments,
J. Geophys. Res., v. 67, pp. 2537-2541.

_____ and Haskin, M.A. (1968) Rare-earth elements in the Skaergaard
intrusion, Geochim. Cosmochim. Acta, v. 32, pp. 433-447.

_____, Wilderman, T.R. and Haskin, M.A. (1968a) An accurate
procedure for determination of the rare-earth elements by
neutron-activation, J. Radioanal., Chem., v. 1, pp. 337-348.

_____, Frey, F.A., Schmitt, R.A. and Smith, R.H. (1966a)
Meteoritic, solar and terrestrial rare-earth distributions,
Phys. Chem. Earth, v. 7, pp. 167-321.

Haskin, L.A., Haskin, M.A., Frey, F.A. and Wildeman, T.R. (1968b) Relative and absolute terrestrial abundances of the rare earths, in-Origin and Distribution of the Elements (editor, L.H. Ahrens), pp. 889-912, Pergamon.

_____, Wildeman, T.R., Frey, F.A., Collins, K.A., Keedy, C.R. and Haskin, M.A. (1966b) Rare earths in sediments, J. Geophys. Res., v. 71, pp. 6091-6105.

Hawley, J.E. (1962) The Sudbury ores; their mineralogy and origin, Can. Mineral., v. 7, pp. 1-207.

Helmke, P.A. and Haskin, L.A. (1973) Rare-earth elements, Co, Sc· and Hf in the Steens Mountain basalts, Geochim. Cosmochim. Acta, v. 37, pp. 1513-1529.

Herrman, A.G. (1968) Die Verteilung der Lanthaniden in basaltischen gesteinen, Contrib. Mineral. Petrol., v. 17, pp. 274-314.

_____ (1970) Yttrium and lanthanides, in Handbook of Geochemistry (editor K.H. Wedepohl), II-2, pp. 57-71, Springer Verlag.

_____, Blanchard, D.P., Haskin, L.A., Jacobs, J.W., Knake, D. and Korotev, R.L. (1974) Rare earths and other trace elements in some greenstone from the Precambrian crust of southern Africa, Trans. Amer. Geophys. Union, v. 55, p. 473.

Hewins, R. H. (1971) The petrology of some marginal mafic rocks along the
    north range of the Sudbury Irruptive, Ph. D. Thesis, University
    of Toronto.

Higuchi, H. and Nagasawa, H. (1969) Partition of trace elements be-
    tween rock-forming minerals and the host volcanic rocks,
    Earth Planet. Sci. Lett., v. 7, pp. 281-287.

_____, Tomura, K. and Hamaguchi, H. (1970) Determination of rare-
    earth elements in rock samples by neutron activation analysis,
    J. Radioanal. Chem., v. 5, pp. 209-222.

Holden, N. E. and Walker, F. W. (1973) Chart of the Nuclides, 11th edition,
    Knolls Atomic Power Laboratory.

Hunter, D. R. (1974) Crustal development in the Kaapvaal craton, II. the
    Proterozoic, Precambrian Res., v. 1, pp. 295-326.

Hurst, R. W. and Wetherill, G. W. (1974) Rb-Sr study of the Sudbury
    Nickel Irruptive, Trans. Amer. Geophys. Union, v. 55,
    p. 466.

Irvine, T. N. (1970) Crystallization sequences in the Muskox intrusion
    and other layered intrusions, Geol. Soc. South Africa, Spec.
    Publ., v. 1, pp. 441-476.

Jackson, E. D. (1967) Ultramafic cumulates in the Stillwater, Great Dyke,
    and Bushveld intrusions, in Ultramafic and Related Rocks
    (editor, P. J. Wyllie), pp. 20-38, J. Wiley and Sons.

Jahn, B.M., Shih, C.Y. and Murthy, V.R. (1974) Trace element geo-
chemistry of Archean volcanic rocks, Geochim. Cosmochim.
Acta, v. 38, pp. 611-627.

Jakes, P. and Gill, J. (1970) Rare earth elements and the island arc
tholeiitic series, Earth Planet. Sci. Lett., v. 9, pp. 17-28.

Kay, R.W. and Gast, P.W. (1973) The rare earth content and origin of
alkali-rich basalts, J. Geol., v. 81, pp. 653-682.

_____, Hubbard, N.J. and Gast, P.W. (1970) Chemical characteristics
and origin of oceanic ridge volcanic rocks, J. Geophys. Res.,
v. 75, pp. 1585-1613.

Keays, R.R. and Crocket, J.H. (1970) A study of precious metals in the
Sudbury Nickel Irruptive ores, Econ. Geol., v. 65, pp. 438-450.

Knight, C.W. (1917) Report of the Ontario Nickel Commission, pp. 110-121.

_____ (1923) The chemical composition of the norite-micropegmatite,
Sudbury, Ontario, Econ. Geol., v. 18, pp. 592-594.

Koljonen, T. and Rosenberg, R.J. (1974) Rare earth elements in granitic
rocks, Lithos, v. 7, pp. 249-261.

Kosiewicz, S.T. (1973) Rare-earth elements in USGS rocks SCo-1 and STM-1,
basalts from the Servilleta and Hindale formations, and rocks
from the Stillwater and Muskox intrusions, Ph.D. Thesis,
The University of Wisconsin.

Krough, T. E. and Davis, G. L. (1974) The age of the Sudbury Nickel

Irruptive, Annual Report of the Director, Geophys. Lab.,

Carnegie, Inst., pp. 567-569.

Mossart, D. L. and Hoste, J. (1968) Activation analysis of rare earths,

Anal. Chim. Acta, v. 42, pp. 21-28.

Masuda, A. (1962) Regularities in variation of relative abundances of

lanthanides elements and an attempt to analyze separation-

index patterns of some minerals, J. Earth Sci., Nagoya Univ.,

v. 10, pp. 173-187.

_____ (1966) Lanthanides in basalts of Japan with three distinct types,

Geochem. J., v. 1, pp. 11-26.

_____ and Kushiro, I. (1970) Experimental determination of partition

coefficients of ten rare earth elements and barium between

clinopyroxene and liquid in the synthetic silicate system at

20 kilobar pressure, Contrib. Mineral. Petrol., v. 26,

pp. 42-49.

McCall, G. J. H. and Leishman, J. (1971) Clues to the origin of

Archean eugeosynclinal peridotites and the nature of serpen-

tinization, Geol. Soc. Australia Spec. publ., v. 3, pp. 281-299.

McIntire, W.L. (1963) Trace element partition coefficients - a review

of theory and applications to geology, Geochim. Cosmochim.

Acta, v. 27, pp. 1209-1264.

Melsom, S. (1970) Precision and accuracy of rare earth determinations

in rock samples using instrumental neutron activation analysis

and a Ge(Li) detector, J. Radioanal. Chem., v. 4, pp.

355-363.

Moeller, T. and Kremers, H. (1945) The basicity characteristics of

scandium, yttrium and the rare earth elements, Chem. Rev.,

v. 37, pp. 97-159.

Moorhouse, W.W. (1969) Nipissing diabase composition, quoted in Gates

(1971).

Morrison, G.H., Gerard, J.T., Travesi, A., Currie, R.L.,

Peterson, S.F. and Potter, N.M. (1969) Multielement neutron

activation analysis of rock using chemical group separations

and high resolution gamma spectrometry, Anal. Chem., v. 41,

pp. 1633-1637.

Mosen, A.W., Schmitt, R.A. and Vasilevskis, J. (1961) A procedure

for the determination of the rare earth elements, lanthanum

through lutetium, in chondritic, achondritic and iron meteorites

by neutron-activation analysis, Anal. Chem. Acta, v. 25,

pp. 10-24.

Nagasawa, H. (1970) Rare earth concentration in zircon and apatite and their host dacite and granites, Earth Planet. Sci. Lett., v. 9, pp. 359-364.

_____ (1971) Partitioning of Eu and Sr between coexisting plagioclase and K-feldspar, Earth Planet. Sci. Lett., v. 13, pp. 139-144.

_____ (1973) Rare-earth distribution in alkali rocks from Oki-Dogo Island, Japan, Contrib. Mineral. Petrol., v. 39, pp. 301-308.

_____ and Schnetzler, C.C. (1971) Partitioning of rare earth, alkali and alkaline earth elements between phenocrysts and acidic igneous magma, Geochim. Cosmochim. Acta, v. 35, pp. 953-968.

_____, Wakita, H., Higuchi, H. and Onuma, N. (1969) Rare earths in peridotite nodules: an explanation of the genetic relationship between basalt and peridotite nodules, Earth Planet. Sci. Lett., v. 5, pp. 377-381.

Naldrett, A.J. and Kullerud, G. (1967) A study of the Strathcona mine and its bearing on the origin of the nickel-copper ore of the Sudbury district, Ontario, J. Petrol., v. 8, pp. 453-531.

_____ and Mason, G.D. (1968) Contrasting Archean ultramafic igneous bodies in Dundonald and Clergne township, Ontario, Can. J. Earth Sci., v. 5, pp. 111-143.

Naldrett, A.J., Greenman, L. and Hewins, R.H. (1972) The main

    Irruptive and the sub-layer at Sudbury, Ontario, Proc.

    24th Int. Geol. Cong., v. 4, pp. 206-214.

_____, Bray, J.G., Gasparrini, E.L., Podolsky, T. and Rucklidge,

    J.C. (1970) Cryptic variation and the petrology of the Sudbury

    Nickel Irruptive, Econ. Geol., v. 65, pp. 122-155.

Nesbitt, R.W. (1971).Skeletal crystal forms in the ultramafic rocks of

    the Yilgarn block Western Australia; evidence for an Archean

    ultramafic liquid, Geol. Soc. Australia Spec. Publ., v. 3,

    pp. 331-350.

Onuma, N., Higuchi, H., Wakita, H. and Nagasawa, H. (1968) Trace

    element partition between two pyroxenes and the host lava,

    Earth Planet. Sci. Lett., v. 5, pp. 47-51.

Paster, T.P., Schauwecker, D.S. and Haskin, L.A. (1974) The behavior

    of some trace elements during solidification of the Skaergaard

    layered series, Geochim. Cosmochim. Acta, v. 38, pp. 1549-

    1577.

Paul, D.K., Potts. P.J., Gibson, I.L. and Harris, P.G. (1975)

    Rare-earth abundances in Indian kimberlites, Earth Planet.

    Sci. Lett., v. 25, pp. 151-158.

Peredery, W.V. (1972) The origin of rocks at the base of the Onaping

    Formation, Sudbury, Ontario, Ph.D. Thesis, University of

    Toronto.

Phemister, T.C. (1925) Igneous rocks at Sudbury and their relation

    to the ore deposits, Annual Rept. Ont. Dept. Mines, XVIII,

    part 8.

Philpotts, J.A. and Schnetzler, C.C. (1968) Genesis of continental

    diabases and oceanic tholeiites considered in light of rare-

    earth and barium abundances and partition coefficients, in

    Origin and Distribution of the Elements (editor L.H. Ahrens),

    pp. 934-947, Pergamon.

_____, _____ and Thomas, H.H. (1972) Petrogenetic implications

    of some new geochemical data on eclogitic and ultrabasic

    inclusions, Geochim. Cosmochim. Acta, v. 36, pp. 1131-1166.

Potts, M.J. and Condie, K.C. (1971) Rare earth element distribution in

    a proto-stratiform ultramafic intrusion, Contrib. Mineral.

    Petrol., v. 33, pp. 245-258.

Price, R.C. and Taylor, S.R. (1973) The geochemistry of the Dunedin

    volcano, East Otago, New Zealand: rare earth elements,

    Contrib. Mineral. Petrol., v. 40, pp. 195-205.

Pyke, D.R., Naldrett, A.J. and Eckstrand, O.R. (1973) Archean

    ultramafic flows in Munro township, Ontario, Geol. Soc. Am.

    Bull., v. 70, pp. 981-1018.

Ragland, P.C., Brunfelt, A.O. and Weigand, P.W. (1971) Rare-earth abundances in Mesozoic dolerite dikes from Eastern United States, in Activation Analysis in Geochemistry and Cosmo-chemistry (editor A.O. Brunfelt and E. Steinnes), pp. 227-236, Universitetsforlaget.

Randle, K. (1974) Some trace element data and their interpretation for several new reference samples obtained by neutron activation analysis, Chem. Geol., v. 13, pp. 237-256.

Rankama, K. and Sahama, T.G. (1950) "Geochemistry", University of Chicago Press.

Rankin, D.W., Lopez-Escabar, L. and Frey, F.A. (1974) Rhyolites of the upper Precambrian Mt. Rogers (Virginia) volcanic center: geochemistry and petrogenesis, Trans. Amer. Geo-phys. Union, v. 55, pp. 475.

Reid, Jr., J.B. and Frey, F.A. (1971) Rare earth distributions in lherzolite and garnet pyroxenite xenoliths and the constitution of the upper mantle, J. Geophys. Res., v. 76, pp. 1184-1196.

Rey, P., Wakita, H. and Schmitt, R.A. (1970) Radiochemical neutron activation analysis of indium, yttrium and the 14 rare-earth elements in rocks, Anal. Chim. Acta, v. 51, pp. 163-178.

Rhodes, R.C. and Elston, W.E. (1974) A meteorite-impact model of the Bushveld-Vredefort complex, South Africa, Trans. Amer. Geophys. Union, v. 55, pp. 336-337.

Sadlor, J.F. (1958) A detailed study of the Onwatin Formation, M.Sc. Thesis, Queen's University, quoted in Dence (1972).

Schilling, J.G. and Winchester, J.W. (1966) Rare earths in Hawaiian basalts, Science, v. 153, pp. 867-869.

_____ and _____ (1967) Rare-earth fractionation and magmatic processes, in Mantles of the Earth and Terrestrial Planets (editor S.K. Runcorn), pp. 267-283, Interscience.

_____ and _____ (1969) Rare-earth contribution to the origin of Hawaiian lavas, Contrib. Mineral. Petrol., v. 23, pp. 27-37.

Schmitt, R.A., Mosen, A.W., Suffredini, C.S., Lasch, J.E., Sharp, R.A. and Olehy, D.A. (1960) Abundances of the rare earth elements, lanthanum to lutetium, in chondritic meteorites, Nature, v. 186, pp. 863-866.

_____, Smith, R.H., Lasch, J.E., Mosen, A.W., Olehy, D.A. and Vasilevskis, J. (1963) Abundances of the fourteen rare-earth elements, scandium, and yttrium in meteoritic and terrestrial matter, Geochim. Cosmochim. Acta, v. 27, pp. 577-622.

Schnetzler, C. C. and Philpotts, J. A. (1968) Partition coefficients
of rare-earth elements and barium between igneous matrix
material and rock-forming mineral phenocrysts - I, in
Origin and Distribution of the Elements (editor L. H. Ahrens),
pp. 929-938, Pergamon.

_____ and _____ (1970) Partition coefficients of some rare-
earth elements between igneous matrix material and rock-
forming mineral pher ɔcrysts - II, Geochim. Cosmochim.
Acta, v. 34, pp. 331-340.

_____, _____ and Thomas, H. H. (1967) Rare-earth and barium
abundances in Ivory Coast tektites and rocks from the Bosumtwi
Crater area, Ghana, Geochim. Cosmochim. Acta, v. 31,
pp. 1987-1993.

Shaw, D. M. (1970) Trace element fractionation during anatexis, Geochim.
Cosmochim. Acta, v. 34, pp. 237-243.

_____ (1972) Development of the early continental crust, part I, use
of trace element distribution coefficient models for the
protoArchean crust, Can. J. Earth Sci., v. 9, pp. 1577-1595.

Shih, C. and Jahn, B. (1973) Geochemistry of volcanic rocks from the
Overwacht Group, Swaziland sequence, South Africa, part I,
trace element study, Trans. Amer. Geophys. Union, v. 54,
pp. 502.

Shoemaker, E.M. and Chao, E.C.T. (1961) New evidence for the impact

origin of the Ries Basin, Bavaria, Germany, J. Geophys. Res.,

v. 66, pp. 3371-3378.

Souch, B.E., Podolsky, T. and Geological Staff (1969) The sulfide ores

of Sudbury: their particular relationships to a distinctive

inclusion-bearing facies of the Nickel Irruptive, in Magmatic

Ore Deposits (editor H.D.B. Wilson), Econ. Geol. Mono.

4, pp. 252-261.

Speers, E.C. (1957) The age relations and origin of the common Sudbury

breccia, J. Geol., v. 65, pp. 497-514.

Stevenson, J.S. (1961) Recognition of the quartzite breccia in the

Whitewater series, Sudbury basin, Ontario, Trans. Roy. Soc.

Canada, 3rd series, v. 55, pp. 57-66.

_____ (1963) The upper contact phase of the Sudbury micropegmatite,

Can. Mineral., v. 7, pp. 413-419.

_____ (1972) The Onaping ash-flow sheet, Sudbury, Ontario, in

New Developments in Sudbury Geology (editor J.V. Guy-Bray),

Geol. Assoc. Canada Spec. Paper, No. 10, pp. 41-48.

_____ and Colgrove, G.L. (1968) The Sudbury Irruptive: some

petrogenetic concepts based on recent field work, 23rd

Internat. Geol. Cong., v. 4, pp. 27-35.

Taylor, S.R. (1966) Australiates, Henbury impact glass and subgreywacke: a comparison of the abundances of 51 elements, Geochim. Cosmochim. Acta, v. 30, pp. 1121-1136.

_____ (1973) Tektites: a post-Apollo view, Earth Sci. Rev., v. 9, pp. 101-123.

_____, Ewart, A. and Capp, A.C. (1968) Leucogranites and rhyolites: trace element evidence for fractional crystallization and partial melting, Lithos, v. 1, pp. 179-186.

Thomson, J.E. (1956) Geology of the Sudbury basin, Ont. Dept. Mines, v. 65, pp. 1-56.

_____ (1969) A discussion of Sudbury geology and sulfide deposits, Ont. Dept. Mines misc. paper No. 30, 22 p.

Thomson, R. (1935) The offset dikes of the Nickel Irruptive, Sudbury, Ontario, Amer. J. Sci., v. 30, pp. 356-367.

Tomura, K., Higuchi, H., Miyaji, N., Onuma, N. and Hamaguchi, H. (1968) Determination of rare-earth elements in rock samples by neutron activation analysis with a lithium-drifted germanium detector after chemical group-separation, Anal. Chim. Acta, v. 41, pp. 217-228.

Topp, N.E. (1965) "The Chemistry of the Rare Earth Elements", Elsevier.

Towell, D.G., Winchester, J.W. and Spirn, R.V. (1965) Rare-earth distributions in some rocks and associated minerals of the batholith of southern California, J. Geophys. Res., v. 70, pp. 3485-3496.

Viljoen, M.J. and Viljoen, R.P. (1969) The geology and geochemistry of the lower ultramafic unit of the Overwacht Group and a proposed new class of igneous rocks, Geol. Soc. South Africa, Spec. publ., v. 2, pp. 55-85.

Wager, L.R. (1968) Rhythmic and cryptic layering in mafic and ultra-mafic plutons, in Basalts (editor H.H. Hess and A. Poldervaart), v. 2, pp. 573-622, Interscience.

_____ and Brown, G.M. (1967) Layered Igneous Rocks, W.H. Freeman and Co.

_____, _____ and Wadsworth, W.J. (1960) Types of igneous cumulates, J. Petrol., v. 1, pp. 73-85.

Walker, T.L. (1897) Geological and petrographical studies of the Sudbury nickel district, Canada, Quart. J. Geol. Soc., v. 53, pp. 40-66.

Weill, D.F. and Drake, M.J. (1973) Europium anomaly in plagioclase feldspar: experimental results and semiquantitative model, Science, v. 180, pp. 1059-1060.

Wildeman, T.R. and Condie, K.C. (1973) Rare earths in Archean graywackes from Wyoming and from the Fig Tree Group, South Africa, Geochim. Cosmochim. Acta, v. 37, pp. 439-453.

_____ and Haskin, L.A. (1973) Rare earths in Precambrian sediments, Geochim. Cosmochim. Acta, v. 37, pp. 419-438.

Williams, H. (1956) Glowing avalanche deposits of the Sudbury Basin, Ont. Dept. Mines, v. 65, pp. 57-89.

Wilson, H.D.B. (1956) Structure of lopoliths, Geol. Soc. Amer. Bull., v. 67, pp. 289-300.

Wright, E.P. (1961) The geology of the Gaberones district, Thesis, University Oxford, quoted in Hunter (1974).

Wyllie, P.J. (1967) Ultramafic and Related Rocks, J. Wiley and Sons.

Yates, A.B. (1938) The Sudbury intrusion, Trans. Roy. Soc. Canada, 3rd series, No. 32, pp. 151-172.

_____ (1948) Properties of International Nickel Company of Canada, in Structure Geology of Canadian Ore Deposits, Can. Inst. Min. Metal., Jubilee Volume, pp. 549-617.

Zielinski, R.A. and Frey, F.A. (1970) Gough Island: evaluation of a fractional crystallization model, Contrib. Mineral. Petrol., v. 29, pp. 242-254.

_____ and _____ (1974) An experimental study of the partitioning of a rare earth element (Gd) in the system diopside-aqueous vapour, Geochim. Cosmochim. Acta, v. 38, pp. 545-565.

APPENDICES

APPENDIX A. MAJOR ELEMENT CONCENTRATIONS (%) OF ROCKS AT SUDBURY

	SiO_2	TiO_2	Al_2O_3	Fe_2O_3	FeO	MnO	MgO	CaO	Na_2O	K_2O	H_2O	P_2O_5	CO_2	TOTAL
1	67.8	0.7	13.4	1.3	4.4	0.07	1.5	2.0	3.4	3.8	1.2	0.2	0.2	100.0
2	55.2	0.8	16.9	1.9	6.5	0.1	5.2	7.4	2.9	1.4	1.3	0.2	0.2	100.0
3	50.0	0.48	14.7	-	-	0.13	7.5	6.4	2.8	0.99	-	-	-	-
4	53.9	0.46	10.0	-	-	0.17	11.8	4.7	2.0	1.24	-	-	-	-
5	60.12	0.83	16.63	1.04	5.65	0.10	4.06	5.46	2.06	2.54	1.51	0.16	0.03	100.19
6	57.90	0.93	17.57	1.78	5.89	0.07	4.29	3.81	2.90	3.40	1.35	0.11	0.09	100.09
7	59.76	0.84	15.65	1.90	5.96	0.10	4.05	5.90	2.90	1.88	1.04	0.21	0.00	100.19
8	60.15	1.03	15.23	1.46	7.07	0.08	3.33	5.35	2.30	2.36	1.03	0.18	0.31	99.88
9	59.48	0.91	16.27	1.54	6.14	0.09	3.93	5.13	2.54	2.54	1.23	0.16	0.11	100.07
10	47.7	2.5	11.9	3.4	12.7	0.2	4.7	9.8	2.8	0.7	1.2	-	0.1	97.7
11	50.3	1.4	13.9	4.0	10.8	0.3	4.8	9.6	3.0	1.0	1.4	-	0.1	100.6
12	50.6	0.5	14.8	3.0	6.1	0.2	9.1	10.4	1.8	1.4	1.6	0.2	-	99.7
13	45.9	3.1	15.1	2.9	12.1	0.2	4.2	8.5	3.5	1.2	1.7	-	0.1	98.5
14	59.6	0.65	15.6	-	-	0.06	2.5	5.4	4.1	0.88	-	-	-	-

APPENDIX A (continued)

	SiO_2	TiO_2	Al_2O_3	Fe_2O_3	FeO	MnO	MgO	CaO	Na_2O	K_2O	H_2O	P_2O_5	CO_2	TOTAL
15	60.99	0.48	12.82	0.95	7.86	0.35	4.46	1.90	0.75	1.98	3.28	0.23	2.32	98.37
16	61.48	0.54	11.85	4.04	4.99	0.15	4.17	4.79	3.25	2.17	1.66	0.15	0.006	99.25
17	66.47	0.49	12.01	2.41	3.43	0.06	3.78	2.76	5.06	1.69	1.72	0.10	-	99.98
18	71.94	0.44	12.18	0.94	2.98	0.09	1.09	0.82	2.02	4.86	-	-	-	97.26
19	67.10	0.53	13.15	1.61	3.71	0.14	2.94	2.17	3.18	2.76	-	-	-	97.29
20	60.1	0.42	15.5	-	-	0.03	2.3	4.4	4.9	1.0	-	-	-	-

References:

1.   micropegmatite (Collins, 1934, average of 34)

2.   norite (Collins, 1934, average of 38)

3.   north range felsic norite (Cowan, 1968, average of 2)

4.   north range mafic norite (Cowan, 1968, 1 analysis)

5.   Copper Cliff offset (Thomson, 1935)

6.   Foy offset (Thomson, 1935)

7.   Frood Stobie offset (Thomson, 1935)

8.   Worthington offset (Thomson, 1935)

9.   average offset (Thomson, 1935, average of 5,6,7,8)

10.   Mackenzie diabase (Fahrig et al., 1965)

11.   Matachewan diabase (Fahrig et al., 1965)

12.   Nipissing diabase (Moorhouse, 1969)

13.   Sudbury diabase (Fahrig et al., 1965)

14.   Superior Province tonalitic gneiss (Cowan, 1968, average of 5)

15.   Onwatin slate (Sadler, 1958)

16.   black Onaping (Stevenson, 1972, average of 2)

17.   grey Onaping (Stevenson, 1972, average of 3)

18.   basal breccia matrix of Onaping Formation (Peredery, 1972, 1 analysis)

19.   melt rocks in Onaping Formation (Peredery, 1972, average of 22)

20.   north range leucocratic sub-layer (Cowan, 1968, average of 2)

–   not reported.

APPENDIX B. REGIONAL GEOLOGICAL HISTORY AT SUDBURY

(after Brocoum and Dalziel, 1974)

b. y.	Events
0.8-1.1	Late Faulting
	Grenvillian Orogeny Thermal Overprint
1.46	Olivine Diabase Dikes
1.6-1.8	Uplift and Cooling
1.7-1.95	**Penokean Orogeny** — Kink Bands in Onaping Formation
	Low Grade Metamorphism
	Deformation of Basin. Folding / Flattening of Whitewater Group. Deformation of Irruptive on South Range.
2.0	Nickel Irruptive
	Sudbury-Type Breccias. Initiation of Whitewater Group Deposition. Cryptoexplosion Event
2.15	Nipissing Diabase
2.2	Creighton and Murray Granite
2.3-2.5	Deposition of Huronian. Initiation of Faulting.
2.5+	Kenoran Orogeny

APPENDIX C.   RARE EARTH DISTRIBUTION COEFFICIENTS FOR SEVERAL ROCK FORMING MINERALS

Basic rock systems[1]

	La	Ce	Sm	Eu	Tb	Yb	Lu
Clinopyroxene	0.073	0.17	0.40	0.46	0.51	0.42	0.39
Orthopyroxene	0.010	0.013	0.023	0.027	0.037	0.11	0.14
Olivine	0.0074	0.0076	0.0094	0.010	0.012	0.019	0.020
Plagioclase	0.14	0.10	0.039	0.39	0.020	0.0085	0.0075
Garnet	0.022	0.058	1.7	3.8	12	38	34

Acid rock systems

	La	Ce	Sm	Eu	Tb	Yb	Lu
Plagioclase[2]	(0.29)	0.24	0.11	1.96	(0.073)	0.044	0.041
K-feldspar[3]	(0.055)	0.044	0.018	1.13	(0.08)	0.012	(0.006)
Biotite[4]	0.27	0.32	0.26	0.24	0.26	0.44	0.33
Hornblende[5]	(0.82)	1.25	6.23	4.20	(7.50)	6.76	4.56
Clinopyroxene[6]	0.50	0.65	1.81	2.01	(1.30)	1.14	1.28

References:

1: compiled by Helmke and Haskin (1973)

2: Nagasawa and Schnetzler (1971), average of 5

3: Schnetzler and Philpotts (1970), 1 sample

4: Higuchi and Nagasawa (1969), 1 sample

5: Nagasawa and Schnetzler (1971), average of 4

6: Schnetzler and Philpotts (1970), 1 sample

( ): value by interpolation.

APPENDIX D. RARE EARTH CONCENTRATIONS (PPM) IN CHONDRITES USED IN SAMPLE

NORMALIZATIONS (after Haskin et al., 1968b)

La	Ce	Pr	Nd	Sm	Eu	Gd	Tb	Dy	Ho	Er	Tm	Yb	Lu
—	—	—	—	—	—	—	—	—	—	—	—	—	—
0.330	0.88	0.112	0.60	0.181	0.069	0.249	0.047	0.317	0.070	0.200	0.030	0.200	0.034